

**SYNTHESIS OF SURFACE CAPPED MOLYBDENUM
SULPHIDE NANOPARTICLES AS AN ANTIWEAR
ADDITIVES FOR BIO-BASED LUBRICANT OIL**

SHARUL HAFIQ BIN ROSLAN

**INSTITUTE OF GRADUATE STUDIES
UNIVERSITY OF MALAYA
KUALA LUMPUR**

2017

**SYNTHESIS OF SURFACE CAPPED MOLYBDENUM
SULPHIDE NANOPARTICLES AS AN ANTIWEAR
ADDITIVES FOR BIO-BASED LUBRICANT OIL**

SHARUL HAFIQ BIN ROSLAN

**DISSERTATION SUBMITTED IN FULFILMENT OF
THE REQUIREMENTS FOR THE DEGREE OF MASTER
OF PHILOSOPHY**

**INSTITUTE OF GRADUATE STUDIES
UNIVERSITY OF MALAYA
KUALA LUMPUR**

2017

UNIVERSITY OF MALAYA
ORIGINAL LITERARY WORK DECLARATION

Name of Candidate: **SHARUL HAFIQ BIN ROSLAN**

Matric No: **HGA 140023**

Name of Degree: **The Degree of Master of Philosophy**

Title of Dissertation (“this Work”):

**Synthesis of Surface Capped Molybdenum Sulphide Nanoparticles as
an Antiwear Additives for Bio-based Lubricant oil**

Field of Study: **Chemistry**

I do solemnly and sincerely declare that:

- (1) I am the sole author/writer of this Work;
- (2) This Work is original;
- (3) Any use of any work in which copyright exists was done by way of fair dealing and for permitted purposes and any excerpt or extract from, or reference to or reproduction of any copyright work has been disclosed expressly and sufficiently and the title of the Work and its authorship have been acknowledged in this Work;
- (4) I do not have any actual knowledge nor do I ought reasonably to know that the making of this work constitutes an infringement of any copyright work;
- (5) I hereby assign all and every right in the copyright to this Work to the University of Malaya (“UM”), who henceforth shall be owner of the copyright in this Work and that any reproduction or use in any form or by any means whatsoever is prohibited without the written consent of UM having been first had and obtained;
- (6) I am fully aware that if in the course of making this Work I have infringed any copyright whether intentionally or otherwise, I may be subject to legal action or any other action as may be determined by UM.

Candidate’s Signature

Date:

Subscribed and solemnly declared before,

Witness’s Signature

Date:

Name: **NURIN WAHIDAH MOHD ZULKIFLI**

Designation:

ABSTRACT

Protecting metal surfaces from wear damage is of great concern in internal combustion engine systems. Using suitable additives in lubricant oil is one way of addressing this problem. Molybdenum sulphide additives are widely known for their antiwear and antifriction capabilities, and is fast becoming one of the main ingredients in lubricants. The preparation steps were modified accordingly to obtain nanosized molybdenum sulphide particles, which allows it to be directly blended into the lubricant to form relatively stable particle dispersion. In order to achieve better dispersion and tribological features, the surface of the inorganic material can be protected using various capping agents. In this research, the surface-capped molybdenum sulphide nanoparticles were synthesised, while various alkyl lengths of fatty acids were used as a capping agent. Hexacarbonylmolybdenum was used as a precursor to synthesise molybdenum (II) acetate, which is an organometallic compound intermediate. This compound was then modified with the capping agent to form capped-surface molybdenum sulphide. The properties of surface-capped molybdenum sulphides were determined using Fourier Transform Infrared Spectroscopy (FTIR), Raman Spectroscopy, X-ray Diffractometry (XRD), Field Emission Scanning Electron Microscopy (FESEM), Energy-dispersive X-ray spectroscopy (EDX), and Thermal Gravimetric Analyser (TGA). It was then blended into a bio-base oil at concentrations between 0.025-0.125 (w/w) %. The prepared bio-lubricants were then tested using the four-ball tribometer setup, viscometer, and densitometer to determine the friction coefficient (CoF), viscosity, and density, respectively. Scanning Electron Microscopy (SEM) were used to image the wear scars. It is expected that the surface-capped molybdenum sulphide will result in the better antiwear properties and enhanced friction modifying capability.

ABSTRAK

Perlindungan permukaan logam daripada haus adalah amat penting di dalam sistem enjin pembakaran dalaman. Bahan tambah seperti molibdenum sulfida telah digunakan secara meluas dan turut dikenali sebagai bahan tambah antihaus dan antigeseran, serta telah menjadi salah satu daripada bahan utama dalam penghasilan minyak pelincir. Pelbagai langkah penyediaan dan pengubahsuaian telah dilakukan oleh para penyelidik untuk mencapai zarah molibdenum sulfida bersaiz nano. Ia boleh dicampur terus ke dalam minyak pelincir, dan membentuk zarah yang terserak secara stabil. Dalam usaha untuk memiliki ciri-ciri tribologi dan serakan yang lebih baik, permukaan nanobahan takorganik boleh dilindungi dengan pelbagai jenis ejen penutup. Dalam kajian ini, permukaan bertukup nanozarah molibdenum sulfida (SCMS) telah berjaya dihasilkan dan asid lemak daripada pelbagai panjang alkil telah digunakan sebagai ejen penutup. Heksakarbonilmolibdenum telah digunakan sebagai bahan permulaan untuk mensintesis sebatian perantaraan molibdenum (II) asetat. Kemudian sebatian ini terus digunakan bersama agen penutup untuk membentuk permukaan bertukup nanozarah molibdenum sulfida. Sifat-sifat permukaan bertukup nanozarah molibdenum sulfida telah dianalisa melalui kaedah spektroskopi Inframerah Transformasi Fourier (FTIR), Spektroskopi Raman, Kristalografi Sinar-X (XRD), Bidang Pelepasan Mikroskop Elektron Pengimbas (FESEM), Spektroskopi Tenaga-serakan Sinar-X (EDX) dan Analisis Gravimetrik Haba (TGA). Kemudian, produk itu telah dicampur ke dalam minyak berasaskan bio pada kepekatan 0.025-0.125 (w/w) %. Selepas itu, minyak bio-pelincir yang terhasil telah diuji dengan pengukur tribometer empat-bola, meter kelikatan dan meter ketumpatan untuk menentukan pekali geseran (CoF), kelikatan dan ketumpatan. Mikroskop Elektron Pengimbas (SEM) telah dilakukan untuk menentukan sifat-sifat parut yang terbentuk. Dijangkakan bahawa permukaan bertukup nanozarah molibdenum sulfida akan memberikan ciri-ciri antihaus dan antigeseran yang diperbaiki.

ACKNOWLEDGEMENTS

First and foremost, I would like to express the deepest gratitude to Allah for giving me strength and capability to proceed successfully. This thesis appears in its form due to the assistance and guidance of several people. I would like to offer my sincere thanks to all of them.

I would like to express special thanks to my supervisor, Dr. Nurin Wahidah Mohd Zulkifli for constant support, thoughtful guidance, insightful comments throughout the experimental and thesis work. I wish to extend my appreciation to all members in Centre for Research in Nanotechnology and Catalysis (NANOCAT) and Centre for Energy Science (CFES), University of Malaya and all my colleagues. In addition, I thank my fellow labmates in both research centres for the stimulating discussion, for the sleepless we were working together before deadlines and for all the fun we have had in the last two years.

I would also like to express my special thanks to my beloved parents, Roslan bin Tasimin and Sahlah binti Haji Idris, my siblings, and my best friends for their endless love and encouragement. I will not be who I am today without their encouragement. My deepest appreciation goes to those who indirectly contributed in this research. This research would not be possible without the financial support from the Ministry of Higher Education Malaysia (MOHE) through MyBrain15, University of Malaya through research grant BKP103-2014A, FP063-2015A and PG269-2015B (PPP).

I am indebted to my late supervisor, Allahyarhamah Prof. Dr. Sharifah Bee Abd Hamid, for her love, guidance, concern, constant encouragement, kind and support throughout the development of this research project. May her soul rest in peace.

Al-Fatihah

TABLE OF CONTENTS

Abstract	iii
Abstrak	iv
Acknowledgements	v
Table of Contents	vi
List of Figures	x
List of Tables.....	xiii
List of Symbols and Abbreviations.....	xv
List of Appendices	xvii
CHAPTER 1: INTRODUCTION.....	1
1.1 Research background.....	1
1.2 Problem statement	5
1.3 Objective of the research	7
1.4 Scope of present work	7
1.5 Organisation of dissertation.....	8
CHAPTER 2: LITERATURE REVIEW.....	10
2.1 Introduction.....	10
2.2 Basic theory of lubricant oil	10
2.2.1 Lubricant base oil	11
2.2.2 Additives in lubricant oil.....	12
2.3 Antifriction, antiwear and extreme pressure additives	14
2.4 Nanoparticles as an additive in lubricant oil.....	17
2.4.1 Molybdenum sulphide nanoparticles.....	19
2.4.2 Disadvantages of unmodified nanoparticles.....	22

2.4.3	Surface capped nanoparticles	22
2.5	Bio-based lubricant oil.....	24
2.6	Physiochemical and tribological study of bio-based lubricant oil.....	26
2.6.1	Viscosity	26
2.6.2	Density.....	26
2.6.3	Nanoparticles characterisation of dispersions and sedimentations	27
2.6.4	Tribological study.....	29
2.7	Research gaps and novelty of dissertation.....	31
CHAPTER 3: METHODOLOGY		34
3.1	Introduction.....	34
3.2	Materials and chemicals	37
3.3	Phase 1: Nanoparticles synthesis	39
3.3.1	Phase 1A: Synthesis of MOAC compound	39
3.3.2	Phase 1B: Synthesis of SCMS nanoparticles	40
3.4	Phase 2: Characterisations	41
3.4.1	Ultraviolet–Visible Spectroscopy (UV-Vis)	41
3.4.2	Field Emission Scanning Electron Microscopy Analysis (FESEM).....	41
3.4.3	Energy Dispersive X-Ray Spectroscopy (EDX)	42
3.4.4	Fourier Transform Infrared Spectroscopy (FTIR).....	42
3.4.5	Raman Spectroscopy	43
3.4.6	X-ray Powder Diffraction Spectroscopy (XRD)	43
3.4.7	Thermal Gravimetric Analysis (TGA)	44
3.5	Phase 3: Formulation and blending of bio-based lubricant oil with SCMS nanoparticles	44
3.5.1	Bio-base oil material	44

3.5.2	Preparation of bio-based lubricant oil with SCMS nanoparticles	46
3.6	Phase 4: Tribological Analysis	47
3.6.1	Friction Reduction Analysis	48
3.6.2	Extreme Pressure Analysis	49
3.6.3	Wear Scar Analysis	50
3.7	Phase 5: Physiochemical measurement of optimized bio-based lubricant oil with SCMS nanoparticles	51
3.7.1	Sedimentation Test	51
3.7.2	Optical Microscopic Study	52
3.7.3	Viscosity and Density Analysis	52
CHAPTER 4: RESULTS AND DISCUSSION		53
4.1	Introduction	53
4.2	Study of molybdenum (II) acetate	53
4.2.1	UV-Vis Spectroscopy	53
4.2.2	FTIR Spectroscopy	54
4.2.3	Raman Spectroscopy	55
4.3	Study of surface capped molybdenum sulphide nanoparticles	56
4.3.1	FESEM Microscopy	57
4.3.2	EDX Spectroscopy	58
4.3.3	FTIR Spectroscopy	60
4.3.4	Raman Spectroscopy	63
4.3.5	XRD Spectroscopy	65
4.3.6	TGA Analysis	66
4.4	Tribological Study	67
4.4.1	Coefficient of Friction (CoF) Analysis	67

4.4.2	Extreme Pressure (EP) Analysis.....	69
4.4.3	Wear Scar Study.....	72
4.5	Physiochemical study of formulated bio-based lubricant oil	81
4.5.1	Sedimentation Study.....	81
4.5.2	Microscopic Dispersion Analysis.....	85
4.5.3	Viscosity Analysis	87
4.5.4	Density Analysis.....	89
CHAPTER 5: CONCLUSIONS AND RECOMMENDATIONS.....		91
5.1	Conclusion	91
5.2	Recommendations for future work	94
	References	95
	List of Publications and Papers Presented	106
	Appendix.....	107

LIST OF FIGURES

Figure 1.1: Lubricant additives market volume by product, Year 2014-2024 (Kilo Tonnes).....	3
Figure 1.2: 2015 Global consumption of lubricant oil additives	4
Figure 2.1: Schematic diagram of Stribeck curve where η is the fluid viscosity, v is relative speed of the surface and P is the load on the interface per unit bearing width ..	14
Figure 2.2: Percentage of nanoparticles shape and morphology based on literature	18
Figure 2.3: Type of nanoparticles used in lubricants and examples	19
Figure 2.4: Research gaps between literature studies and current research based on type of nanoparticles and characterisation methods	32
Figure 2.5: Research gaps between literature studies and current research based on type of nanoparticles and base oil	33
Figure 3.1: Flowchart of synthesising MOAC compound and SCMS nanoparticles in Phase 1 and Phase 2 respectively	35
Figure 3.2: Flowchart of SCMS nanoparticles blending, tribological analysis and physiochemical study in Phase 3 to Phase 5	36
Figure 3.3: Reaction set up.....	40
Figure 3.4: Chemical structure of PETC ester where R represent a mixture of 7 or 9 carbon alkyl chain	45
Figure 3.5: PETC ester used as bio-base oil	45
Figure 3.6: Additive and base oil blending process	47
Figure 3.7: Four-ball arrangement	47
Figure 3.8: Four-ball schematic diagram and point contact after test.....	48
Figure 4.1: UV-Vis Spectra of (a) hexacarbonylmolybdenum precursor and (b) MOAC compound.....	54
Figure 4.2: FTIR Spectrum of MOAC compound	55
Figure 4.3: Chemical structure of MOAC.....	55
Figure 4.4: Raman spectrum of MOAC	56

Figure 4.5: FESEM images of (a) SCMS-CA, (b) SCMS-LA, (c) SCMS-SA and (d) SCMS-OA nanoparticles.....	57
Figure 4.6: EDX mapping of (a) SCMS-CA, (b) SCMS-LA, (c) SCMS-SA and (d) SCMS-OA nanoparticles.....	58
Figure 4.7: FTIR Spectra comparison of (a) MoS ₂ nanoparticles (b)SCMS-LA nanoparticles, and (c) lauric acid	61
Figure 4.8: FTIR Spectra of surface capped molybdenum sulphides nanoparticles where (a) SCMS-CA, (b) SCMS-LA, (c) SCMS-SA and (d) SCMS-OA nanoparticles.....	62
Figure 4.9: Raman Spectra of surface capped molybdenum sulphides nanoparticles where (a) MoS ₂ , (b)SCMS-CA, (c) SCMS-LA (d) SCMS-SA and (e) SCMS-OA nanoparticles	64
Figure 4.10: XRD Spectra of surface capped molybdenum sulphides nanoparticles where (a) SCMS-CA, (b) SCMS-LA (c) SCMS-SA and (d) SCMS-OA nanoparticles.....	65
Figure 4.11: TGA Analysis of SCMS nanoparticles.....	66
Figure 4.12: Average Coefficient of friction (CoF) of bio-based lubricant oil without additive and bio-based lubricant oil containing 0.025 to 0.125 (w/w) % additive	68
Figure 4.13: Average Coefficient of friction (CoF) of bio-based lubricant oil only and bio-based lubricant oil containing 0.075 (w/w) % SCMS-LA nanoparticles at different load.....	70
Figure 4.14: Variation of COF with load from 400 N to 1800 N in 10 seconds for (a) bio based lubricant oil without additive and (b) bio-based lubricant oil with addition 0.075 (w/w) % SCMS-LA nanoparticles	72
Figure 4.15: Average wear scar diameter (WSD) of bio-based lubricant oil only and bio-based lubricant oil containing 0.025 to 0.125 (w/w) % additives.....	73
Figure 4.16: Relationship between load and wear scar diameter (WSD) of bio-based lubricant oil only and bio-based lubricant oil containing 0.075 (w/w) % SCMS-LA nanoparticles at different load 400 to 1,800 N.....	77
Figure 4.17: Schematic plot of WSD against applied load	77
Figure 4.18: Model of SCMS nanoparticles where R is long alkyl chain with carbon number (n), n=4,10,16 (saturated) and 16 (unsaturated) for SCMS-CA, SCMS-LA, SCMS-SA and SCMS-OA respectively.....	84
Figure 4.19: Schematic diagram of single layer of fatty acid capped molybdenum sulphide nanoparticles in bio-based lubricant oil (PETC ester)	84

Figure 4.20: Relationship between additive concentration and viscosity index of UCMS and SCMS-LA nanoparticles added bio-based lubricant oil..... 89

University of Malaya

LIST OF TABLES

Table 2.1: Base oil classifications	12
Table 2.2: Summary and development of lubricant oil additives	13
Table 2.3: Designation of antifriction additives.....	15
Table 2.4: Physical properties of MoS ₂	20
Table 2.5: Different methods of synthesising molybdenum sulphide nanoparticles	21
Table 2.6: Synthesised surface capped nanoparticles for various applications	23
Table 2.7: Summary on sources, advantages and applications of bio-based lubricant oil	25
Table 2.8: Techniques used to study dispersibility of nanoparticles	28
Table 2.9: Instrumentation used by previous research on tribological study for lubricant oil.	30
Table 3.1: List of chemicals and material used throughout research study	37
Table 3.2: Composition of bio-based lubricant in this research.....	46
Table 3.3: Friction test parameters at normal load.....	49
Table 3.4: Extreme Pressure test parameters at different load.....	50
Table 4.1: Average particles size of SCMS nanoparticles.....	58
Table 4.2: Elemental composition of SCMS nanoparticles	59
Table 4.3: Chemical composition and composition of capping agent present in SCMS nanoparticles	59
Table 4.4: FTIR band comparison between various types of SCMS nanoparticles.....	62
Table 4.5: Characteristics Raman bands assignation	64
Table 4.6: Wear scar images of bio-based lubricant oil without additive and bio-based lubricant oil containing 0.025 to 0.125 (w/w) % additive.....	75
Table 4.7: Surface morphology of wear scar formed on the ball after EP test using calibrated optical microscope.....	79

Table 4.8: Digital images of the dispersion and sedimentation behaviour of SCMS-LA and UCMS nanoparticles after loading after 7 and 30 days for various additive concentration	82
Table 4.9: Metallographic micrographs of UCMS and SCMS-LA nanoparticles at different loading percentage.....	86
Table 4.10: Kinematic viscosity at 40 and 100 °C and viscosity index of formulated bio-based lubricant oil, loaded with SCM-LA and UCMS nanoparticles at concentration up to 0.125 (w/w) %.....	88
Table 4.11: Density at 15 °C of formulated bio-based lubricant oil, loaded with SCM-LA and UCMS nanoparticles at concentration up to 0.125 (w/w) %.....	90

University of Malaysia

LIST OF SYMBOLS AND ABBREVIATIONS

API	:	American Petroleum Institute
ASTM	:	American Society for Testing and Materials
SCMS-CA	:	Caproic acid capped molybdenum sulphide
C	:	Carbon
cSt	:	Centistokes
CFES	:	Centre for Energy Science
NANOCAT	:	Centre for Research in Nanotechnology and Catalysis
CoF	:	Coefficient of friction
S	:	Sulphide
DLS	:	Dynamic Light Scattering
EDX	:	Energy Dispersive X-ray Spectroscopy
EVA	:	Ethylene–vinyl acetate copolymer
EP	:	Extreme pressure
FESEM	:	Field Emission Scanning Electron Microscopy
η	:	Fluid viscosity
FTIR	:	Fourier Transform Infrared Spectroscopy
HFRR	:	High-Frequency Reciprocating Rig Tester
HRTEM	:	High Resolution Transmission Electron Microscopy
LLS	:	Laser Light Scattering
SCMS-LA	:	Lauric acid capped molybdenum sulphide
Mo	:	Molybdenum
MOAC	:	Molybdenum acetate
MoDTP	:	Molybdenum dialkyldithiophosphates
MoS ₂	:	Molybdenum disulphide

MoDTC	:	Molybdenum dithio-carbamates
SCMS-OA	:	Oleic acid capped molybdenum sulphide
O	:	Oxygen
p.a.	:	Per annum
PETC	:	Pentaerythrityl tetracaprylate/tetracaprate
PAO	:	Polyalphaolefin
Raman	:	Raman Spectroscopy
RBD	:	Refined, bleach and deodorised
v	:	Relative speed
rpm	:	Revolutions per minute
SEM	:	Scanning Electron Microscopy
SCMS-SA	:	Stearic acid capped molybdenum sulphide
St	:	Stokes
SCMS	:	Surface capped molybdenum sulphide
SI	:	System of Units
P	:	The load on the interface per unit bearing width
TGA	:	Thermal Gravimetric Analyser
UV-Vis	:	Ultraviolet-Visible Spectroscopy
UCMS	:	Uncapped/unmodified molybdenum sulphide
VI	:	Viscosity index
WSD	:	Wear scar diameter
(w/w) %	:	Weight to weight percent
XRD	:	X-ray Diffractometry
ZDDP	:	Zinc dialkyldithiophosphate

LIST OF APPENDICES

Appendix A-1: CoF value for each SCMS nanoparticles added bio-based lubricant oil with concentration varies from 0.025 (w/w) % - 0.125 (w/w) %	107
Appendix A-2: CoF value for no additive and 0.075 (w/w) % SCMS-LA nanoparticles of bio-based lubricant oil with load varies from 400 N – 1800 N	108

University of Malaya

CHAPTER 1: INTRODUCTION

1.1 Research background

The global population is currently expanding at a rate of 25 %, from 7.2 billion in 2014, to 9 billion in 2040, with India expected to have a population of 1.6 billion by 2040, surpassing China as the most populous country in the world (Mobil, 2016). Currently, the world household incomes are increasing and poverty is decreasing, which increases demand for many manufactured finished daily products. Subsequently, industries need to expand their production capacities to meet this demand. The manufacturers rely heavily on machineries for this, which increases demand for lubricant oil and grease that would help increase the efficiency of such equipment and prevent failure (Analysts, 2015).

Lubricant is essential to machines, and it has been pivotal since the invention of the wheel (Panchal *et al.*, 2017). There are many base oil available in the market, encompassing petroleum oil, synthetic oil, refined oil, and vegetable oil (R. V. Sharma & Dalai, 2013). Petroleum crude oil is a well-known major source of conventional lubricant oil used worldwide. The total world lubricant oil demand is estimated to approach 42.1 million metric tons by 2017, at a growth rate of ~2 % p.a. (B. K. Sharma & Biresaw, 2016). The rate of utilisation of total lubricants remains moderate, with a 2.2 % growth due to lubricant producers focussing mainly on formulating high quality lubricants and using enhanced materials in machineries, which results in reduced need for lubricants in the near future. On the contrary, Asia Pacific, Latin America, and Africa/Mideast regions showed the opposite trend due to the fast paced industrialisation and growing car ownership in those regions (Bart *et al.*, 2012).

The automotive sector represents the largest product market, with engine oil making up its main revenue. The increasing demand for light passenger and heavy-duty vehicles and the improvement of the average lifespan of vehicles had further propped up the lubricant oil market. Strict quality standards imposed by governments vis-à-vis exhaust gas emissions from vehicles is also a factor. The lubricant oil industry, seeing these needs, are constantly coming up with new products that increase fuel efficiency in combustion engine via the reduction of friction between contacting surfaces (Markets, 2015).

Many lubricant companies have invested in research and development (R&D) for formulating lubricant product that comply with consumer expectations and environmental regulations. Additives in lubricant oil enhance its subsequent performance. Additives are selected for its capability to achieve one or more specific functions alongside other functional additives, such as wear and friction inhibitor, viscosity improver of base oil, and antioxidant and corrosion inhibitor. They can also improve engine performance, withstand extreme pressure, and extend drain interval period of lubricant oils.

Recent studies show that the international lubricant oil additives market size was \$14.35 billion in 2015. Dispersant and viscosity modifier additives are in high demand, with both jointly accounting for over 40 % of the total market volume, as shown in Figure 1.1. The global need for lubricant oil additives is expected to expand at an average annual rate of 1-2 % by 2020 (Markit, 2015). The demand for lubricants in the industrial and automotive sectors fluctuates worldwide, where it depends on the automotive production and possession required in each region, as shown in Figure 1.2. The main drivers for lubricant oil additives consumption are the nations in the Asia Pacific region, especially China, India, Malaysia, and other ASEAN countries. They are undergoing rapid economic development and industrialisation, which results in increasing consumption of

lubricants for machinery and automobiles. However, in developed countries such as in Central and Eastern Europe where the market is more mature, growth remains minimal due to ever-changing technology in the end-use industries, focussing more on automotive engine design and government regulations of lowering pollution emission and reducing fuel consumption.

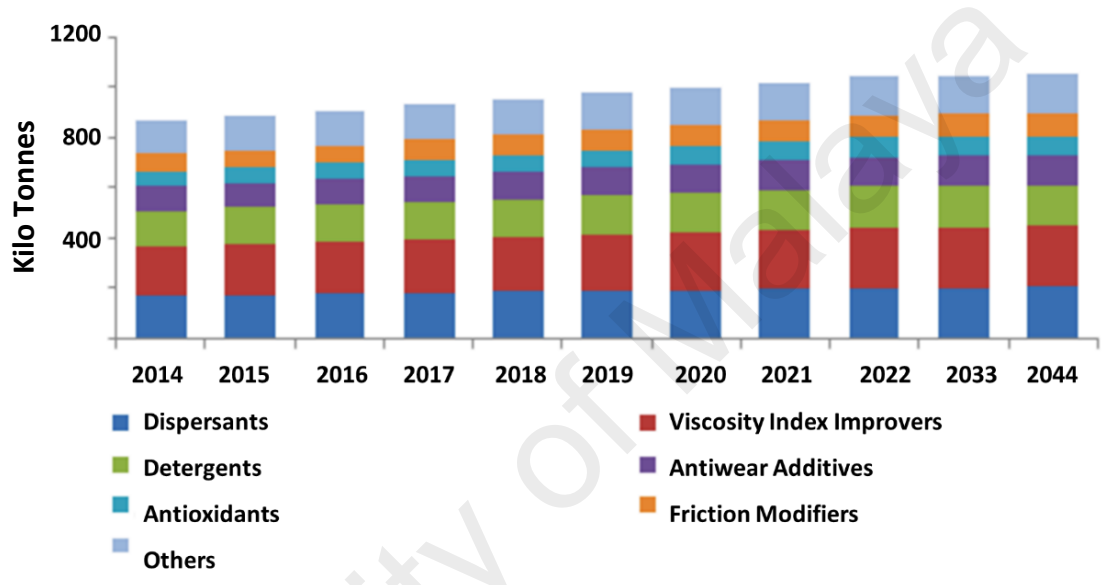


Figure 1.1: Lubricant additives market volume by product, Year 2014-2024 (Kilo Tonnes) (Research, 2016)

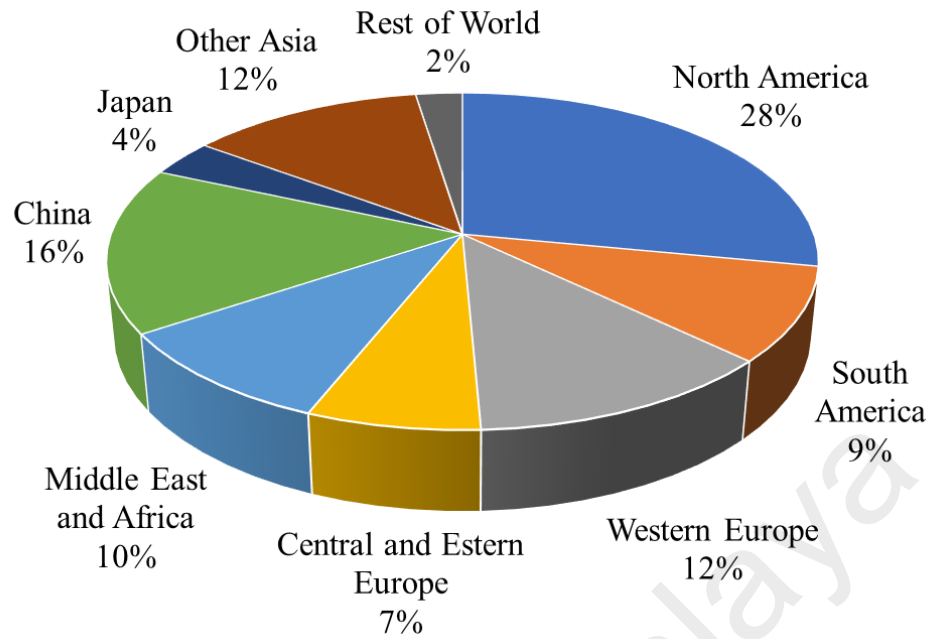


Figure 1.2: 2015 Global consumption of lubricant oil additives (IHS, 2015)

Friction and wear modifier additives are chemical compounds that can alter the friction coefficient of a lubricant. They are specially designed to reduce the amount of energy required to encourage contacting surfaces to the other. Friction modifiers is heavily reliant on its application. For example, in internal combustion engines, the intent is to reduce friction, which is expected to increase fuel consumption efficiency. However, in industrial applications, automatic transmission, and in clutches, additives are expected to minimise slippage. The additives improves the oil transition process from dynamic to static, especially during gear changes in transmission or the engagement of a clutch (Green, 2015).

The use of nanomaterials in lubricant oil formulation have been reported, and many researches confirm that nanotechnology can certainly improve the lubrication properties of oil and grease (Zhmud & Pasalskiy, 2013). These nanoadditives are far superior to lubricant oil, as they are small enough to infiltrate contact asperities, are of high thermal stability, diverse particle chemistry, and its reaction period with the surface lack induction periods (Shahnazar *et al.*, 2016). Moreover, the individual feature of nanoparticles such as its shape, size, and physiochemistry help control systemic friction property and wear reduction behaviour of the base oil.

Environmental concerns will continue to play a major role in the formulation of lubricant oil, as a fraction of total lubricant used worldwide end up polluting the environment via spillage, accident, or volatility (Schneider, 2006). Furthermore, the widely used petroleum-based lubricant oil are unsustainable as they are heavily tied to the availability of limited resources (i.e. Petroleum). Oil prices are also subjected to constant fluctuations (Yang *et al.*, 2002). Therefore, there is renewed interest in bio-based lubricant oil. They exhibit positive significant environmental impact, are sustainable, and reports acceptable performance in a wide array of applications (Nagendramma & Kaul, 2012; Ramezani & Schmid, 2015).

1.2 Problem statement

A typical internal combustion engine depletes around 15 % - 20 % of fuel due to frictional force (Nakada, 1994). In order to improve fuel efficiency, a lubricant with excellence friction and wear reducing behaviour is required. Molybdenum sulphide nanoparticles are widely used as additives in the lubricant sector, providing oil with excellent antiwear and antifriction capabilities. It reports low friction characteristics due to its crystal structure, which allows for easy shearing of MoS₂ layers (Mutyala *et al.*, 2016; Parenago *et al.*, 2002).

Recent advances in nanoprocessing resulted in many possible approaches for synthesising molybdenum sulphide nanoparticles with varying shapes, sizes, and physiochemistry. However, preventing nanoparticles from aggregating into bigger clusters remains a problem due to its intrinsic properties. It is driven by high particle-particle interaction and/or by the reduction of energy correlated to the high surface-to-volume ratio of the nanoparticles.

To enhance the stability of nanoparticle dispersion in lubricant base oil, modifying and capping the surface of the nanoparticles using modifiers (polymers, surfactant and small organic molecules) results in the creation of an active repulsive force. The coating agent that could afford sufficient repulsive interactions to counter agglomeration must be able to balance the antifriction and antiwear properties and the van der Waals attractive forces acting on the nanoparticles, contain non-harmful elements, and needs to be economically affordable.

Previous studies showed that a huge amount of lubricants pollute the environment either during or after its use by vehicles and machineries. Approximately 5-10 million tonnes of petro-based oleochemicals waste are produced annually, with 40 % originating from industrial and municipal waste, spills, refinery process, urban runoff, and condensation from engine exhaust (Syahrullail *et al.*, 2011). Bio-based oil from vegetable oils are proposed as substitute to petroleum-based oil, as they are environmentally compatible and demonstrate adequate tribological performance. Since the early 1980s, bio-based lubricant oil had been developed, starting with neopentylpolyol ester, which consist of branched-chain fatty acids as the base fluid, later expanding to neopentylglycol, pentaerythritol, and trimethylolpropane (TMP) ester (Adhvaryu *et al.*, 2002; Lugo *et al.*, 2007).

This research focuses on a potential modified and upgraded nanoparticle for use as antifriction and antiwear additive to induce better dispersibility in bio-based oil with enhanced tribological performance. The study undertakes the use of promising biodegradable and sustainable substitute of petroleum-based oil for better eco-friendliness and minimise reliance on mineral oil. Moreover, the study also involves the tribological analyses of lubricant oil formulated using bio-based sources with the addition of newly synthesised nanoparticles for antiwear and antifriction additives.

1.3 Objective of the research

The objectives of this study are:

1. To synthesise and characterise surface-capped molybdenum sulphide (SCMS) nanoparticles using various types of fatty acid as capping agent.
2. To determine the suitable type of SCMS nanoparticles and optimum concentration from tribological analyses.
3. To study the physiochemical properties of formulated bio-based lubricant oil with the addition of SCMS nanoparticles based on optimised tribological performances.

1.4 Scope of present work

To synthesise SCMS nanoparticles, its precursor, molybdenum acetate (MOAC), was synthesised using hexacarbonylmolybdenum, acetic acid, and acetic anhydride. Then, freshly prepared MOAC, together with thioacetamide, capping agent, and hexane were used to prepare SCMS nanoparticles using the solvothermal method. Capping agents used for this study were caproic (C6:0), lauric (C12:0), stearic (C18:0), and oleic (C18:1) acid. MOAC was characterised using UV-Vis, Fourier Transform Infrared spectroscopy

(FTIR), and Raman spectroscopy, while SCMS nanoparticles were characterised using FTIR, Raman spectroscopy, X-ray Diffraction (XRD), Field Emission Scanning Electron Microscopy (FESEM), Energy Dispersive Spectrometer (EDX), and Thermal Gravimetric Analyser (TGA). After confirming the properties of the SCMS nanoparticles, each were blended into the PETC ester (bio-base oil) at various concentrations between 0.025 - 0.125 (w/w) %. Then, the formulated bio-based lubricant oils were tested on a four-ball wear tester instrument to determine their tribological properties such as friction improver, extreme pressure performance, and wear reduction behaviour. Among them, the bio-based lubricant oil containing SCMS nanoparticles with the best tribological performance was selected in order to further analyse physiochemical properties, such as dispersibility, sedimentation, viscosity, and density, followed by comparison study of SCMS nanoparticles with uncapped molybdenum sulphide (UCMS) nanoparticles.

1.5 Organisation of dissertation

This dissertation is divided into five sections, organised in the following order:

Chapter 1 - Overview of lubricant oil and antiwear additives issue dealt with in this research, problem statement, the objectives of the study, and the scope of the dissertation.

Chapter 2 - Literature review on the technology of synthesising molybdenum sulphide nanoparticles, friction and wear reduction study, development of bio-based lubricant oil, and physiochemical analyses of formulated lubricant oil.

Chapter 3 - Describe the research steps and methodologies, beginning from synthesising SCMS nanoparticles, up till physiochemical study of formulated bio-based lubricant oil blended with SCMS nanoparticles

Chapter 4 - Present and discuss the experimental results obtained on the characterisation of synthesised SCMS nanoparticles, tribological study of formulated bio-based lubricant oil, as well as its physiochemical characteristics.

Chapter 5 - Summarise the overall research study and provide recommendations for future research development.

University of Malaya

CHAPTER 2: LITERATURE REVIEW

2.1 Introduction

This chapter discusses reports and publications to provide an understanding of the topic and issues pertaining to this study. This chapter also covers the basics on lubrication and additives, feasibility of bio-based oil to be used as lubricant base oil, and recent achievements of formulated lubricant oil on friction improver and wear reduction. Finally, the performance of bio-based lubricant oil and the effect of the addition of nanoparticles will also be reviewed.

2.2 Basic theory of lubricant oil

Studies on the chemical effects of lubrication started in the early 1900. At that time, researches were unscientific, and the test results depends on the source of lubricant and focussed on the metal in bearings and how the bearings were made (Dalmaz *et al.*, 1995). Lubricant, by definition, is a material introduced to a system to reduce friction between surfaces in mutual contact in order to minimise heat formation when the surfaces move and provide a protection medium to carry loads (pressure generated) between opposing surface. Nowadays, lubricants are needed for every mechanical machine. The coarseness and irregularities on the surface generate macroscopic ridges and valleys, which leads to friction (Panchal *et al.*, 2017).

The development of lubricants, especially additives, is done to improve properties and performance. These additives are chemical compounds that are added to the oil in quantities of few wt. % to improve the lubricating properties and durability of the oil. Typically, lubricants contain around 90 % base oil and less than 10 % additives (Rudnick, 2009). Lubricants have been used in various industries, such as drilling, factories,

automotive, aviation, and food processing sector. Emerging technology require intense and varied requirements from the lubricant itself, as the suitable formulation of lubricant oil for specific applications is complex.

2.2.1 Lubricant base oil

Base oil/base stock is the term used to describe plain oil being used as a major component when formulating lubricant oil. The physical properties of lubricant oils depend on its chemically inert stock. Lubricants are formulated from three different source of base oil, namely mineral, synthetic, and bio-based, all of which exhibit contradictory features and are suitable for diverse applications (Shahnazar et al., 2016). Mineral oil is derived from petroleum-based fluid, and is widely utilised in engine, turbine, bearings, and gears. Synthetic base oil is a fluid form of a chemical compound that are artificially made or produced using chemically modified petroleum with exceptional properties such as lubricating at low/high temperatures (Gwidon W. Stachowiak & Batchelor, 2006). Bio-based oil is derived from natural sources such as vegetables oils and animal fats. It is typically used in pharmaceutical and food processing, where contamination risks are of serious concern.

The American Petroleum Institute (API) designates several types of lubricant base oil. The first three groups are refined from the petroleum crude oil. Group IV base oils are fully synthetic (polyalphaolefin) oils, while Group V is for all other base oils not included in Groups I – IV, as shown in Table 2.1 (Prince, 2010).

Table 2.1: Base oil classifications

Group	Base stock Properties		
	Saturates	Sulphur	Viscosity index
I	< 90	> 0.03 %	≥ 80 and < 120
II	≥ 90	≤ 0.03 %	≥ 80 and < 120
III	≥ 90	≤ 0.03 %	≥ 120
IV	Includes polyalphaolefin (PAO)		
V	All other base oil stock not constituted in Group I, II, III or IV		

(Prince, 2010)

2.2.2 Additives in lubricant oil

Advances in the technology of lubricant additives can result in further improvements. The prevalence of environmental issues, cost, and energy efficiency problems require the use of new additives. The absence of additives could result in lubricant oil easily broken down and contaminating the system, or failing to protect the mechanical parts in a system.

Additives are required to enhance properties such as antifriction and antiwear, anticorrosion, viscosity modifier, detergents and dispersant, antioxidant stability, and pour-point depressant (Mortier *et al.*, 2010). Certain additives enhance the performance of lubricants under harsh conditions such as extreme pressures and temperatures and high levels of contamination. Typical classification of additives and its corresponding properties are summarised in Table 2.2.

Table 2.2: Summary and development of lubricant oil additives

Additive classification	Additives used	Properties	References
Antifriction and wear improver	Polyvinyl-pyrrolidone protected copper microparticles	Decrease CoF and reduce wear scar size. Form tribological reaction film on the worn surface.	(M. Qu <i>et al.</i> , 2016)
Extreme pressure improver	Fullerene (C ₆₀) nanoparticles	Improve lubrication performance on the friction surfaces by reducing metal surface contacts at high load and temperature. Enhance load carrying capacity of oil.	(Ku <i>et al.</i> , 2010)
Anticorrosion	Imidazolium, Ionic Liquids, Bearing, Benzotriazole Group.	Prevent undesirable chemical reactions on contacting surface by forming passive layer. Give significant anticorrosion capacity due to the presence of benzotriazole groups.	(Cai <i>et al.</i> , 2011)
Viscosity modifier	Ethylene–vinyl acetate copolymer (EVA), and ethyl cellulose	Upgrade viscosity index and improve lubricant viscosity at high temperature. Presence of hydroxyl functional group help in elevating viscosity and oil polarity.	(Quinchia <i>et al.</i> , 2014)
Detergents and dispersant	Poly-isobutylene succinic anhydride derivatives	Contain base component neutralising acids that can attack metal surface. Suspend polar oxygenated component, insoluble particles and contaminant in lubricant oil.	(Beck <i>et al.</i> , 2014)
Antioxidant stability	Zinc dialkyl-dithio-phosphates (ZDDP)	Retard the degradation process of base oil by oxidation thus preventing formation of corrosion product. Protect the designated functionalities of lubricant oil.	(Barnes <i>et al.</i> , 2001)
Pour point dispersant	Isooctyl-acrylate polymers	Improve cold flow ability of lubricant oil at low temperature. Modify the wax crystallisation process and control their shape during growth.	(P. Ghosh & Das, 2014)

2.3 Antifriction, antiwear and extreme pressure additives

There are four types of lubrication regimes: boundary lubrication, mixed lubrication, elasto-hydrodynamic lubrication, and hydrodynamic lubrication. The lubrication regime region, as well as viscosity optimisation, can best be described using a Stribeck curve shown in Figure 2.1. This curve shows the coefficient of friction as a function of a lubricant parameter, and a combination of boundary lubrication and a viscous friction curve (Kondo *et al.*, 2013). During boundary lubrication, lubricants are at low viscosities and speeds and higher loads, where the hydrodynamic pressure is insufficient to completely separate the surface and asperities on the opposing surfaces when it comes into contact, while at higher viscosities and speeds or lower load, sufficient hydrodynamic pressure separates two opposing surfaces completely by a thin film of lubricant. This phenomenon is known as hydrodynamic lubrication (Dorinson & Ludema, 1985).

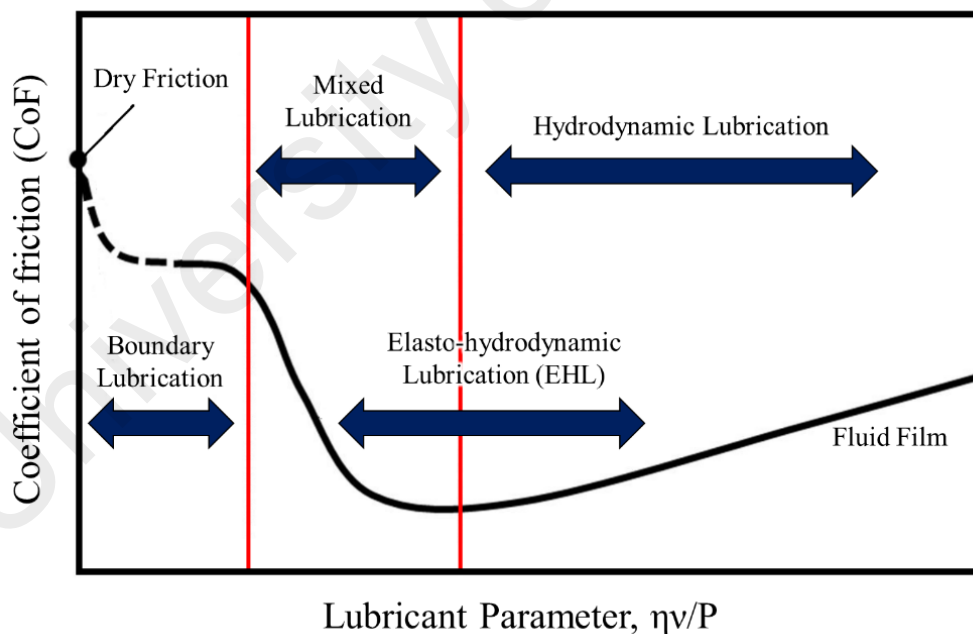


Figure 2.1: Schematic diagram of Stribeck curve where η is the fluid viscosity, v is relative speed of the surface and P is the load on the interface per unit bearing width (Kondo *et al.*, 2013)

Friction and wear are commonly high at boundaries of mixed lubrications, which results in increased friction, high surface wear, and surface damages. In this condition, antifriction or friction modifier are mostly used to modify friction characteristics, increase lubricity, and prevent seizure. Antifriction additives are able to corral CoF and is widely used in gear and engine oil applications. It can be classified into two main type for liquid lubricant, namely organomolybdenum compounds and organic friction modifiers, as shown in Table 2.3 (Tang & Li, 2014).

Table 2.3: Designation of antifriction additives

Antifriction classification	Group	Additives	Properties	References
Organic friction modifiers		Stearic acid	Can be adsorbed physically or chemically on rubbing metal surfaces to form monolayers preventing direct metal-metal contact.	(Choo <i>et al.</i> , 2007)
Organo-molybdenum compounds	Sulphur- and phosphorus-containing compounds	Molybdenum dialkyldithio-phosphates (MoDTP)	Able to form molybdenum compounds in the rubbing surfaces, but lesser than MoDTC.	(Yamamoto & Gondo, 1989)
	Sulphur-containing and phosphorus-free compounds	Molybdenum dithio-carbamates (MoDTC)	Reduces friction at contacting area under boundary lubrication. Demonstrate the mechanisms of friction-reduction by attributing MoDTC to the sliding effect between single layers of MoS ₂ .	(Grossiord <i>et al.</i> , 1998)
	Sulphur- and phosphorus-free compounds	Molybdate ester	Display good friction improver behaviour in comparison with traditional MoDTC.	(Gorbachev <i>et al.</i> , 2016)

Antiwear additives deposit layers of surface film under normal operating conditions that helps minimise continuous and moderate wears. The working mechanism of antiwear additives can be divided into several methods. Some deposit sufficiently thick multilayer films to enhance marginal hydrodynamic film and hinder asperity contact altogether, while others create easily-restored monolayer film that can reduce the local shear stress between contacting asperities. Other methods chemically bond layers with the metal surface and slowly alter the surface asperity geometry via the controlled removal of the surface material until the condition is favourable for the hydrodynamic film generation to reappear (Farnig, 2009). Zinc dialkyldithiophosphate (ZDDP) is the most typical antiwear additive used in industry, which is a very effective wear protection coating that prevents scuff damages (J. Qu *et al.*, 2014).

Extreme pressure (EP) additives are designed to react rapidly with surfaces under severe distress and prevent further disastrous failures such as seizure, scuffing, and galling. They can also prevent welding or metal-metal adhesion when the surface active species in lubricants are not strong enough to deposit a protective film, especially under harsh conditions, such as high load, high speed, and high temperature operation. They behave in a similar manner to antiwear additives, but the reaction rate of EP additives with the metal surface is higher, the formation rate of the EP film is faster, and its protective film is stronger (Y.-C. Lin *et al.*, 2012). Nanomaterials such as copper oxide (CuO) and titanium dioxide (TiO₂) nanoparticles are widely accepted by industries for use as EP additives, as they can improve load carrying capacity and the seizure load of lubricant oil (Peña-Parás *et al.*, 2016).

2.4 Nanoparticles as an additive in lubricant oil

Over the past few decades, nanoparticles are fast becoming more prominent as lubricant additives due to their potential in reducing emission and enhancing fuel efficiency. Extensive research has been carried out on both organic and inorganic nanoparticles, especially to reduce friction, improve wear, and as EP additives. Preceding studies demonstrated that nanoparticles possess exceptional tribological capabilities compared to conventional solid lubricant additives (Hwang *et al.*, 2011). Synthesising inorganic nanoparticles and stabilising it in a liquid medium were reported in literature, such as synthesising inorganic nanoparticles in reverse microemulsion environment (López-Quintela, 2003), vapour-phase method (Swihart, 2003), thermal decomposition of organometallic precursor (Talpin *et al.*, 2002), and preparation in polymeric system (Schmidt & Malwitz, 2003).

The reduction of friction, improving wear, and EP behaviours in lubricants containing nanoparticles largely rely on the characteristics of nanoparticles, such as shape, size, and loading concentration. Typically, the size of nanoparticles are ~1 - 100 nm (S. K. Ghosh *et al.*, 2004). Under normal conditions, smaller nanoparticles are prone to forming a surface protection film that permits easy entry into the contacting surface of friction pair for load bearing, which helps improve antiwear properties (J. Zhou *et al.*, 1999). However, under the high frequency of surface-to-surface interaction, larger particles perform better, while nanoparticles are applicable for greater load and lesser frequency (N. Xu *et al.*, 2013).

Shape and morphology can also influence friction, wear, and EP. The morphology of the nanoparticles utilised in lubricants include spherical, tube, onion, sheet, and granular. The statistical analyses on shape and morphology has been carried out and shown in Figure 2.1 (Dai *et al.*, 2016). Most of the nanoparticles' morphology used in lubrication

are spherical, as they reported remarkable rolling, reduce affinity to metal surfaces, possess higher elasticity, minimise contact temperature, and is more resistant to chemicals (Rapoport *et al.*, 1999). They also improve the tribological characteristics at very low concentrations. Previous studies reported that nanoparticles loaded into lubricant oil at concentrations as low as 0.05 (w/w) % results in the best antiwear and antifriction properties (S. Chen *et al.*, 1998).

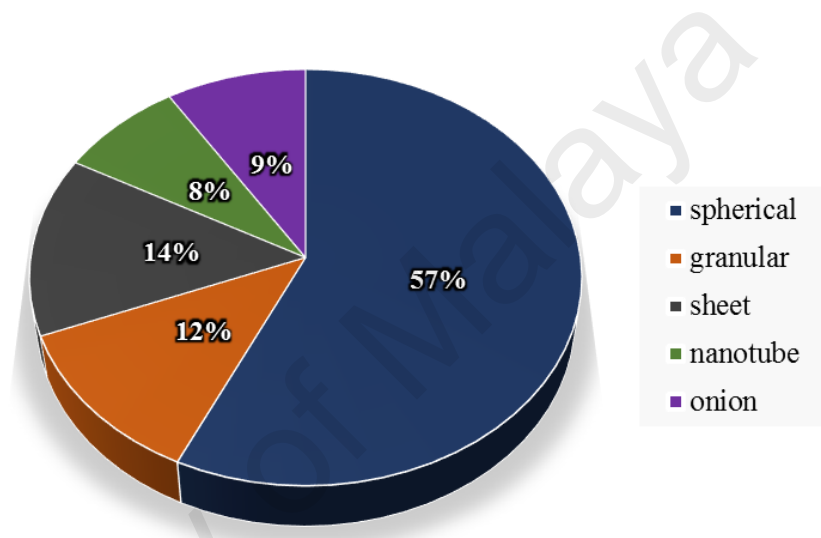


Figure 2.2: Percentage of nanoparticles shape and morphology based on literature (Dai et al., 2016)

Nanoparticles possess diverse chemical composition and physical and chemical properties, which subsequently influence how they interact with surfaces. W. Dai (Dai et al., 2016) posited that nanoparticles can be classified into seven classes based on their respective chemical characteristics, which are metal oxide, metal, sulphides, rare earth compound, nanocomposites, carbon, and its corresponding derivatives. As shown in Figure 2.3, metal oxides, metals, and sulphur are the major types of nanoparticles used as additives in lubrication. The metals and metal oxides are mostly from the transition metal group. Some elements in the rare earth element group are suitable as additives in lubricants, such as yttrium, lanthanum, and cerium. Nanocomposites, on the other hand, are a combination of the aforementioned elements, such as copper/silicon dioxide

(Cu/SiO₂), serpentine/lanthanum hydroxide (serpentine/La(OH)₂), and aluminium oxide/titanium oxide (Al₂O₃/TiO₂).

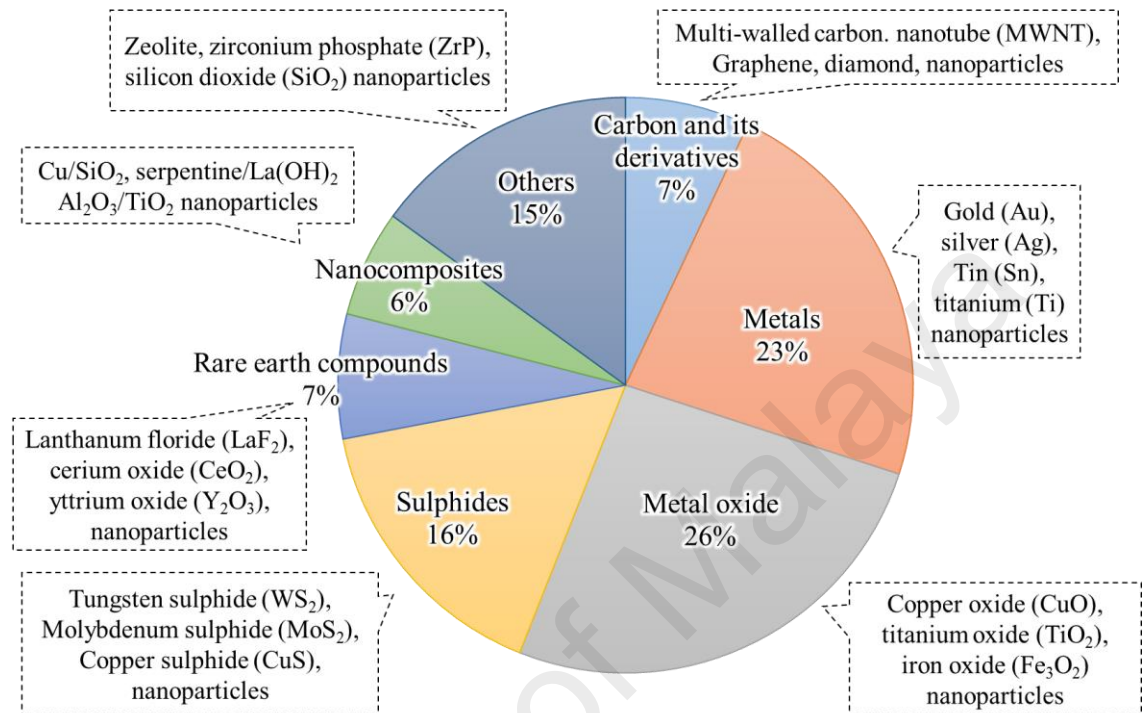


Figure 2.3: Type of nanoparticles used in lubricants and examples (Dai et al., 2016)

2.4.1 Molybdenum sulphide nanoparticles

Studies on molybdenum disulphide, or MoS₂, as additives in lubricants have been carried out since the early 19th century (Lansdown, 1999). It is a hexagonal-structured material made up of molybdenum atoms that are layer sandwiched between double layers of sulphur atoms linked by Van der Waals forces (Panigrahi & Pathak, 2013).

MoS₂ is able to provide lubrication at high contact stress and work by settling a solid lubricant layer on the contacting surfaces (Mutyala et al., 2016). Molybdenum disulphide is extracted from Molybdenite ore via the floatation process, which results in relatively pure MoS₂, with carbon as its major contaminant (Wie & Fuerstenau, 1974). MoS₂ is also a very stable compound, with a high melting point and a service temperature of 371 °C (Rudnick, 2009). The properties of molybdenum disulphide is tabulated in Table 2.4.

Table 2.4: Physical properties of MoS₂ (H. Wang *et al.*, 2013)

Properties	Value
Molecular weight (g.mol⁻¹)	160.08
Crystal type	Hexagonal crystal system
Density (g.cm⁻³)	4.5-4.8
Melting point (°C)	1185
Adhesivity	Strong bonding force, cannot damage the metal surface
Friction Coefficient	851
Heat conductivity (W.m⁻¹.K⁻¹)	0.13 (40 °C); 0.19 (430 °C)

There are many synthetic approaches that are viable for synthesising MoS₂ nanoparticles, such as hydrothermal reaction, precursor decomposition, solution reaction, surfactant assisted reaction, and sulphide sulphidation. These approaches are summarised in Table 2.5 (Afanasiev, 2008).

Table 2.5: Different methods of synthesising molybdenum sulphide nanoparticles

Synthesis method	Experimental condition	Product morphology	Advantages	References
Direct solid-state reaction	Elemental Mo&S, reaction at 700 °C under high pressure (2.0-5.0 GPa)	Poorly crystalline MoS ₂	Display hexagonal structure product (2H-MoS ₂).	(S. Wang & He, 2011)
Hydrothermal reaction	MoO ₃ , Na ₂ S, 0.4 M HCl	MoS ₂ nanowires	Simple technique and convenient chemicals, Random & loosely stacked MoS ₂ layer.	(Li <i>et al.</i> , 2003)
Solvothermal reaction	(NH ₄) ₆ Mo ₇ O ₂₄ .4H ₂ O, elemental sulphur, LiOH.H ₂ O, N ₂ H ₄ .H ₂ O, pyridine solvent	Ball-like and tube-like amorphous MoS ₂	Energy-favourable reaction for the single layer of MoS ₂ synthesis.	(Peng <i>et al.</i> , 2002)
Solution reaction	MoCl ₄ dissolved in tenery-tridodecylmethyl-ammonium iodide hexanol & octane, H ₂ S/ (NH ₄) ₂ S (aqueous)	Single-layer MoS ₂ discs nanocluster	Form fine size control of MoS ₂ nanocluster (3.5-8 nm), capable technique for morphological control.	(Wilcoxon & Samara, 1995) (Chikan & Kelley, 2002)
Surfactant assisted reaction	(NH ₄) ₆ Mo ₇ O ₂₄ .4H ₂ O, elemental S, LiOH.H ₂ O, N ₂ H ₄ .H ₂ O, cetyl-trimethyl-ammonium bromide (CTAB), thermal activation at 400 – 500 °C in H ₂ S/H ₂ mixture	Closely perfect MoS ₂ monolayer	High specific surface area product, no mesophase product formed.	(Afanasiev <i>et al.</i> , 1999)
Precursor decomposition reaction	(NH ₄) ₂ Mo ₂ S ₁₂ .2H ₂ O, isothermal heating at 120 °C,	Formation of Mo ₂ S ₁₁ intermediate, further heating lead to stepwise decomposition into crystalline MoS ₂	Better textural properties of MoS ₂ formed (70-80 m ² /g, mesoporosity ranging 2-8 nm).	(Genuit <i>et al.</i> , 2005)

2.4.2 Disadvantages of unmodified nanoparticles

Despite the fact that MoS₂ nanoparticles can be synthesised via various methods, unmodified MoS₂ nanoparticles tend to agglomerate. Inorganic nanoparticles are of high activity, due to the large surface area of nanoparticles, poor compatibility with oil, and its tendency to agglomerate (Zhang *et al.*, 2014b). Although nanoparticles are relatively stable as dispersion in oil, problems appear later due to the vigorous Brownian motion (Hwang *et al.*, 2008). These nanoparticles undergo intense collective bombardment, which slowly lead to agglomeration (Kebinski *et al.*, 2002). Agglomeration increase particle size and reduce its surface area, which subsequently prompts it to undergo fast settling from the effect of gravitational force (Choi & Jung, 2012). Reported studies homogenously disperse nanoparticles in fluids using physical treatment techniques, such as stirrers, ultrasonic baths, and high pressure homogeniser (Hwang *et al.*, 2008). Besides physical treatment techniques, the use of dispersing agent and surfactants has proven effective in inducing repulsion between the nanoparticles and minimising agglomeration (G. Zhou *et al.*, 2013).

2.4.3 Surface capped nanoparticles

There are many alternatives to tribologically active nanoparticles as additives in lubricants. One is to prepare what is called surface capped nanoparticles, where the nanoparticles' surface are encapsulated by compounds that strongly interact/react with organic materials (Suslov *et al.*, 2003). This organic surface capping agent possess long hydrocarbon chains and functional groups that are able to interact with the molybdenum sulphide nanoparticles, such as fatty acid, alkyl phosphate, and alkyl amine (Hu *et al.*, 2010). This modification improves the interfacial interaction between the inorganic nanoparticles and the surrounding fluids.

Previous studies show that several researches have been conducted on the synthesis of surface capped nanoparticles, as tabulated in Table 2.6.

Table 2.6: Synthesised surface capped nanoparticles for various applications

Nanoparticles	Capping agent	Properties	Applications	References
Molybdenum Trisulphide, MoS₃	Zinc dialkyldithio-phosphates, (ZDDP)	ZDDP capped MoS ₃ reduce wear and friction even at low concentration.	Oil based Lubricant	(Bakunin <i>et al.</i> , 2006)
Platinum, Pt	Poly-(vinyl-pyrrolidone), (PVP).	Capped nanoparticles provide better catalysis than uncapped analogue and do not prevent nanoparticle catalysis under reaction condition.	Catalysis	(Park <i>et al.</i> , 2009)
Cadmium sulphide (CdS), Zinc sulphide (ZnS), Lead sulphide (PbS)	Oleic acid	Strong Interaction between the fatty acid and metal sulphide nanocrystal enhance stability and dispersion in non-polar solvent.	Semi-conductor	(Jayesh D. Patel <i>et al.</i> , 2012)
Copper, Cu	Methoxyl-polyethylene-glycol xanthate	Capped Cu nanoparticles able to form a boundary lubricating film on the rubbed steel surface.	Water based Lubricant	(Zhang <i>et al.</i> , 2014b)

2.5 Bio-based lubricant oil

The public need for a pollutant-free environment is increasing, leading to the demand for environmentally-friendly lubricants (Zeng *et al.*, 2007). The lubricant industry and academic researchers have been trying to design better bio-based lubricant in terms of renewability, biodegradability, and performance (Sevim Z Erhan & Asadauskas, 2000).

Bio-based oil can be defined as the main component used in the lubricant formulation that generally comes from vegetable oil or other renewable sources. Usually, the major compositions of bio-based oil are triesters (triacylglycerol ester), derived from plants and animals, such as rich oleic canola oil, palm oil, rapeseed oil, and sunflower seed oil (Campanella *et al.*, 2010). Triacylglycerol esters contain fatty acid of almost similar alkyl length (14 - 22 carbon numbers), with different levels of unsaturation (Fox & Stachowiak, 2007). For lubricant purpose, the bio-base oil used from vegetable-derived substance are preferred, and this type of oil is classified as a Group V base oil.

Lubricant oil derived from bio-sources possess many desirable properties, such as high viscosity indices due to the strong intermolecular interaction between the long polar fatty acid, making them resilient to temperature changes and leading to a more stable viscosity (Fox & Stachowiak, 2007). In terms of volatility, bio-based lubricant oil exhibit superior quality compared to petroleum based lubricant oil due to the high molecular weight of triacylglycerol molecules (Sevim Z. Erhan *et al.*, 2008). Bio-based lubricant oil also shows efficient boundary lubricants properties, and the entire base oil is of high polarity, which permit strong interactions with lubricated surfaces. The ester linkages bear implicit lubricity and help the oil adhere to the surface of the metal (Soni & Agarwal, 2014).

Numerous studies have shown that bio-based lubricant oil is suitable for use as alternatives to petroleum-based oil. Table 2.7 summarises the sources, benefits, and various applications of bio-based lubricant oil.

Table 2.7: Summary on sources, advantages and applications of bio-based lubricant oil

Bio-based lubricant oil	Sources	Advantages	Applications	References
Modified jatropha oils	Crude jatropha oil, jatropha methyl ester and trimethylol-propane	Exhibits superior performance in wear and friction reduction, better cutting force with outstanding cutting temperature.	Metalworking fluid (MWF)	(Talib & Rahim, 2016)
Esterified pentaerythritol	Palm oil methyl ester and pentaerythritol	Capable to endure a high temperature surrounding with a flash point of 302 °C and viscosity of 12.7 cSt at 100 °C.	Oven chain lubricant for food industry	(Aziz <i>et al.</i> , 2014)
Esterified epoxy canola oil	Epoxy canola oil, acetic anhydride, sulphated Ti-SBA-15 (10) catalyst	Demonstrate excellent lubricity property.	Suitable as replacement for synthetic lubricant	(R. V. Sharma & Dalai, 2013)
Refined bleached and deodorised palm stearin oil	Palm oil	Able to lower the extrusion load compared to mineral oil without additive, can generate a surface product with a low value of surface roughness.	Cold work forward plane strain extrusion process	(Syahrullail <i>et al.</i> , 2011)

2.6 Physiochemical and tribological study of bio-based lubricant oil

The performance of bio-based lubricant oil with nanoparticles can be elucidated using its physiochemical properties, such as viscosity, density, and the dispersibility of nanoparticles in the lubricant oil medium.

2.6.1 Viscosity

Detailed knowledge of the viscometric properties of lubricant oil is required especially in the context of its intended application(s). Viscosity can be defined as a measure of fluid resistance to gradual deformation by shear or tensile stresses. It specifies the thickness of the lubricant oil and is obtained by calculating the time needed for a given measure of oil to pass through a specific orifice (Raj & Sahayaraj, 2010). This property is derived from the collisions of nearby particles in a fluid moving at different velocities.

Viscosity encompasses dynamic viscosity, kinematic viscosity, and bulk viscosity, all of which can be tested at multiple temperatures. Kinematic viscosity is widely used in lubricants. Based on The International System of Units (SI) system, viscosity carry the unit Stokes (St), or as m^2/s , where 1 St is equivalence to $10^{-4} \text{m}^2/\text{s}$. As the Stoke unit is a large unit, it is normally divided into much smaller scale unit called Centistokes (cSt) (Dutt *et al.*, 2007).

2.6.2 Density

Density, or specific gravity, can be defined as the ratio of the mass of the given volume at temperature ' t_1 ' to the mass of an equal volume of pristine water at temperature ' t_2 '. Normally, for petroleum products, the specific gravity is quoted using the same standard temperature of 15.6 °C. In the petroleum industry, a typical mineral oil is $\sim 850 \text{ kg}/\text{m}^3$, and since the density of water is $\sim 1000 \text{ kg}/\text{m}^3$, the specific gravity of mineral oil can be expressed as 0.85 (G.W. Stachowiak & Batchelor, 1993). The density of a lubricant oil is an important parameter when determining its performance, since the kinematic viscosity

received in testing instrument (in cSt) must be multiplied by the density to obtain the absolute viscosity for characterising lubricant film (Khonsari & Booser, 2001). The density of the liquid lubricant changes with temperature and pressure, where it decreases linearly with temperature. Moreover, it provides an indication of its chemical component and nature, as the rate of change of density is affected. For instance, aromatic oil is more dense compared to paraffinic oil at similar viscosities (Stepina & Vesely, 1992).

2.6.3 Nanoparticles characterisation of dispersions and sedimentations

The characterisation of the colloidal stability of nanoparticles in a liquid medium is required when formulating lubricant oil. Colloidal stability is technically defined as the ability of particle dispersion to resist aggregation for a specified time (Dobias, 1993). It is an important parameter, as it ensures uniform dispersion without any agglomeration of solid additives used in base oil. There are several methods that can be used to study the dispersibility, as well as the agglomeration and sedimentation of nanoparticles. These methods include the use of dynamic light scattering (DLS) technique, in situ optical microscopy, UV-Vis, and laser light scattering (LLS).

DLS is an instrumental technique that are frequently used to determine the size and distribution of particles with diameters ranging from several nanometres to microns. It detects the scattered light intensity fluctuation generated by the Brownian motion of the particles in a liquid (Barth, 1984). UV-Vis is also suitable for the evaluation of dispersion stability. Based on the Beer-Lambert law, absorbance increase linearly with absorbance. The concentration of nanoparticles in a supernatant fluid implies supernatant behaviour, where higher concentration is correlated to better dispersion properties, thus the stability of nanoparticles is determined by determining absorbance (J. Lin *et al.*, 2011).

In the in-situ optical microscopic technique, the size of the interconnected fractal aggregates was estimated at a micrometer scale. A suspension containing a known mass fraction of nanoparticles were taken and carefully dipped on a glass slide to settle so that we can analyse its morphology under a microscope (Jiang *et al.*, 2003). Another suitable method for analysing dispersibility is the LLS technique. It is a competent instrument for determining sizes and analysing cluster formation in solutions that relies on measurements of autocorrelation function of light scattered by translational and rotary Brownian diffusion of the particles (Nepomnyashchaya *et al.*, 2016). The overall summary of the applications of these techniques in the latest research findings are tabulated in Table 2.8.

Table 2.8: Techniques used to study dispersibility of nanoparticles

Method	Nanoparticles	Dispersing medium	Advantages	References
Dynamic light scattering (DLS)	Gold	Nanopure water	Efficiently track aggregate growth from nanosized primary particles to micrometer-sized aggregates.	(Zheng <i>et al.</i> , 2016)
In-situ optical microscopy	Surfactant-modified TiO ₂	Ethanol, tetrahydrofuran, methyl-methacrylate and toluene.	Capable in estimating the size of the TiO ₂ aggregates formed.	(Kamiya & Iijima, 2010)
UV-vis spectroscopy	Nanoscale zerovalent iron	Water	Able to determine sedimentation rates and colloidal aggregation.	(Phenrat <i>et al.</i> , 2007)
Laser Light Scattering (LLS)	Graphene oxide (GO)	Pure water, electrolyte aqueous solution	Can assess the effects of salt on the dispersions stability of GO.	(M. Wang <i>et al.</i> , 2016)

2.6.4 Tribological study

The word ‘tribology’ is a combination of two Greek words: “tribos”, which means rubbing, and “logos”, which means word. Tribology, in its technical definition, is the scientific and technical studies of managing and controlling wear, friction, and lubrication (Tzanakis *et al.*, 2012). This is of immense practical concern due to many mechanical, electromechanical, and biological system being reliant on suitable friction and wear values (Menezes *et al.*, 2013).

Various equipment had been designed to evaluate the tribological properties of lubricating material, and the most prevalent wear tester used in the oil industry is the four-ball wear tester. It has been extensively used to study the lubrication behaviour of oils and chemical interactions at wear contacts (Hsu & Klaus, 1978). Besides generating CoF from real-time recording the shaft torque, wear can be measured under a calibrated microscope and reported as a wear scar diameter (WSD) (Zulkifli *et al.*, 2014).

Another method for determining the lubricity of oil samples is the high-frequency reciprocating rig (HFRR) tester. The testing plate is settled in an oil groove, while the testing ball is controlled using an electromagnetic oscillator in the front/back direction at a high frequency and short stroke under certain load. The value of CoF can be obtained from the frictional force and normal load based on Column friction law, while the wear scar can be calculated from the testing ball (Y. Xu *et al.*, 2010).

Other than four-ball and HFRR, pin and ball on disc wear tester can be used to study the tribological behaviour and lubricity on oil. Each instrumentation and methods used for tribological testing and determination of CoF and wear scar are summarised in Table 2.9.

Table 2.9: Instrumentation used by previous research on tribological study for lubricant oil.

Equipment	Method	Tribological Advantages	References
Fourball Machine	ASTM D4172 ASTM D2783	Able to establish the relative wear-preventing properties of lubricating fluids and greases in sliding and rolling applications.	(Yadav <i>et al.</i> , 2016)
High-Frequency Reciprocating Rig (HFRR) Tester	ISO-12156 ASTM D6079	Can characterise friction under lubricated condition using a ball on disc configuration. Suited for wear testing relatively poor lubricants such as diesel fuels, wear.	(Sulek <i>et al.</i> , 2010) (Y. Xu <i>et al.</i> , 2010)
Pin on Disc Sliding Wear Tester	ASTM F732	Capable of analysing lubricant under multidirectional wear condition. can replicate multiple modes of wear such as unidirectional, bidirectional, omnidirectional, and quasi-rotational.	(Watanabe <i>et al.</i> , 2016)
Ball on Disc Sliding Wear Tester	ASTM G133	Able to determine the wear resistance and friction generated in uniaxial sliding contacts between lubricant films. sliding contact is delivered by pushing a ball specimen onto a rotating disc specimen under a consistent load.	(Singh, 2011)

2.7 Research gaps and novelty of dissertation

Lubricant oil consists of mainly base oil and the mixture of various types of additives. Among these additives, friction and wear improvement is some of the most prominent properties needed in lubricant oil that enhances its lubricity and performance. An example of an additive that does this is MoS₂. Various synthesis methods were reported for obtaining nano-sized compound with specific physiochemical properties based on the required applications, and different characterisation approaches were selected by previous researchers to determine the properties of nanoparticles, while the similarities and gaps between current works and literature is summarised in Figure 2.4.

Generally, nanoparticles are used as additives in lubricant oil, but dispersion instability in lubricant oil and its tendency to coagulate poses problems, as it minimises the quality of the lubricant and creates sedimentation. Several suitable techniques and instrumentation were used to help us understand the additives dispersion performance and the tribology of the formulated lubricant oil. This could be resolved by modifying the surface of the nanoparticles using a suitable capping agent, such as Zinc dialkyldithiophosphates (ZDDP), fatty acid, and polymeric compound. Increased environmental awareness resulted in higher demands for a bio-based lubricant oil derived from vegetable oil.

Many research on the synthesis of nanoparticles for lubricant additives and the production of bio-based lubricant oil from various sources were conducted, however, only a few intended to understand the tribological effect of the addition of surface-modified nanoparticles and its behaviour towards bio-based lubricant oil, as shown in Figure 2.5. This research intends to elucidate suitable modifications of molybdenum sulphide nanoparticles using various alkyl lengths of fatty acid as its capping agent and its effect on the dispersibility and lubricity of bio-based lubricant oil.

Characterisation Methods	Uncapped/undoped/unmodified nanoparticles				Capped/doped/modified nanoparticles			
HRTEM	(Hu <i>et al.</i> , 2009)	(Ingole <i>et al.</i> , 2013)			(Chen <i>et al.</i> , 2005)	(Wang <i>et al.</i> , 2006)		
FESEM			(Padgurskas <i>et al.</i> , 2013)	(Peng <i>et al.</i> , 2010)			(Park <i>et al.</i> , 2009)	This research
EDX								
FTIR		(Ingole <i>et al.</i> , 2013)			(Chen <i>et al.</i> , 2005)	(Wang <i>et al.</i> , 2006)		
Raman								
XRD	(Hu <i>et al.</i> , 2009)					(Wang <i>et al.</i> , 2006)		
TGA								
XPS	(Hu <i>et al.</i> , 2009)						(Park <i>et al.</i> , 2009)	
	MoS ₂	TiO ₂	Fe, Cu & Co	SiO ₂	MWC-SA	TiO ₂ -DBS	Pt-PVP	
Nanoparticles	Uncapped/undoped/unmodified nanoparticles				Capped/doped/modified nanoparticles			

Abbreviations: MWC-SA (multi-walled carbon nanotube-stearic acid), DBS (sodium dodecylbenzenesulfonate), PVP (poly(vinylpyrrolidone))

Figure 2.4: Research gaps between literature studies and current research based on type of nanoparticles and characterisation methods

Modified nanoparticles	Modified molybdenum sulphide		(Xu <i>et al.</i> , 2015) (Tannous, 2011)						This research
	Modified multi-walled carbon nanotube	(Chen <i>et al.</i> , 2005) (Ahmadi <i>et al.</i> , 2013)							
	Surface coated Serpentine	(Yu <i>et al.</i> , 2010)	(Zhang <i>et al.</i> , 2016)						
Unmodified nanoparticles	Zinc dialkyl-dithiophosphate (ZDDP)	(Gorbachev <i>et al.</i> , 2016)	(Demydov <i>et al.</i> , 2010) (Gorbachev <i>et al.</i> , 2016)						
	MoS ₂	(Hu <i>et al.</i> , 2009)	(Demydov, <i>et al.</i> , 2010)			(Lovell <i>et al.</i> , 2010)			
	Boric Acid	(Canter N., 2010)						(Canter <i>et al.</i> , 2009)	
	TiO ₂	(Ingole <i>et al.</i> , 2013)						(Zulkifli <i>et al.</i> , 2013)	
	Copper	(Padgurskas <i>et al.</i> , 2013)			(Qu <i>et al.</i> , 2016)				
No additive			(Shahbuddin, 2013) (Demydov, 2010)	(Shahbuddin, 2013) (Husnawan, 2007)	(Quinchia <i>et al.</i> , 2014)	(Lovell <i>et al.</i> , 2010)	(Zulkifli <i>et al.</i> , 2013)	(Aziz <i>et al.</i> , 2014)	
Additives		Paraffin/ mineral oil	PAO/ Synthetic oil	Petroleum/ bio-base mixture	Sunflower oil derivatives	Canola oil derivatives	TMP Ester	Pentaerythritol ester	
	Base oil	Petroleum-base oil		Mixture	Bio-base oil				

Figure 2.5: Research gaps between literature studies and current research based on type of nanoparticles and base oil

CHAPTER 3: METHODOLOGY

3.1 Introduction

This chapter encompasses the main phases of work, from sample preparation to physiochemical analysis. In the first phase (**Phase 1A**), molybdenum acetate (MOAC) was synthesised using a hexacarbonylmolybdenum precursor. Then (**Phase 1B**), the freshly prepared MOAC sample was used as a precursor to synthesise surface capped molybdenum sulphide (SCMS) nanoparticles via the solvothermal method. Four different samples of SCMS nanoparticles were prepared using different types of capping agent, namely SCMS-CA, SCMS-LA, SCMS-SA, and SCMS-OA nanoparticles, while the capping agents used were caproic (C6:0), lauric (C12:0), stearic (C18:0), and oleic (C18:1) acid, respectively. In the consequence phase (**Phase 2**), the synthesised MOAC was analysed using UV-Vis, FTIR, and Raman spectroscopy. Then, the SCMS nanoparticles were characterised using FTIR, Raman, XRD, FESEM, EDX, and TGA. The next phase (**Phase 3**) blends the nanoparticles into the bio-base oil. For the tribological study (**Phase 4**), the lubricity of the bio-based lubricant oil was investigated via friction reduction, anti-wear characteristics, and extreme pressure condition using a steel ball. The surface analysis of the wear was performed using SEM and a calibrated optical microscope, and the best performing additive and suitable concentration were determined. In (**Phase 5**), physiochemical analyses were performed on the formulated bio based lubricant oil, which involves dispersibility analysis, viscosity, and density to further confirm the quality of the formulated bio-based lubricant oil. Figure 3.1 shows the flowchart of overall process in Phases 1 and 2, while Figure 3.2 shows the flowchart of the overall process of Phases 3 -5.

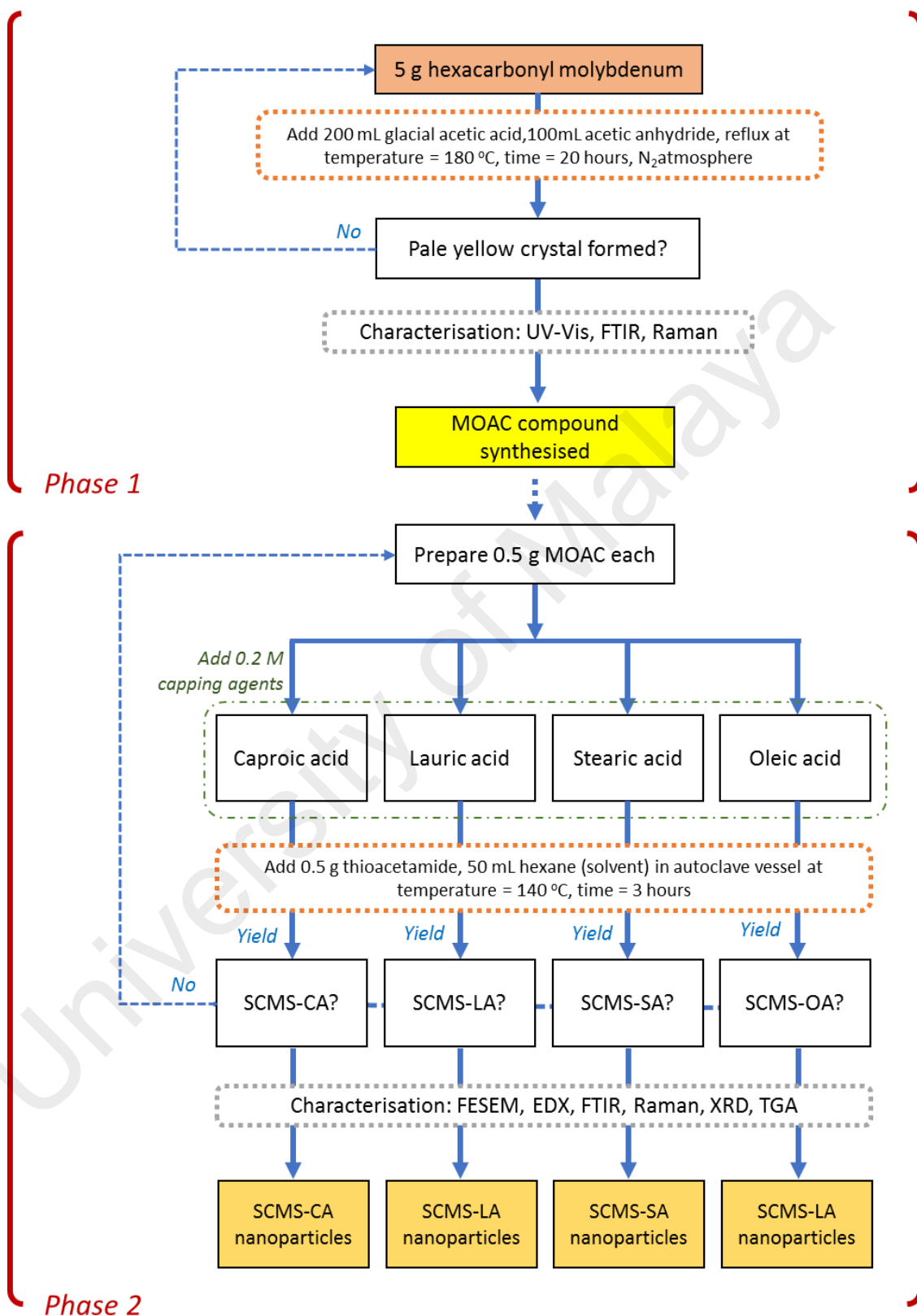


Figure 3.1: Flowchart of synthesising MOAC compound and SCMS nanoparticles in Phase 1 and Phase 2 respectively

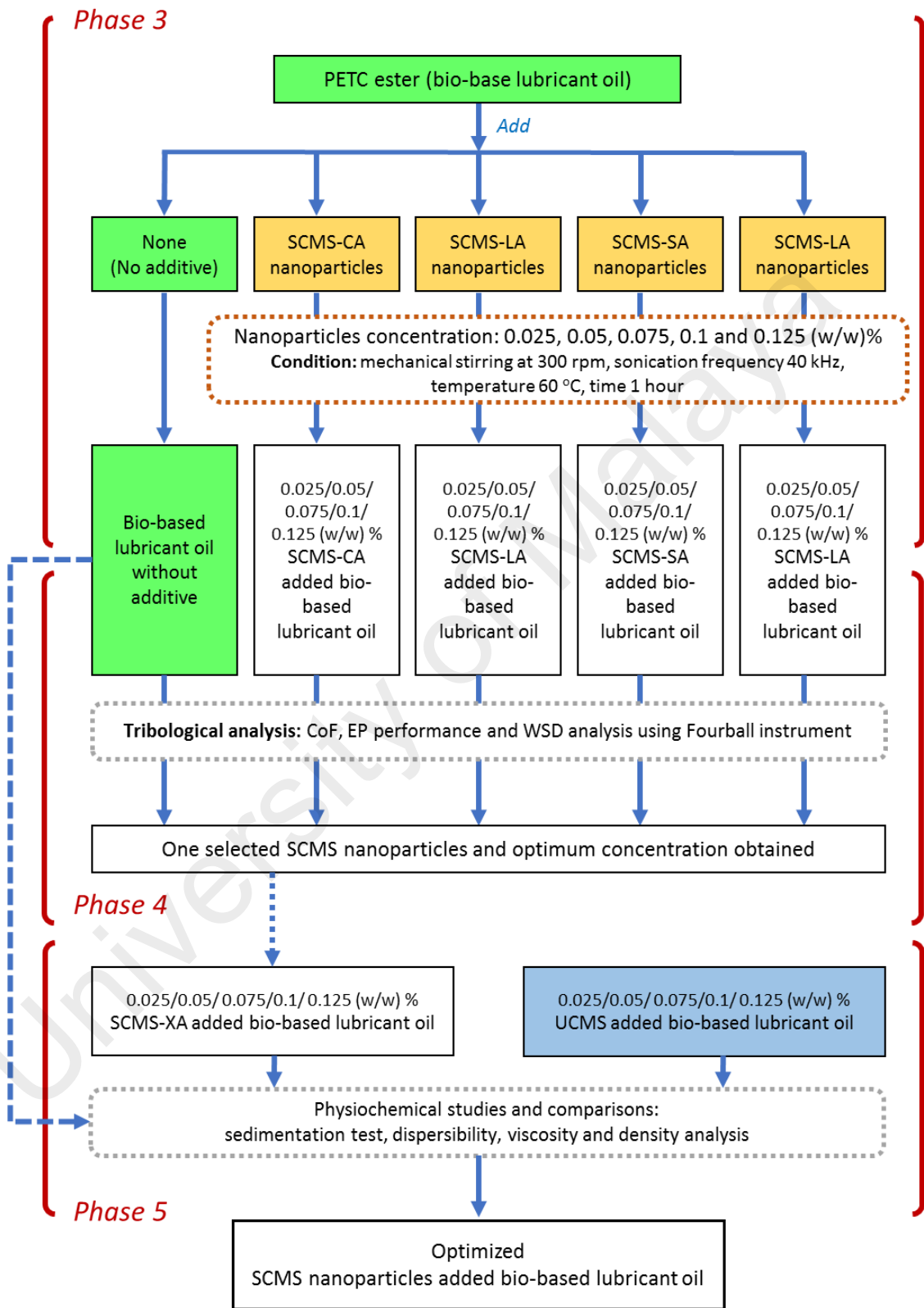


Figure 3.2: Flowchart of SCMS nanoparticles blending, tribological analysis and physiochemical study in Phase 3 to Phase 5

The SCMS nanoparticles were synthesised and blended into the bio-based lubricant oil at the NANOCAT Research Laboratory. The characterisations of products, such as FTIR, Raman, XRD, and TGA were carried out at NANOCAT Spectroscopic Hall, while FESEM and EDX analyses were conducted at the Physics Department of UM. The tribological and physiochemical analysis were carried out in the Tribological Laboratory of the Department of Mechanical Engineering of UM.

3.2 Materials and chemicals

The list of chemicals, solvents, and materials used are tabulated in Table 3.1.

Table 3.1: List of chemicals and material used throughout research study

Phase	Material	Functions	Supplier	Other information
1A	Hexacarbonyl molybdenum	MOAC precursor	Merck	Chemical formula: $\text{Mo}(\text{CO})_6$ Molar mass: 264 g/mol Purity: $\geq 99.0\%$ Appearance: White powder
	Acetic acid glacial		Merck	Chemical formula: CH_3COOH Molar mass: 60.05 g/mol Purity: $\geq 99.0\%$ Appearance: colourless liquid
	Acetic anhydride		Merck	Chemical formula: $(\text{CH}_3\text{CO})_2\text{O}$ Molar mass: 102.08 g/mol Purity: $\geq 98.5\%$ Appearance: colourless liquid
	Ethanol Absolute	Solvent	Merck	Chemical formula: $\text{C}_2\text{H}_5\text{OH}$ Molar mass: 46.07 g/mol Purity: $\geq 99.5\%$ Appearance: colourless liquid
1B	n-Hexane	Solvent	Merck	Chemical formula: $\text{CH}_3(\text{CH}_2)_4\text{CH}_3$ Molar mass: 86.18 g/mol Purity: $\geq 96.0\%$ Appearance: colourless liquid

Table 3.1, continued

Table 3.1, continued

Phase	Material	Functions	Supplier	Other information
1B	Caproic acid (Hexanoic acid)	Capping agent	Sigma-Aldrich	Chemical formula: $\text{CH}_3(\text{CH}_2)_4\text{COOH}$ Molar mass: 116.16 g/mol Purity: $\geq 99.0\%$ Appearance: Oily liquid
	Lauric acid (Dodecanoic acid)		Sigma-Aldrich	Chemical formula: $\text{CH}_3(\text{CH}_2)_{10}\text{COOH}$ Molar mass: 200.32 g/mol Purity: $\geq 98.0\%$ Appearance: White powder
	Stearic acid (Octadecanoic acid)		Sigma-Aldrich	Chemical formula: $\text{CH}_3(\text{CH}_2)_{16}\text{COOH}$ Molar mass: 284.48 g/mol Purity: $\geq 98.5\%$ Appearance: White solid
	Oleic acid (cis-9-Octadecenoic acid)		Sigma-Aldrich	Chemical formula: $\text{CH}_3(\text{CH}_2)_7\text{CH}=\text{CH}(\text{CH}_2)_7\text{COOH}$ Molar mass: 282.46 g/mol Purity: $\geq 99.0\%$ Appearance: viscous liquid
	MOAC	SCMS nanoparticles precursor	Freshly prepared in Phase 1A	Chemical formula: $\text{C}_8\text{H}_{12}\text{Mo}_2\text{O}_8$ Molar mass: 428.10 g/mol Appearance: yellow solid
	Thioacetamide		Merck	Chemical formula: CH_3CSNH_2 Molar mass: 75.13 g/mol Purity: $\geq 99.0\%$ Appearance: Colourless crystals
4	Steel ball for fourball test	Surface analysis	Taat Bestari	Brand: SKF Model: RB-12.7/G20 Weight: 0.0084 kg Diameter: 12.7 mm Material: Bearing steel
	Acetone	Solvent	Merck	Chemical formula: CH_3COCH_3 Molar mass: 58.08 g/mol Purity: $\geq 99.0\%$ Appearance: colourless liquid
5	UCMS nanoparticles	For comparison study	Self-prepared	Chemical formula: MoS_2 Molar mass: 160.07 g/mol Appearance: black powder

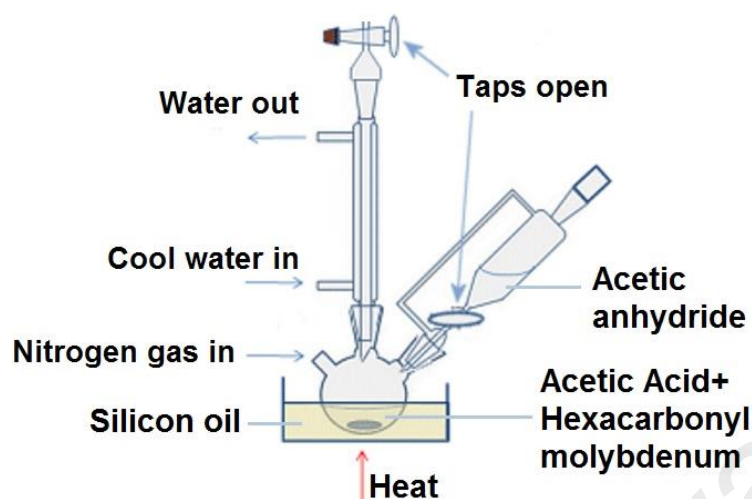
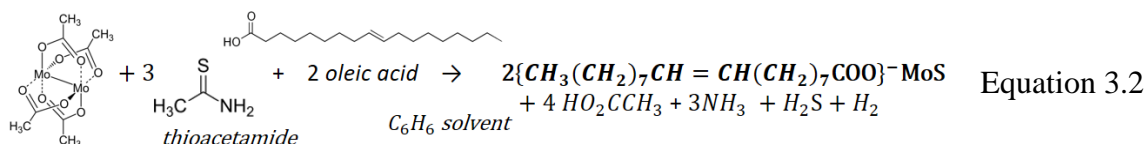


Figure 3.3: Reaction set up

3.3.2 Phase 1B: Synthesis of SCMS nanoparticles

The following chemicals were used in this experimental work: freshly synthesised MOAC, thioacetamide (CH_3CSNH_2), different types of alkyl substituent of fatty acid, which were caproic ($\text{C}_6\text{H}_{12}\text{O}_2$), lauric ($\text{C}_{12}\text{H}_{24}\text{O}_2$), oleic ($\text{C}_{18}\text{H}_{34}\text{O}_2$), stearic ($\text{C}_{18}\text{H}_{36}\text{O}_2$) acids, hexane (C_6H_{14}), and ethanol ($\text{C}_2\text{H}_6\text{O}$).

Mo-O complexes were prepared using the solvothermal reaction between MOAC and fatty acid in a hexane medium. 0.5 g of freshly prepared MOAC, 0.2 M caproic acid, and 0.5 g thioacetamide were dissolved in 50 mL n-hexane under sonication, then transferred into stainless steel autoclaves. The autoclave was closed and heated to 140 °C for 3 hours, and when done, it was left to cool to room temperature. The precipitate was centrifuged and washed several times with n-hexane, followed by ethanol. Finally, the fine dark product was dried in an oven at 50 °C for 3 hours. The same procedure was repeated, but the caproic acid was replaced with different fatty acids, such as lauric, stearic, and oleic acid. The chemical equation involved in synthesising SCMS-OA nanoparticles is described in Equation 3.2 below.



3.4 Phase 2: Characterisations

The characterisation technique used in Phase 1A were UV-Vis, FTIR, and Raman spectroscopy, while in Phase 1B, FESEM, EDX, Raman, FTIR, XRD, and TGA were used to study the surface-capped molybdenum sulphide nanoparticles.

3.4.1 Ultraviolet–Visible Spectroscopy (UV-Vis)

UV-Vis spectroscopy was used to determine the absorption/reflectance spectroscopy in the spectral region within the ultraviolet and visible light wavelengths. The working principle is based on the capability of molecules to absorb light when passing through a sample. In this study, UV-Vis spectra were obtained using UV/Vis Perkin Elmer Lambda 35 instrument. 0.5 g of SCMS nanoparticles were placed onto the sample holder, and the wavelength in which the spectrum was recorded was 350 - 700 nm.

3.4.2 Field Emission Scanning Electron Microscopy Analysis (FESEM)

FESEM is an analytical equipment that provide topological information at high magnification. The FESEM generate images of samples by scanning it using a focused electron beam. The electrons cooperate with atoms in the sample, generating discrete signals that contain information about surface topography and elemental composition. SCMS nanoparticles were scanned using JSM-7500F Jeol Microscope and operated at 5 kV. The samples were sprayed with platinum (Pt) prior to being loaded into sample holder. After that, Pt coated samples were anchored onto the sample holder using double-sided pressure equalising funnel carbon adhesive tapes to prevent the accumulation of

surface charge on the specimens when exposed to the electron beam. Scanning was performed under low vacuum and at a magnification range of 5,000 – 200,000 x.

3.4.3 Energy Dispersive X-Ray Spectroscopy (EDX)

A FESEM, equipped with an EDX can be used to determine elemental composition. The accumulation of energy count in the form of intensity creates a spectrum, where each peak represents each present element. The energy beam used for scanning is commonly around 10 - 20 keV. A higher intensity peak indicates a higher concentration of elements in the scanned area of the sample, which also allows us to obtain the weight and atomic percentages of specific elements in the scanned region.

3.4.4 Fourier Transform Infrared Spectroscopy (FTIR)

FTIR spectroscopic analysis reports qualitative and quantitative values for organic and inorganic samples. It is an effective tool for determining the functional group and characterising covalent bonds. The FTIR instrument used in this research was the Perkin-Elmer 100 spectrophotometer. The sample holder was cleaned using acetone. Around 0.5 mg of SCMS nanoparticles was mixed with 4 mg of potassium bromide (KBr) and subsequently pressed to form a pellet. The pellet was placed on the FTIR sample holder and bombarded with infrared (IR) radiation. The sample absorb some of the infrared radiation, while others passed through, and are detected as transmittance. The resolution of the FTIR was set to 4 cm^{-1} , with 15 scans in the wavelength of 400 cm^{-1} - 4000 cm^{-1} . The spectrum generated were obtained, and the peaks were assigned to distinct functional groups.

3.4.5 Raman Spectroscopy

Raman scattering is a spectroscopic method that complements infrared absorption spectroscopy. It is used to study the vibrational, rotational, and other low frequency transitions in the samples. The instrument used in this work was Renishaw in Via Reflex, with a high performing CCD camera and LEICA microscope. Around 0.05 g of SCMS nanoparticles sample was placed into the sample holder and the Raman spectroscopy. The 5 % of 150 mW laser power at a 30 s exposure time was selected as the parameter to analyse SCMS nanoparticles, as sample degradation might occur throughout this work. Then, the argon gas laser was set at 785 nm due to its 1200 nm^{-1} spectral resolution being sufficient to plot excellent spectra. The laser beam was focussed via $\times 100$ objective lens, which helped compile the scattered radiation. The laser spot on the sample was around 1.13 μm at 785 nm excitation.

3.4.6 X-ray Powder Diffraction Spectroscopy (XRD)

XRD technique is a rapid and non-destructive analysis mainly used for phase identification of a crystalline or amorphous material. It can also provide information on unit cell dimensions based on the diffraction patterns. The crystallinity of SCMS nanoparticles were determined using Bruker AXS D8 Advance XRD Diffractometer, equipped with Cu $K\alpha$ ($\lambda = 1.5406 \text{ \AA}$) and radiation source at 40 kV and 40 mA. It is able to provide information on the phase, structures, and preferred orientations, such as average grain size and material crystallinity. Prior to being placed in a 1 g sample-to-sample holder, the samples were finely grounded and closely packed in a sample holder. The test parameters were set to 0.02° , at a $0.02^\circ/\text{s}$ scanning rate between $5^\circ - 80^\circ$ diffraction angle (2θ).

3.4.7 Thermal Gravimetric Analysis (TGA)

TGA is a thermal analysis technique that monitor changes in the mass of a sample, either as a function of increasing temperature at constant rate, or isothermally as a function of time in surrounding gases of nitrogen, helium, air, other gases, or vacuum. In this research, the thermal stability of SCMS nanoparticles were examined through the degradation temperature of the capping agent and molybdenum sulphide nanoparticles. The samples were examined using TGA instrument (Mettler Toledo, TGA/SDTA-851) by inserting it into 100 μL open alumina crucible. The test temperature was set to an ambient temperature of ~ 900 $^{\circ}\text{C}$ and a heating rate of 10 $^{\circ}\text{C min}^{-1}$ under a nitrogen gas flow rate of ~ 50 mL min^{-1} . After the heating process is completed, it was then cooled to room temperature. This technique helped identify the stability of SCMS nanoparticles at various temperature range, which allows us to study the strength of the monolayer bounds surrounding the SCMS nanoparticles.

3.5 Phase 3: Formulation and blending of bio-based lubricant oil with SCMS nanoparticles

Formulated bio-based lubricant oil is made up of two components: the bio-base oil purchased directly without any modification, and the antiwear additives, which was the synthesised SCMS nanoparticles. The properties of the bio-base oil were determined, and the nanoparticles were mixed with bio-base oil at specific conditions.

3.5.1 Bio-base oil material

Pentaerythrityl tetracaprylate/tetracaprate (PETC) ester was used as a bio-base oil in this research, and its chemical structure is shown in Figure 3.4. It is a tetraester compound that can be prepared from pentaerythritol and a blend of caprylic and capric acids via the alcohol esterification method (Becker *et al.*, 2015).

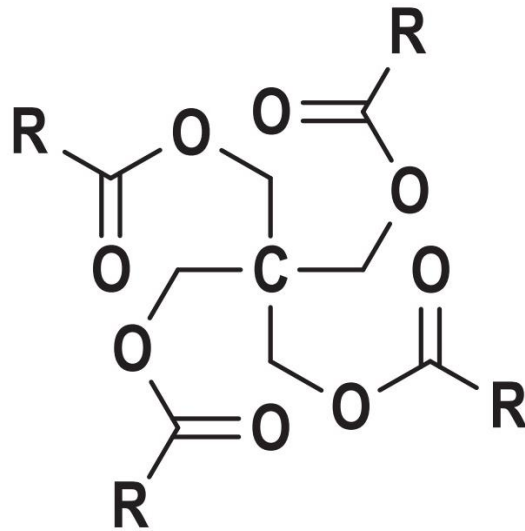


Figure 3.4: Chemical structure of PETC ester where R represent a mixture of 7 or 9 carbon alkyl chain (Becker et al., 2015)



Figure 3.5: PETC ester used as bio-base oil

3.5.2 Preparation of bio-based lubricant oil with SCMS nanoparticles

The antiwear additives (SCMS nanoparticles) and bio-base oil were combined based on weight percentage compositions, as shown in Table 3.2, and transferred into a blending flask. The mixture flask was immersed in the Thermo-6D ultrasonic bath. An RW20 IKA mechanical stirrer was used with two blade propellers, and was inserted into the mixture. The mixture was stirred at a rate of 300 rpm at 60 °C under 40 kHz ultrasonic frequency for an hour to confirm the complete mixing and dispersion of both components. The schematic diagram of the blending process is shown in Figure 3.6.

Table 3.2: Composition of bio-based lubricant in this research

No	Lubricant sample	Composition (w/w) %				
		Bio-base oil	SCMS-CA	SCMS-LA	SCMS-SA	SCMS-OA
1	No Additive	100	-	-	-	-
2	SCMS-CA 0.025	99.975	0.025	-	-	-
3	SCMS-CA 0.05	99.95	0.05	-	-	-
4	SCMS-CA 0.075	99.925	0.075	-	-	-
5	SCMS-CA 0.1	99.9	0.1	-	-	-
6	SCMS-CA 0.125	99.875	0.125	-	-	-
7	SCMS-LA 0.025	99.975	-	0.025	-	-
8	SCMS-LA 0.05	99.95	-	0.05	-	-
9	SCMS-LA 0.075	99.925	-	0.075	-	-
10	SCMS-LA 0.1	99.9	-	0.1	-	-
11	SCMS-LA 0.125	99.875	-	0.125	-	-
12	SCMS-SA 0.025	99.975	-	-	0.025	-
13	SCMS-SA 0.05	99.95	-	-	0.05	-
14	SCMS-SA 0.075	99.925	-	-	0.075	-
15	SCMS-SA 0.1	99.9	-	-	0.1	-
16	SCMS-SA 0.125	99.875	-	-	0.125	-
17	SCMS-OA 0.025	99.975	-	-	-	0.025
18	SCMS-OA 0.05	99.95	-	-	-	0.05
19	SCMS-OA 0.075	99.925	-	-	-	0.075
20	SCMS-OA 0.1	99.9	-	-	-	0.1
21	SCMS-OA 0.125	99.875	-	-	-	0.125

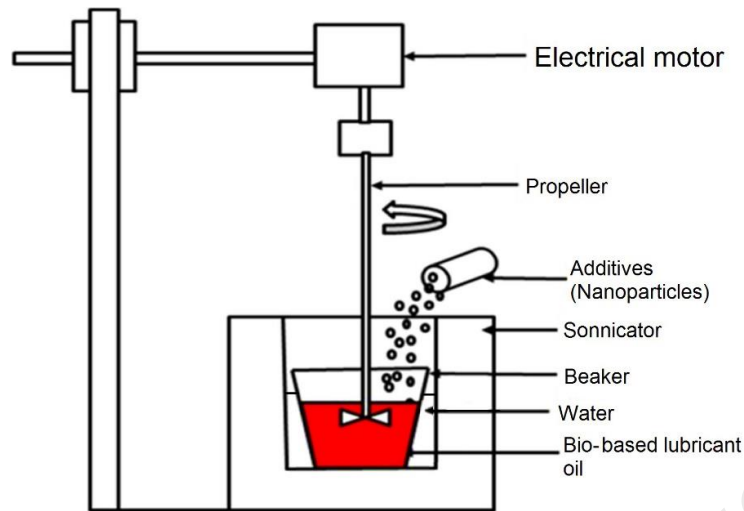


Figure 3.6: Additive and base oil blending process

3.6 Phase 4: Tribological Analysis

The four-ball tester were used to determine the tribological behaviour of the formulated bio-based lubricant oil with the SCMS nanoparticles. The main measurement of four-ball tester was to determine the wear preventive properties, extreme pressure properties, and the friction behaviour of lubricant oil. The four-ball friction and wear tester were made up of three stationary balls in a pot, with the fourth rotating ball sticking to the spindle. The spinning ball was steadily pressed against three stationary balls held together and drenched in lubricant oil, as shown in Figure 3.7. The schematics of the four-ball test is shown in Figure 3.8.



Figure 3.7: Four-ball arrangement

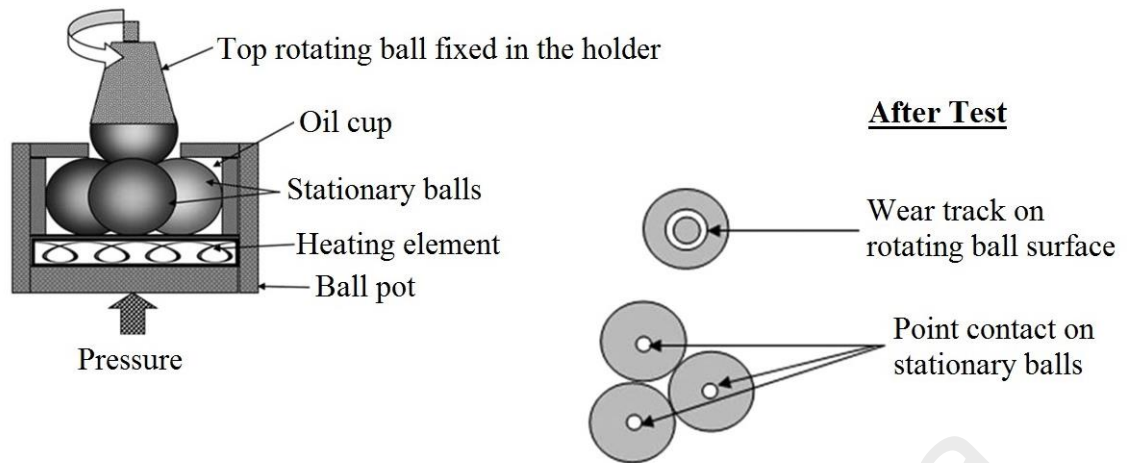


Figure 3.8: Four-ball schematic diagram (left) and point contact after test (right) (Gupta & Harsha, 2016)

This experiment used the Ducom Four-ball Instrument, while the balls were AISI 52-100 steel balls with a diameter of 12.7 mm and 64-66 Rc hardness. Test parameters such as applied load, temperature, test duration, and rotating speed can be set in accordance to the standard test method. The tribological study were divided into three sections, namely friction reduction analysis at ambient load, extreme pressure properties analysis, and wear reduction analysis.

3.6.1 Friction Reduction Analysis

The friction reduction analysis of the formulated bio-based lubricant oil was assessed using CoF, where it is a dimensionless number that define the ratio between friction force that is present between two contacting surface and the normal force simultaneously squeezing them. CoF is vital in demonstrating the transmission efficiency in a lubricating system, where higher efficiency is the results of lower friction and CoF. In the four-ball instrument, the exerted frictional force was controlled and recorded in real-time by the shaft torque. Using the IP-239 standards, the CoF obtained in this experiment can be calculated using Equation 3.3.

$$\mu = \frac{T\sqrt{6}}{3Wr} \quad \text{Equation 3.3}$$

where μ is the CoF, T is the frictional torque (Nm), W is load (N), and r is the contact surface distance from the centre on the bottom balls to the rotation axis, which was determined to be 3.67 mm. This strategy was also used by other researchers (Husnawan *et al.*, 2007) and (Zulkifli *et al.*, 2014).

Before starting the four-ball test, the balls were thoroughly cleaned with acetone. Approximately 10 mL of formulated bio-based lubricant oil are required for each test. The test condition used to obtain the tribological characteristics are tabulated in Table 3.3. The CoF values of the bio-based lubricant oil was calculated, and the type and concentration of nanoparticles that resulted in the best friction improvement was further tested for extreme pressure properties analysis.

Table 3.3: Friction test parameters at normal load

Parameter	Load, N	Temperature	Speed, rpm	Test duration, s
Condition	400	Room Temperature	1200	3600

3.6.2 Extreme Pressure Analysis

Extreme Pressure Analysis was conducted to determine wear preventive characteristics of the formulated bio-based lubricant at different loads. The standard used for this test is the ASTM D2783 using the aforementioned four-ball instrument. In the instrument, a vertical driving spindle rotates a chuck at a speed of 1,770 rpm and the load is elevated 200 N every 10 s until the spinning ball was completely welded to all three stationary balls. The complete test condition for extreme pressure test were shown in Table 3.4. One specific formulated bio-based lubricant oil (the type and concentration of nanoparticles) that exhibited the best friction improvement were used for this test.

Table 3.4: Extreme Pressure test parameters at different load

Parameter	Test	Load, N	Temperature	Speed, rpm	Test duration, s
Condition	1	400	Room Temperature	1770	10
	2	800			
	3	1000			
	4	1200			
	5	1400			
	6	1600			
	7	1800			

3.6.3 Wear Scar Analysis

Wear scar analysis was conducted to show the corresponding wear preventive properties of the formulated bio-based lubricant oil in sliding contact under specific test condition. This analysis is divided into two parts: 1) the average WSD formed on the stationary steel balls in **Section 3.6.1.** under normal conditions, and 2) under EP conditions in **Section 3.6.2.** At the end of four-ball friction test, the stationary ball bearings were collected and washed with acetone, then dried in an oven for an hour at 70 °C. The wear scar on the three stationary ball bearings surface were analysed using SEM spectroscopy (normal condition) and optical microscope (EP condition). The metallograph were analysed and expressed as wear scar diameter (WSD).

SEM works in a manner similar to the FESEM, where it provides the topographical and elemental information at various magnifications. Even though SEM produce lower resolution compared to FESEM, it is much easier to operate, and is able to provide images at magnifications of 10 – 100, 000 x to analyse the surface roughness of the wear scar. The ball bearing samples are mounted onto a sample holder using a double sided electrically conducting carbon adhesive tape to prevent the accumulation of surface charge on the ball when exposed to the electron beam.

3.7 Phase 5: Physiochemical measurement of optimized bio-based lubricant oil with SCMS nanoparticles

The crucial properties of formulated bio-based lubricant oil with SCMS nanoparticles were analysed using several analytical techniques, such as sedimentation test, optical microscopic study, viscosity, and density analysis. In this phase, the optimised bio-based lubricant oil with SCMS nanoparticles from the previous phase was subjected to physiochemical measurement and compared to the UCMS nanoparticles. The UCMS nanoparticles were previously prepared using similar methods for synthesising SCMS nanoparticles, with the exception of the addition of a capping agent.

3.7.1 Sedimentation Test

Sedimentation test is a suitable testing method to evaluate the dispersion stability of nanoparticles via observation. The sedimentation of SCMS nanoparticles were determined alongside the best suppression of friction for concentrations ranging from 0.025 - 0.125 (w/w) %. Each bio-base lubricant oil was collected at the same volume and transferred into a 25 mL sample vial at room temperature in the absence of any distractions (Zahid, 2016). Each sample were constantly observed up till the point the nanoparticles are sedimented at the bottom of the flask and from separate phase from the oil. Sample of bio-based lubricant oil without additive, bio-based lubricant oil with SCMS nanoparticles, and UCMS nanoparticles were also prepared so that they can all be compared to one another.

3.7.2 Optical Microscopic Study

The optical microscopy measurement was used to evaluate the rapid aggregation of inorganic materials from single nanoparticles all the way to micrometer-sized aggregates at different loadings percentages. The dispersion and aggregation of SCMS nanoparticles were detected in situ using Nikon Eclipse TE300 instrument. A drop of each formulated bio-based lubricant oil was dropped onto the glass slide and left at room temperature overnight. Then, the glass slide was placed on a sample holder of a microscope, and images of the SCMS and UCMS nanoparticles dispersion and agglomeration were recorded at 10 x magnification.

3.7.3 Viscosity and Density Analysis

Viscosity and density are key parameters for determining the physical behaviour of lubricant oils. The experiments were conducted on SVM 3000 Stabinger Anton Paar Viscometer Instrument simultaneously. We determined the viscosity and density of fluid according to the Standard Test Method for Dynamic Viscosity and Density of Liquids by Stabinger Viscometer (ASTM D7042,2012). Using ASTM D2270, the viscosity index (VI) was determined using the kinematic viscosities at 40 °C and 100 °C. Around 3 mL of formulated bio-based lubricant oil sample were used for this test. The reproducibility and repeatability for this instrument were 0.35 % and 0.1 %, respectively.

CHAPTER 4: RESULTS AND DISCUSSION

4.1 Introduction

This chapter reports the experimental results obtained from the tests and analyses. It is divided into four main sections. The first discuss the formation of MOAC and characterisation analyses of the product. The second will illustrate the production and characterisation of SCMS nanoparticles using the solvothermal method. The structure and properties of SCMS nanoparticles will be discussed based on characterisation results. The third will discuss the tribological performance of SCMS nanoparticles and pinpoint which of them show the best wear reduction and reduction of friction. The influence of the load applied on EP performance of selected SCMS nanoparticles will be illustrated as well. The fourth will present the physiochemical study and colloidal stability of the formulated bio-based lubricant oil loaded with the SCMS nanoparticles.

4.2 Study of molybdenum (II) acetate

Bright yellow solid MOAC was successfully formed at the end of Phase 1A. Some of it includes very fine needle-like crystal. It was characterised using UV-Vis, FTIR, and Raman analysis.

4.2.1 UV-Vis Spectroscopy

UV-Vis spectra in Figure 4.1 shows the comparison between the product and its precursor, where (a) hexacarbonylmolybdenum, and (b) MOAC. A broad peak is observed at wavelength 370 - 500 nm, with a maximum peak at 398 nm for hexacarbonylmolybdenum (0) UV-Vis spectrum, which disappear in the product spectrum, indicating an increase in the oxidation state of the metal centre from 2Mo^0 to $\text{Mo}^{\text{II}}\text{Mo}^{\text{II}}$ (Feinstein-Jaffe & Maisuls, 1987).

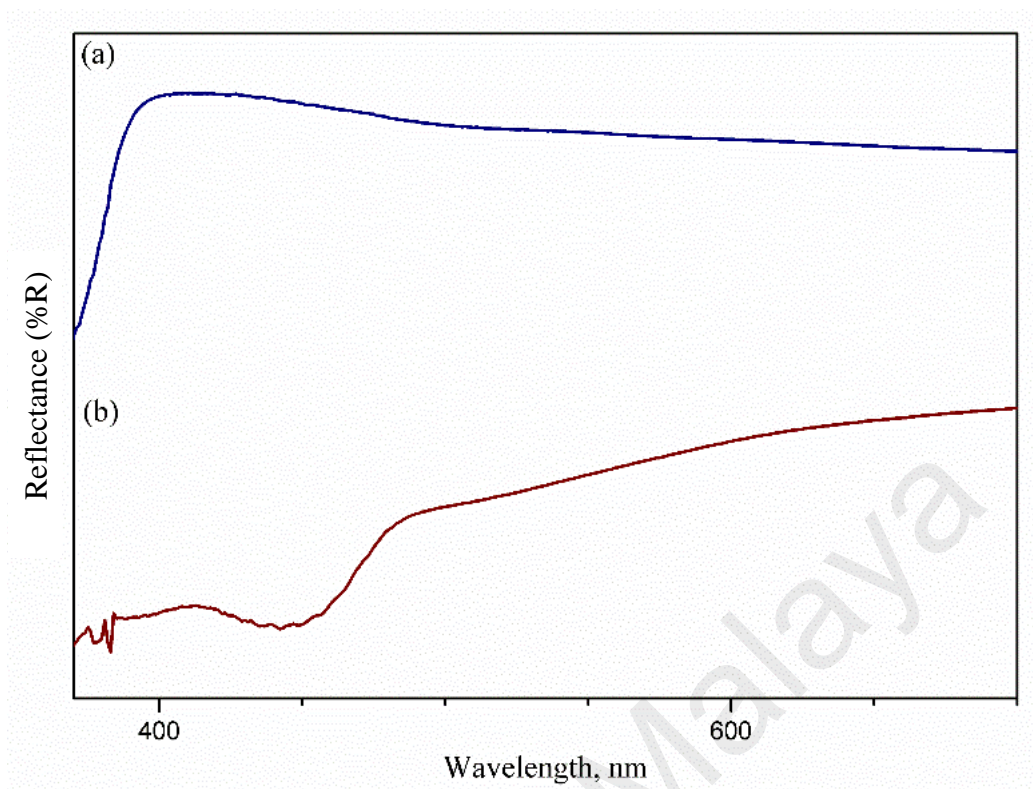


Figure 4.1: UV-Vis Spectra of (a) hexacarbonylmolybdenum precursor and (b) MOAC compound

4.2.2 FTIR Spectroscopy

Figure 4.2 shows the FTIR spectrum for a functional group of molybdenum (II) acetate. It shows a broad band around 3448 cm^{-1} at the high frequency area, which indicate the stretching and bending vibration of the O-H group of water molecules adsorbed on the compound. Large amounts of adsorbed water in MOAC takes place due to the high surface energy of the particles (Stephenson *et al.*, 1964). The characteristic stretching vibration of C=O in acetate can be found in the strong sharp band at 1640 cm^{-1} . The strong band at the absorption frequency region of 1109 cm^{-1} imply that there is stretching vibration of C-O, whereas at 1437 cm^{-1} , it can be assigned to C-H bending in acetate. The chemical structure of MOAC are shown in Figure 4.3.

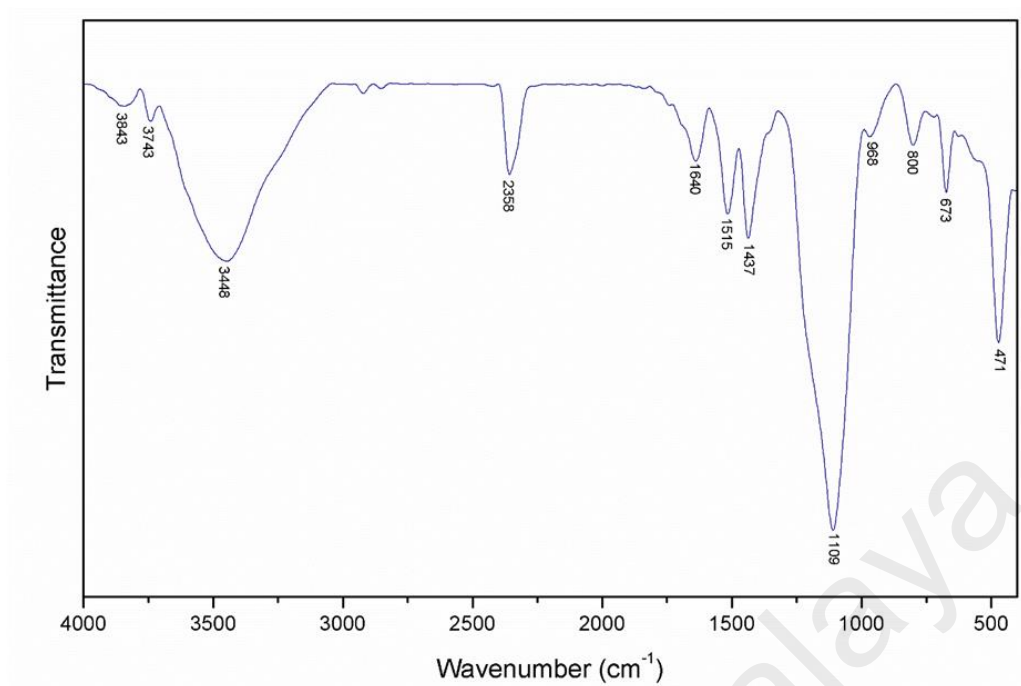


Figure 4.2: FTIR Spectrum of MOAC compound

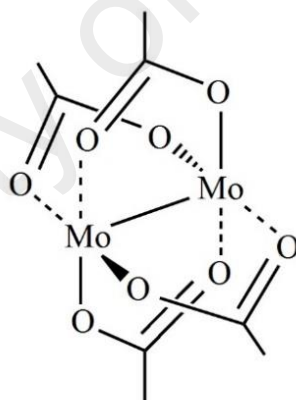


Figure 4.3: Chemical structure of MOAC (Lawton & Mason, 1965)

4.2.3 Raman Spectroscopy

Based on the Raman spectrum shown in Figure 4.4, the strong Raman band focused at 404 cm⁻¹ can be unconditionally assigned to the stretching frequencies of the quadrupole bond between the Mo atoms. The strong band at 1431 cm⁻¹ at 1347 cm⁻¹ indicate the CH₃ asymmetric deformation located at the acetate ligand surrounding the Mo atom. The highest sharp band centred at 691 cm⁻¹ can be said to be the angular deformation of

O-C-O bond. Furthermore, the band at 946 cm^{-1} can prove the presence of a O-O bond vibration. Medium bands at 298 cm^{-1} at 321 cm^{-1} exhibit C-C bond deformation. The weak band at Raman shift 2941 cm^{-1} can be assigned as the vibration mode of C-H bond present in the compound. The Raman signature of this study and literature confirms the formation of an MOAC compound (Bratton *et al.*, 1971).

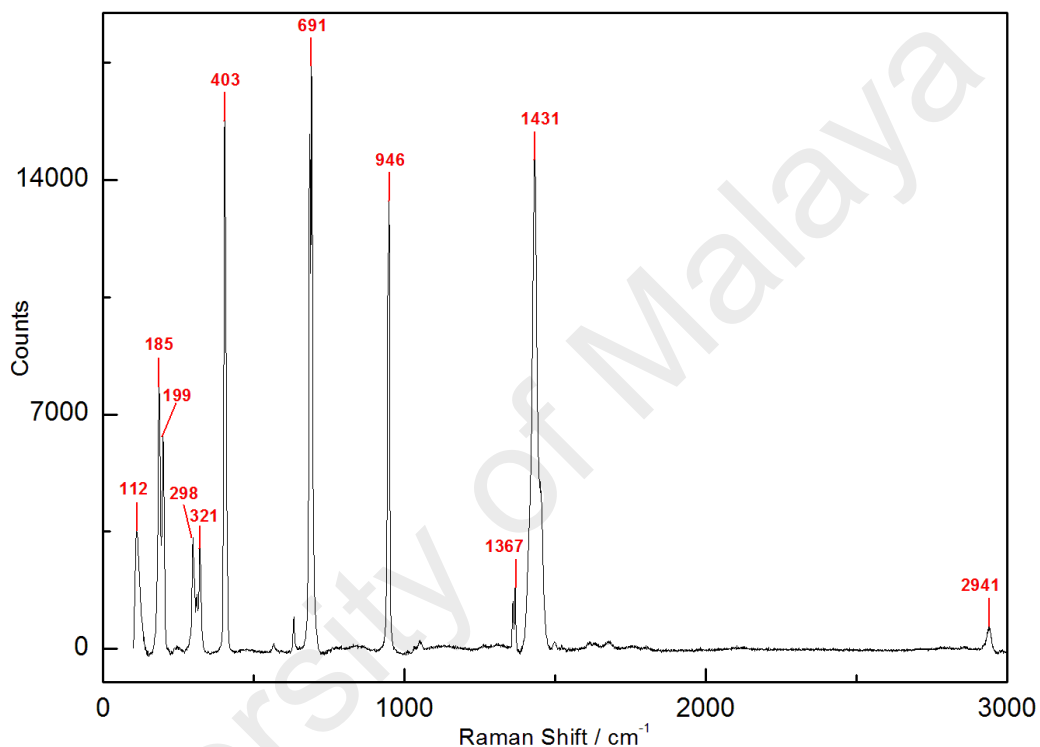


Figure 4.4: Raman spectrum of MOAC

4.3 Study of surface capped molybdenum sulphide nanoparticles

The structural, morphological, chemical, and thermal properties of the SCMSs nanoparticles were further analysed using several characterisation techniques, such as FTIR, Raman, XRD, FESEM, EDX, and TGA analysis.

4.3.1 FESEM Microscopy

The nanoparticles observed in the micrograph of Figure 4.5 are almost spherical and well dispersed. Layers of capping agent encircling the nanoparticles are also present, and the outline of the SCMS nanoparticles is fuzzy because the particles' surfaces are coated with a fatty acid modifier. A typical FESEM micrograph for pristine MoS₂ from literature (Zhao *et al.*, 2015) shows that the MoS₂ nanoparticles appear rose-like in shape and congregate with many ultrathin sheets-like MoS₂ nanoparticles. Therefore, it is assumed that the capping layers are effectively preventing agglomeration and growth of molybdenum sulphide, leading to the formation of nanoparticles. The average particle size proved that the SCMS-SA is the smallest, at 37 nm, while others are within 62 - 84 nm, as shown in Table 4.1.

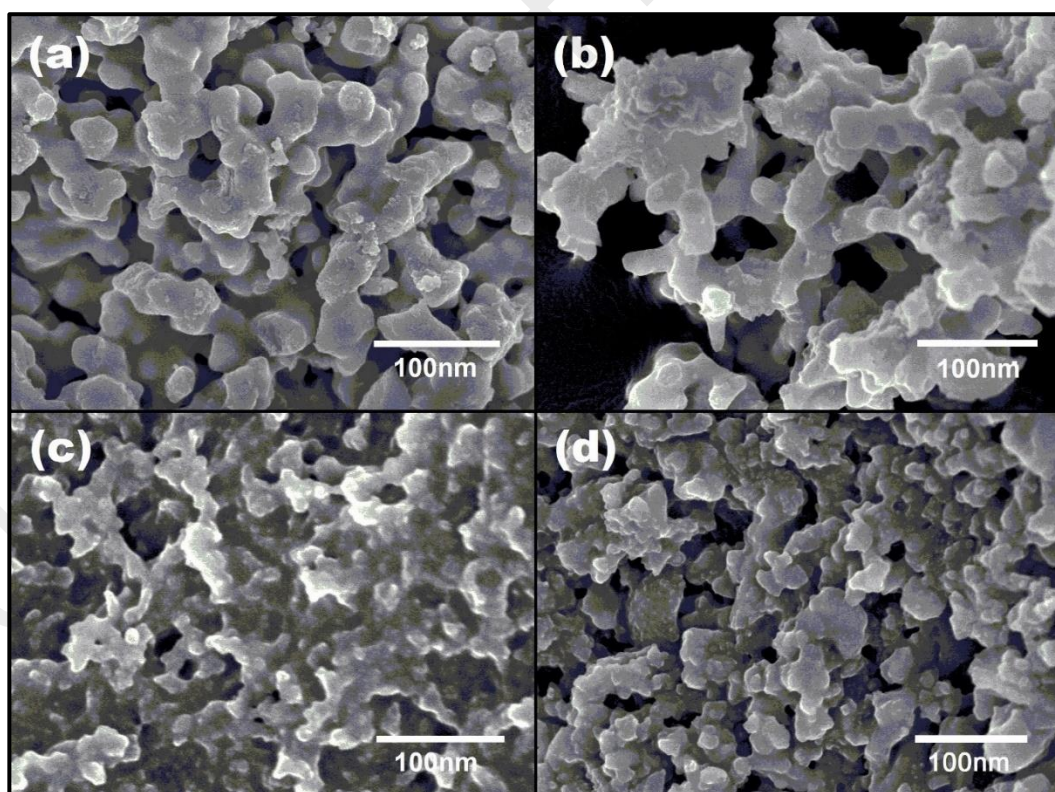


Figure 4.5: FESEM images of (a) SCMS-CA, (b) SCMS-LA, (c) SCMS-SA and (d) SCMS-OA nanoparticles

Table 4.1: Average particles size of SCMS nanoparticles

Micrograph	Nanoparticles	Average size, nm	Standard deviation, nm
a	SCMS-CA	84	17.19
b	SCMS-LA	64	5.12
d	SCMS-SA	37	2.60
e	SCMS-OA	62	2.5

4.3.2 EDX Spectroscopy

EDX spectroscopy is used to confirm the formation of SCMS nanoparticles. Each relevant peak from EDX mapping indicates the elements present in the SCMS nanoparticles, while the functionality of fatty acid on the surface of the SCMS nanoparticles were confirmed by the strong peak at 0.3 keV and 0.5 keV, corresponding to carbon (C) and oxygen (O), respectively, as shown in Figure 4.6. The detected elements include molybdenum (Mo) and sulphur (S), which comes from molybdenum sulphide core nanoparticles, while C and O originated from the capping agent. Quantitative EDX analysis tabulated in Table 4.2 further confirms the formation of a fatty acid layer surrounding molybdenum sulphide nanoparticles in terms of weight and atomic percentages.

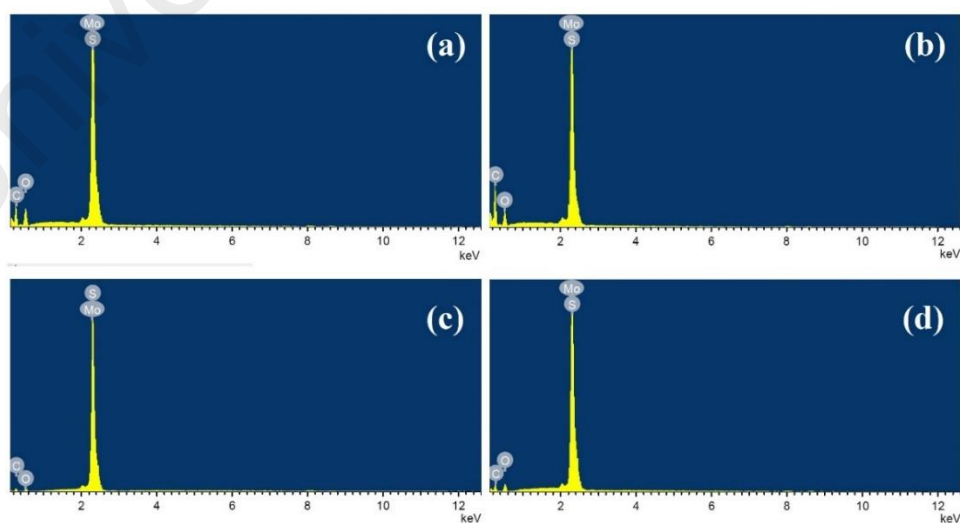


Figure 4.6: EDX mapping of (a) SCMS-CA, (b) SCMS-LA, (c) SCMS-SA and (d) SCMS-OA nanoparticles

Table 4.2: Elemental composition of SCMS nanoparticles

Composition	Sample	Mo	S	C	O	Mo/S ratio
Weight %	SCMS-CA	4.43	1.22	10.42	2.51	3.6
	SCMS-LA	11.48	3.02	34.00	14.68	3.8
	SCMS-SA	7.09	2.80	40.24	7.53	2.5
	SCMS-OA	8.67	3.78	38.48	7.15	2.3
Atomic %	SCMS-CA	4.16	3.42	78.26	14.16	1.2
	SCMS-LA	3.03	2.37	71.44	23.16	1.3
	SCMS-SA	1.86	2.19	84.13	11.82	0.8
	SCMS-OA	2.34	3.06	83.02	11.58	0.8

The chemical formula and percentage composition of the capping agent in SCMS nanoparticles are listed in Table 4.3. Chemical analysis shows that the sulphur content for SCMS-CA, SCMS-SA, and SCMS-OA nanoparticles correspond to MoS₂, while only SCMS-LA nanoparticles are correlated with MoS₃. Furthermore, SCMS-LA nanoparticles appear to have the highest atomic percentage of capping agent compared with other SCMS nanoparticles, followed by SCMS-CA, SCMS-OA, and SCMS-SA nanoparticles.

Table 4.3: Chemical composition and composition of capping agent present in SCMS nanoparticles

Nanoparticles	Composition, MoS _y C _z	Composition capping agent (%)
SCMS-CA	MoS _{1.97} C _{8.46}	78.41
SCMS-LA	MoS _{3.02} C _{19.60}	84.80
SCMS-SA	MoS _{2.09} C _{2.52}	47.19
SCMS-OA	MoS _{1.51} C _{3.47}	63.90

4.3.3 FTIR Spectroscopy

In the current study, FTIR analysis was conducted to study the adsorption of the capping agents on the surface of the SCMS nanoparticles. The resemblances between FTIR spectra were shown in Figure 4.7, where (b) SCMS-LA nanoparticles were being compared with (a) MoS₂, which is the non-capped nanoparticles, and (c) lauric acid. The lauric acid in spectrum (c) display two vibration bands, respectively, at 2918 cm⁻¹ and 2851 cm⁻¹, indicating asymmetric and symmetric stretching of CH₂. Additionally, identical bands at similar wavenumbers (2920 and 2853 cm⁻¹) are also present in SCMS-LA nanoparticles in spectrum (b). Moreover, the band at ~680cm⁻¹ can be identified as the rocking vibration of CH₂, which usually appear in compounds with long alkyl chain -(CH₂)_n- of n greater than three. This band also appear in spectrum (b) at 671 cm⁻¹, confirming the presence of fatty acid in modified nanoparticles. The band at 1698 cm⁻¹ in lauric acid spectrum indicates stretching of the C=O bond, while the band at 1298 cm⁻¹ indicate C-O bond stretching. However, this band did not appear in spectrum (b), suggesting that there are no free lauric acid present in the SCMS-LA nanoparticles. Bands at 1427 cm⁻¹ and 940 cm⁻¹ were present due to the in-plane and out-plane bending of O-H. Nonetheless, FTIR spectrum for SCMS-LA nanoparticles in (b) shows the presence of two new bands at 1530 and 1404 cm⁻¹ as being assigned to the stretching of $\nu_{\text{asymmetric}}$ (COO⁻) and $\nu_{\text{symmetric}}$ (COO⁻) properties, respectively. Its appearance prove that the fatty acid is chemisorbed in the form of carboxylate onto the surface of molybdenum sulphide nanoparticles (Limaye *et al.*, 2009) instead of physical adsorption (S. Chen & Liu, 2006).

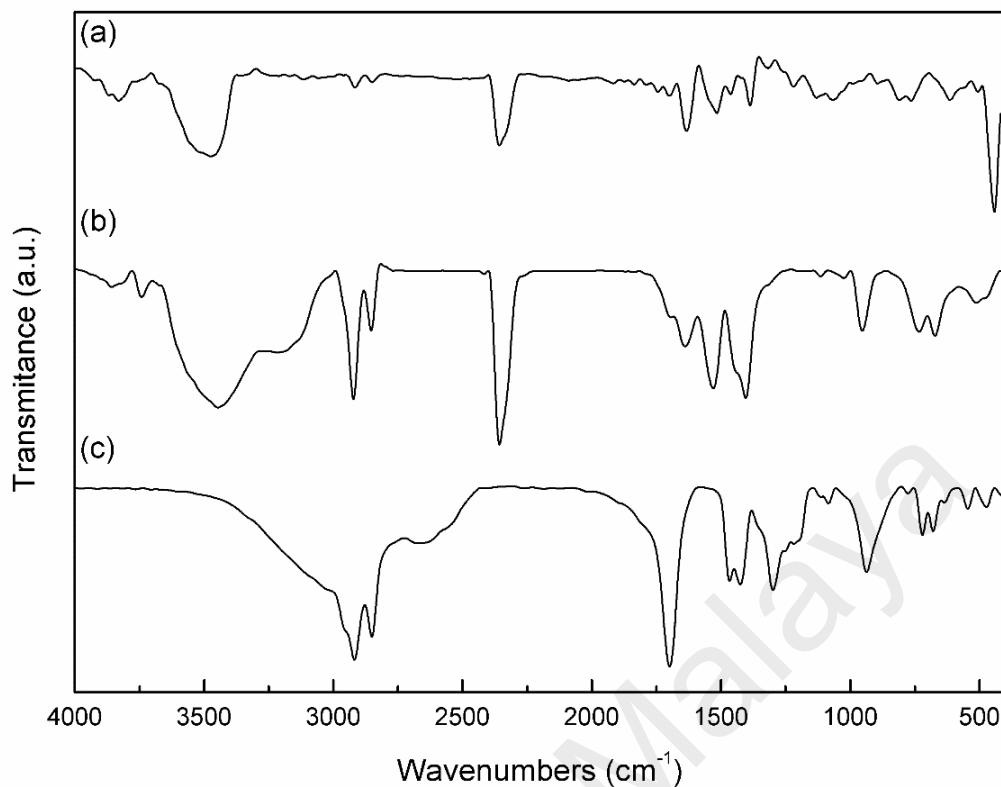


Figure 4.7: FTIR Spectra comparison of (a) MoS₂ nanoparticles (b) SCMS-LA nanoparticles, and (c) lauric acid

A similar interpretation approach was repeated for Figure 4.8, where the FTIR spectra of surface modified molybdenum sulphide nanoparticles with various fatty acid were compared, namely (a) SCMS-CA (b) SCMS-LA (c) SCMS-SA, and (d) SCMS-OA nanoparticles. The assignment of these FTIR peaks can be summarised in the manner shown in Table 4.4. We can assume that the molybdenum sulphide nanoparticles were successfully capped using fatty acid based on the appearance of fatty acid bands in the modified nanoparticles spectra. However, in Figure 4.8 (c) and (d), it can be seen that the appearance of bands at around 2300 cm⁻¹ can barely be seen compared to its (a-c) counterpart. It is suggested that the thick layers of capping layer of stearic and oleic acid cause hindrance to the vibration of the core nanoparticles as both have long 18-carbon alkyl chain length.

Table 4.4: FTIR band comparison between various types of SCMS nanoparticles

Spectrum	Nanoparticles	Wavelength (cm^{-1})	Assignment
a	SCMS-CA	2949.80, 2859.19	CH ₂ asymmetric and symmetric stretching
b	SCMS-LA	2922.30, 2853.38	
c	SCMS-SA	2918.19, 2850.03	
d	SCMS-OA	2928.52	
a	SCMS-CA	1533.70, 1402.65	$\nu_{\text{asymmetric}}$ (COO ⁻) and $\nu_{\text{symmetric}}$ (COO ⁻) stretching of fatty acid on MoS nanoparticles
b	SCMS-LA	1530.08, 1404.37	
b	SCMS-SA	1503.30, 1412.45	
d	SCMS-OA	1519.34, 1435.74	
a	SCMS-CA	669.26	rocking vibration of CH ₂ in alkyl chain of fatty acid
b	SCMS-LA	671.62	
c	SCMS-SA	666.74	
d	SCMS-OA	673.93	

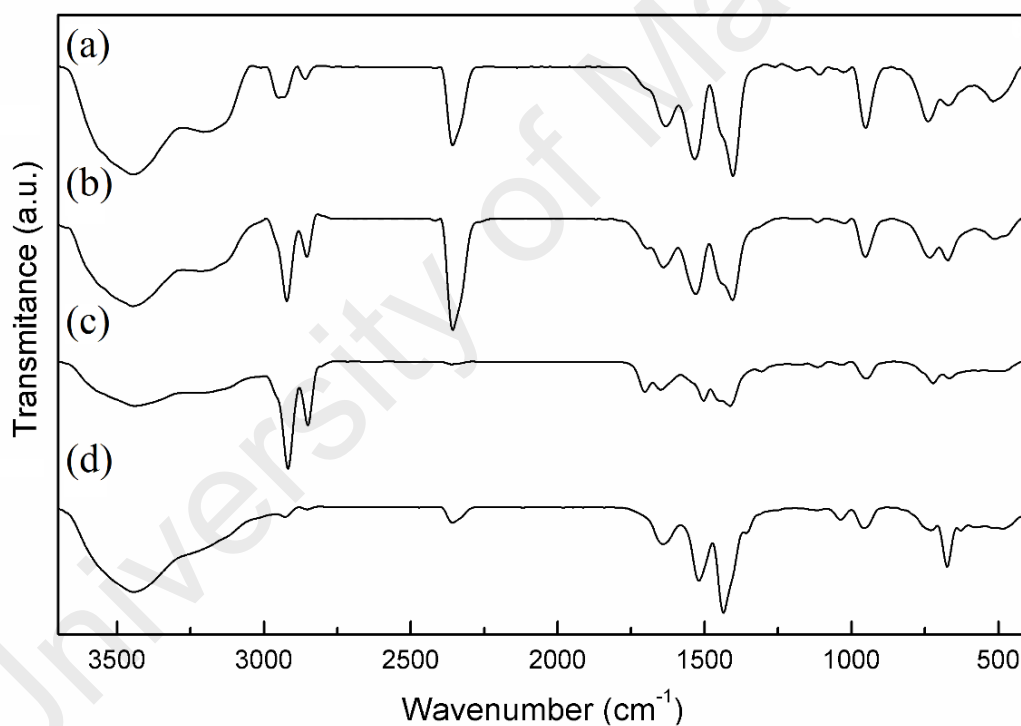


Figure 4.8: FTIR Spectra of surface capped molybdenum sulphides nanoparticles where (a) SCMS-CA, (b) SCMS-LA, (c) SCMS-SA and (d) SCMS-OA nanoparticles

4.3.4 Raman Spectroscopy

The presence of the carboxyl functional group of fatty acids at the surface of molybdenum sulphide nanoparticles determined from Raman spectroscopy are in excellent agreement with the results reported by the FTIR analysis. In this study, Raman data were obtained from 100 - 1800 cm^{-1} . The main characteristics of Raman bands of each nanoparticle are shown in Table 4.5. Each band were interpreted in accordance to (Otero *et al.*, 2014). The main focus of this analysis is that the Raman characteristic bands between 900 - 1800 cm^{-1} , where the Raman shift between 948 - 993 cm^{-1} are linked to the C-C stretching vibrations between alkyl chain for fatty acid, as per Figure 4.9 (b-e). Furthermore, the presence of the symmetric vibration of carboxylate salt (COO^-) is evident in all SCMS nanoparticles at a Raman shift of $\sim 1400 \text{ cm}^{-1}$. However, the different carbon chain length in the SCMS nanoparticles around this region makes it almost undetectable due to the weak intensity of this band. Contrarily, there is a lack of any Raman band within this region in the MoS_2 nanoparticles, as shown in Figure 4.9 (a), which proves that the region beyond 900 cm^{-1} represents fatty acid. Raman data for any motion in molybdenum sulphide were obtained from 100 - 9 cm^{-1} . Comparing the Raman spectra of MoS_2 and SCMSs nanoparticles, it is possible to see multiple bands between 280 - 334 cm^{-1} and 337 - 407 cm^{-1} , which may be assigned to the motion between Mo-S atoms and S-S atoms, respectively (Zabinski & McDevitt, 1996).

Table 4.5: Characteristics Raman bands assignment

Spectrum	Nanoparticles	Raman Shift (cm ⁻¹)	Intensity	Assignment
a	MoS ₂	N/A	N/A	ν _{symmetric} (COO ⁻) of carboxylate salt
b	SCMS-CA	1404	<i>m</i>	
c	SCMS-LA	1432	<i>s</i>	
d	SCMS-SA	1430	<i>m</i>	
e	SCMS-OA	1432	<i>s</i>	
a	MoS ₂	N/A	N/A	ρ(CH ₂) in long alkyl chain of fatty acid
b	SCMS-CA	993	<i>s</i>	
b	SCMS-LA	948	<i>s</i>	
d	SCMS-SA	949	<i>m</i>	
e	SCMS-OA	947	<i>s</i>	
a	MoS ₂	377	<i>m</i>	Motion of the Mo & S atoms
b	SCMS-CA	382	<i>m</i>	
b	SCMS-LA	407	<i>s</i>	
d	SCMS-SA	404	<i>s</i>	
e	SCMS-OA	402	<i>s</i>	
a	MoS ₂	282, 334	<i>s, m</i>	S-S atoms interaction
b	SCMS-CA	280, 334,	<i>s, s</i>	
c	SCMS-LA	292, 322	<i>m, w</i>	
d	SCMS-SA	297	<i>w</i>	
e	SCMS-OA	296, 319	<i>m, w</i>	

s = strong, m = intermediate and w = weak, N/A = not applicable

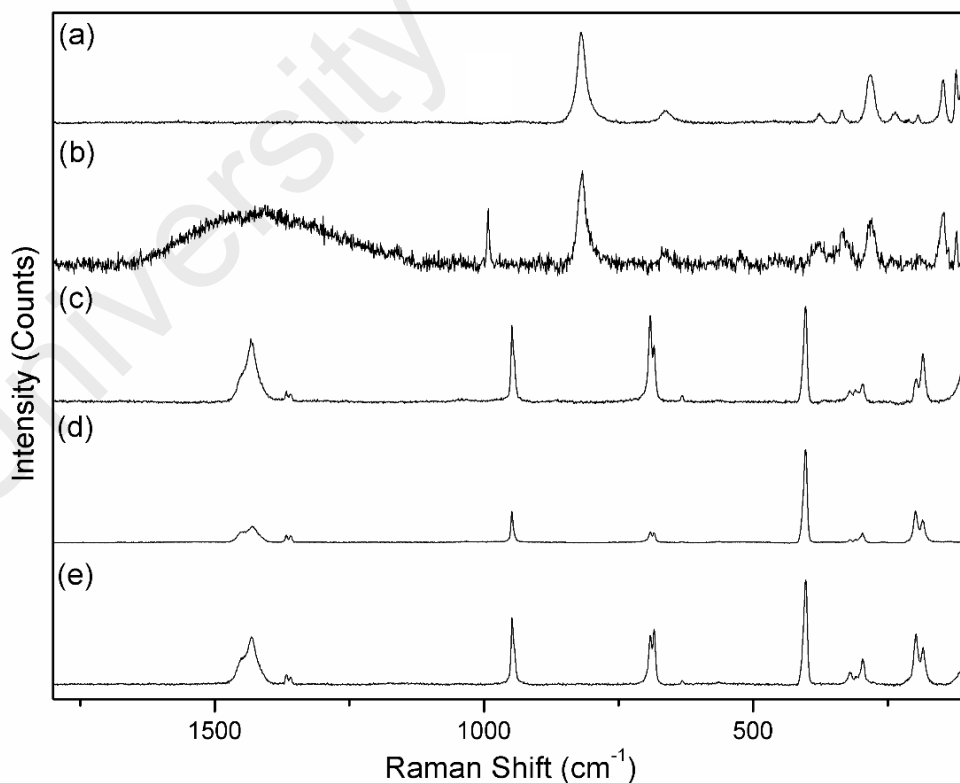


Figure 4.9: Raman Spectra of surface capped molybdenum sulphides nanoparticles where (a) MoS₂, (b)SCMS-CA, (c) SCMS-LA (d) SCMS-SA and (e) SCMS-OA nanoparticles

4.3.5 XRD Spectroscopy

The XRD spectra in Figure 4.10 exhibit one broad peak and a broad feature, proving that long-range order crystalline is absent in all SCMS nanoparticles. XRD spectra is of a typical amorphous product (Duphil *et al.*, 2002). The broad peak located at $2\theta = 8.0^\circ$ correspond to the (002) plane Bragg reflection of the hexagonal 2H-MoS₂ structure (Panigrahi & Pathak, 2013), then continues beyond 15° . Moreover, (002) diffractions at $2\theta = 14.4^\circ$, as shown in literature (Liang *et al.*, 1986), does not appear in the XRD plots, which suggest that the stacking of single layer nanoparticles did not take place.

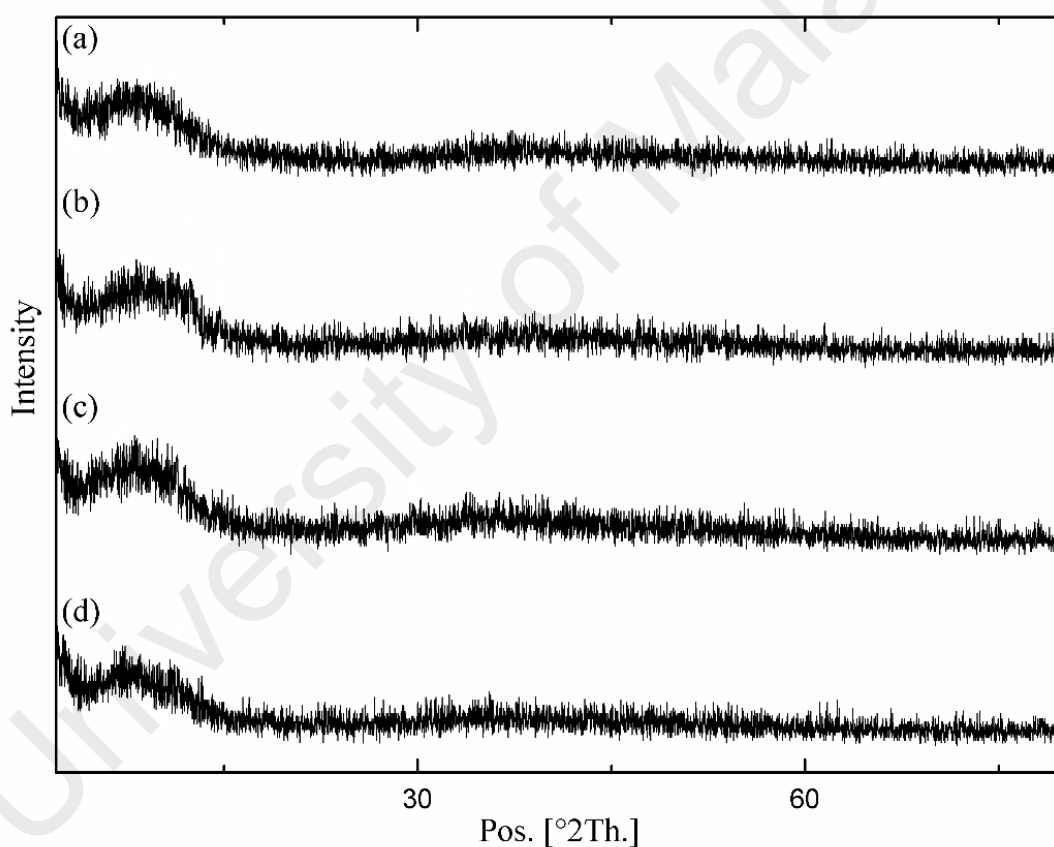


Figure 4.10: XRD Spectra of surface capped molybdenum sulphides nanoparticles where (a) SCMS-CA, (b) SCMS-LA (c) SCMS-SA and (d) SCMS-OA nanoparticles

4.3.6 TGA Analysis

In surface capped nanoparticles, the size and the type of cation on the surface are greatly affected by the amount of coating materials (Jayesh D Patel *et al.*, 2012). Thus, we used TGA to analyse the amount of fatty acid of modified skin on the surface of nanoparticles. Figure 4.11 shows the TGA plots of all SCMS nanoparticles, where the heating temperature are between 30 - 950 °C. For SCMS-CA, SCMS-LA, and SCMS-SA nanoparticles, loss of mass begins at ~200 °C, whereas for SCMS-OA, loss of mass occurs at ~300 °C, due to the decomposition of the fatty acid layer surrounding the surface of the nanoparticles (Kreivaitis *et al.*, 2014). The entire elimination of fatty acid layer falls within 250 - 450 °C. Then, the decomposition of core nanoparticles takes place at a higher temperature, as early as 700 °C, and up to 800 °C. From this TGA plot, the respective weight composition of caproic, lauric, stearic, and oleic acid in each SCMS nanoparticles were 40.80 (w/w) %, 44.19 (w/w) %, 57.30 (w/w) %, and 53.01 (w/w) %. Among these plots, SCMS-OA nanoparticles exhibit sharp decrease in the mass loss, suggesting that oleic acid has the strongest monolayer bound surrounding SCMS nanoparticles.

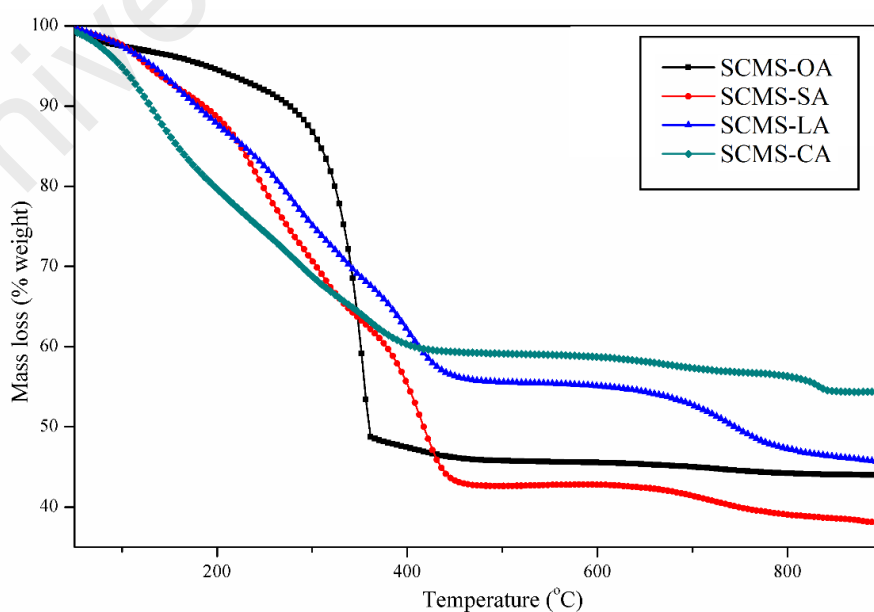


Figure 4.11: TGA Analysis of SCMS nanoparticles

4.4 Tribological Study

To understand the tribological behaviour of SCMS nanoparticles as an additive in PETC ester, quantitative analyses were carried out for different capping agents, concentrations, and load applied on each product. The results of the coefficient of friction, extreme pressure behaviour and wear scar diameters were obtained from four-ball test.

4.4.1 Coefficient of Friction (CoF) Analysis

The CoF data were collected from the four-ball friction test. The variation of CoF as a function of concentration of the additives in bio-based lubricant oil under 400 N load is illustrated in Figure 4.12. From this figure, it can be seen that SCMS nanoparticles can reduce CoF of steel-steel pair compared to those of the bio-based lubricant without the addition of additive. Different SCMS nanoparticles show different friction reduction ability, with each reporting a different concentration of optimum friction improvements.

Among the various types of SCMS nanoparticles, the highest friction reducing properties were obtained when the SCMS-LA nanoparticles concentration is 0.075 (w/w) %, at a percentage of 15.40 %. At this point, they can be embedded into the worn surfaces, while the pan furrows on the metal surface were filled with additives. The boundary film become thicker and smoother, which helps reduce friction between the contacting metal surfaces. Moreover, the ball-like shape of SCMS nanoparticles leads to the rolling effect mechanism between the friction surface, altering the pure sliding friction to mixed sliding-rolling friction (Tang & Li, 2014).

At very low additive concentrations (below optimum concentration), SCMS nanoparticles are highly dispersed in bio-based oil and are able to undergo the rolling mechanism of the sphere-like shape of SCMS nanoparticles between two contacting metal surfaces (Dai et al., 2016). However, the presence of SCMS nanoparticles in the bio-based lubricant oil is limited, and it was unable to form adequate amount of deposited

film to minimise the self-reducing effect of nanoparticles filling the dents of wear surface (M. Qu et al., 2016). Thus, higher concentrations of loaded additives lead to more nanoparticles filling the dents, and subsequently decreased the CoF.

As the concentration of additives increases beyond that of the optimum concentration, friction will also increase. This takes place due to the SCMS nanoparticles filling up all of the furrow and holes up to the point of saturation. At high concentrations of SCMS nanoparticles, the unfilled nanoparticles tend to accumulate and form large agglomerations. They become hard to disperse, making it difficult to penetrate the interface of the bio-based lubricant oil to decrease the shear stress (Ilie & Covaliu, 2016). Nevertheless, these large agglomerated nanoparticles in the bio-based lubricant oil act similarly to debris particles, which lead to the presence of abrasive-like wear.

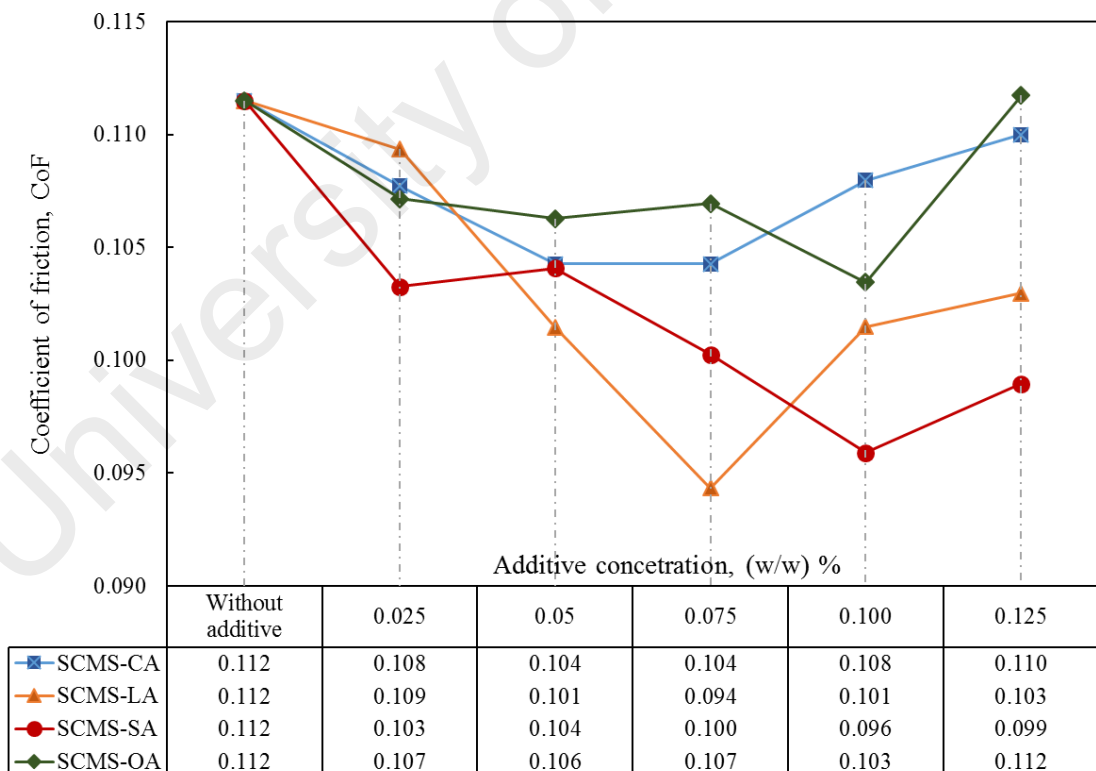


Figure 4.12: Average Coefficient of friction (CoF) of bio-based lubricant oil without additive and bio-based lubricant oil containing 0.025 to 0.125 (w/w) % additive (maximum uncertainty: 8.335×10^{-3})

4.4.2 Extreme Pressure (EP) Analysis

The SCMS-LA nanoparticles at a concentration 0.075 (w/w) % demonstrated the best ability to reduce friction. The sample was then further analysed using EP analysis by varying the applied load from 400 N up to 1800 N for 10 s using the four-ball instrument. Figure 4.13 show the variation of CoF with the load under the lubrication of bio-based lubricant oil without additives and bio-based lubricant oil containing 0.075 (w/w) % of SCMS-LA nanoparticles. It is seen that SCMS-LA nanoparticles can effectively reduce friction. From the figure, we can detect the small differences of the CoF between two samples under a lower test load (800 N). The difference in CoF of both samples gradually increases up to 1,600 N, indicating that SCMS nanoparticles can effectively improve load-carrying capacity of the bio-based lubricant oil over a wide range of the applied load. Among the loads, SCMS nanoparticles shows high load carrying ability specifically at a load of 1,600 N at a reducing factor of 174.77 %. This could be due to the stable dispersion of SCMS nanoparticles in the bio-based lubricant oil that can be readily transferred onto the contact zone of rubbing steel surfaces for deposition to form a protective surface and lubricious layer, thus reducing friction (Zhang *et al.*, 2014a). Moreover, smaller SCMS nanoparticles are able to easily penetrate the interface of base oil to form a continuous oil film in the concave of the rubbing surface, thus exhibiting a lower CoF (Shia *et al.*, 2014).

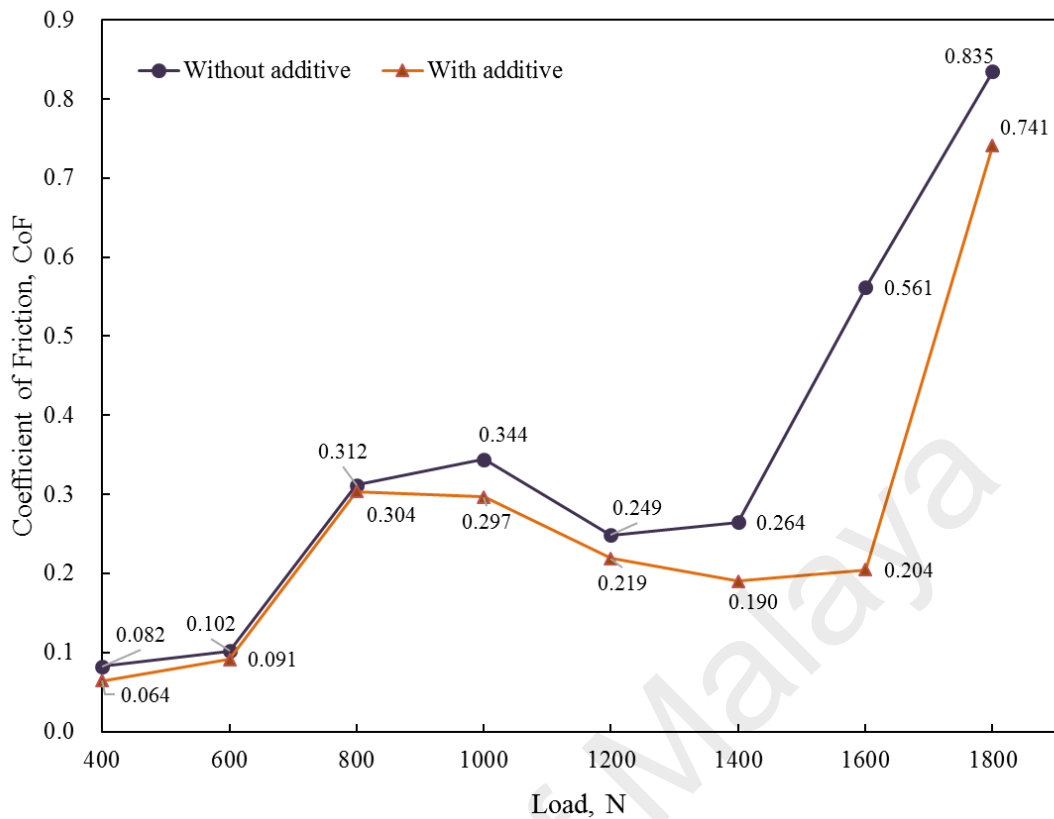


Figure 4.13: Average Coefficient of friction (CoF) of bio-based lubricant oil only and bio-based lubricant oil containing 0.075 (w/w) % SCMS-LA nanoparticles at different load (maximum uncertainty: 5.735×10^{-3})

Figure 4.14 shows the correlation of CoF with different loads using bio-based lubricant oil vs. time. For Figure 4.14 (a), at low loads (400 N), the CoF of bio-based lubricant oil without additive is low. This could be due to the thin film being formed can be used to withstand the load. As the load was increased to 600 N, the thin film starts to degenerate, which increased the CoF. From the same figure, at 600 - 1400 N, the CoF showed a strong increase at the beginning, followed by a sharp decrease.

The sudden fluctuation of CoF could be caused by the “running-in effect”, where the thickness of the oil film is too thin, therefore, contact begins at the top of the asperities, increasing CoF and WSD (Nogueira *et al.*, 2002). This phenomenon is called boundary lubrication, and a sudden increase in localised pressure causes sound turbulence, high

wear rates, and severe damages (Lugt *et al.*, 2001). Later, the contacting surface area becomes smoother, and their wear rate is subsequently decreased and stabilises. At 1800 N, the CoF increases until it reaches maximum point, then rapidly decreases. This situation occurs when surface is welded together as the lubricant evaporates due to the high temperature and pressure.

Figure 4.14 (b) show the relationship between CoF and different loads using bio-based lubricant oil with the presence of an additive. This graph shows an almost similar pattern to the one lacking additive, however, it shows lower peak of asperity and CoF. At maximum load (1800 N), bio-based lubricant oil with an additive is able to retain CoF for a while, before it drops significantly compared to the lubricant without an additive. This shows that the addition of SCMS nanoparticles result in EP properties.

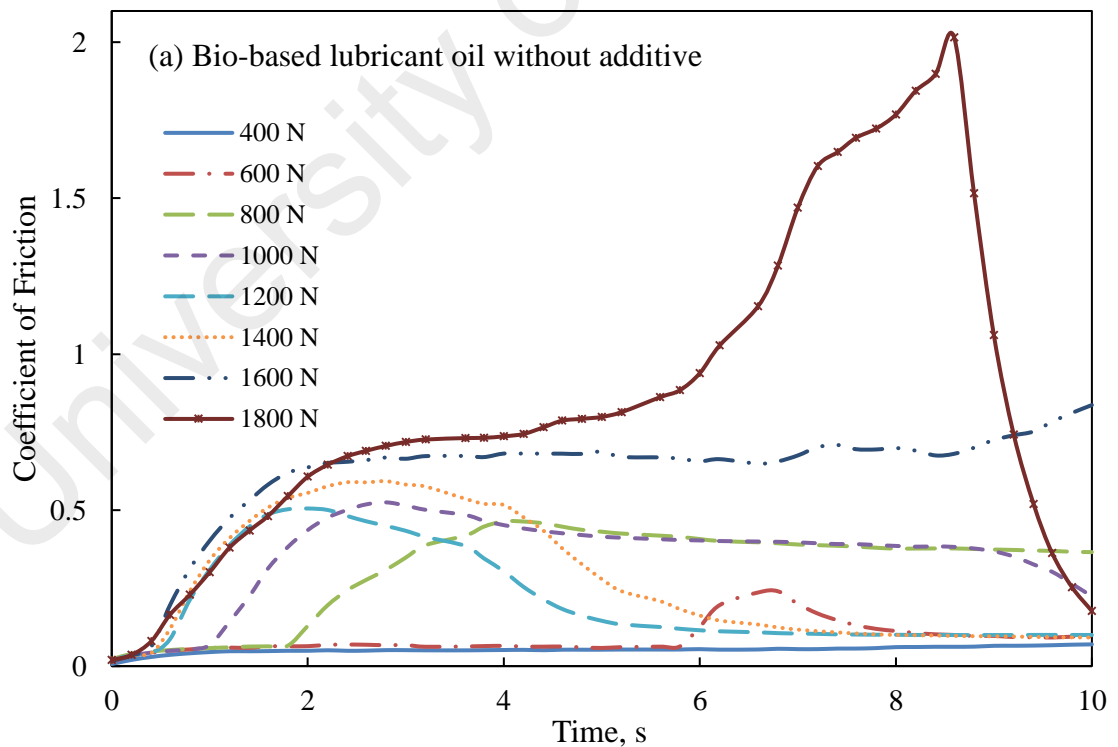


Figure 4.14, continued

Figure 4.14, continued

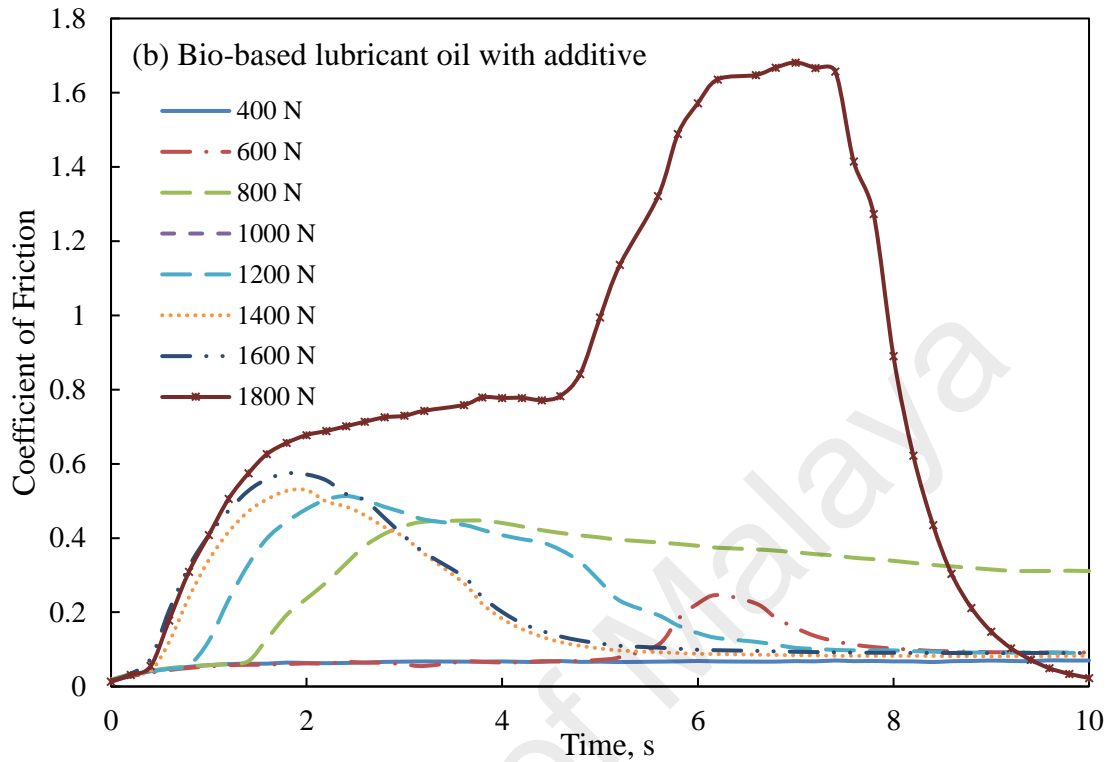


Figure 4.14: Variation of COF with load from 400 N to 1800 N in 10 seconds for (a) bio based lubricant oil without additive and (b) bio-based lubricant oil with addition 0.075 (w/w) % SCMS-LA nanoparticles

4.4.3 Wear Scar Study

In relation to the average CoF discussed in previous section, the use of SCMS nanoparticles as additives in bio-based lubricant oil could also decrease WSD on ball bearing collected from the four ball test. Based on Figure 4.15, bio-based lubricant oil that were infused with additives reduced WSD compared to bio-base lubricant oil without additives. From the graph, the average WSD of the bio-base lubricant oil without additive is 702 μm . The lowest average WSD achieved from this test is 597 μm , where the addition of 0.100 (w/w) % SCMS-OA additives can reduce the WSD by 14.96 %. Most formulated bio-based lubricant oil with the addition of SCMS nanoparticles successfully reduced WSD by 4.81 - 14.96 %.

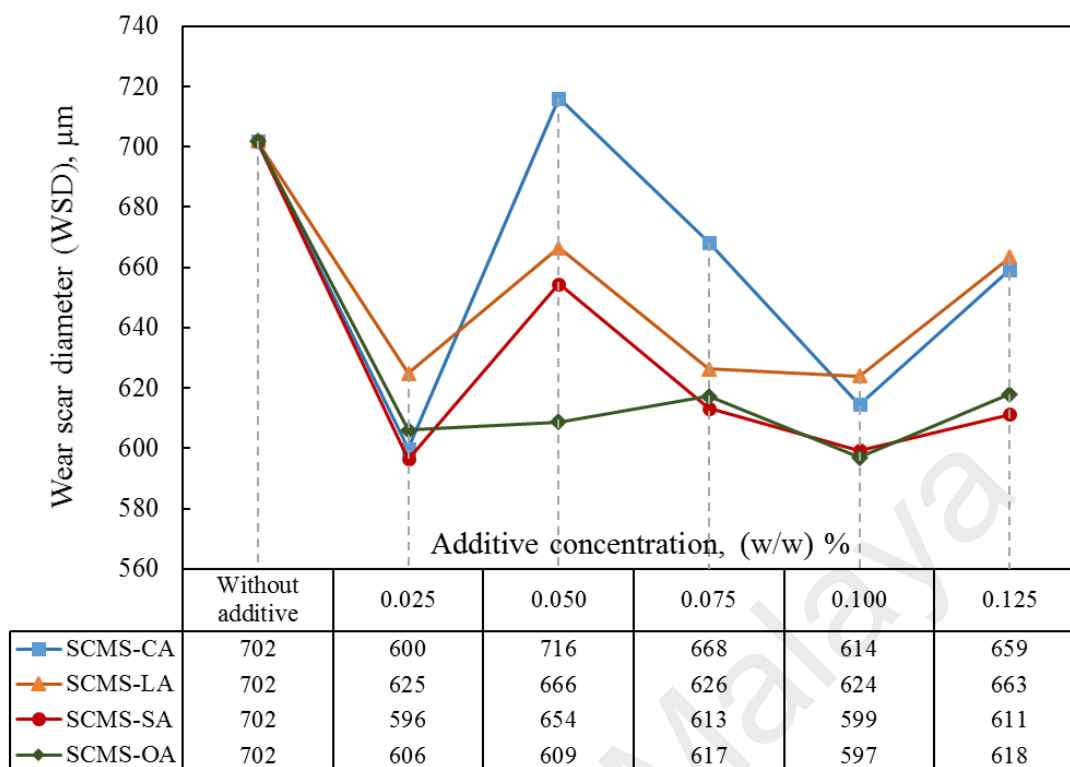


Figure 4.15: Average wear scar diameter (WSD) of bio-based lubricant oil only and bio-based lubricant oil containing 0.025 to 0.125 (w/w) % additives

Impressively, the wear reduction rate of SCMS nanoparticles increased with increasing alkyl chain length of the capping layer. The interpretations for this behaviour could be that SCMS-OA has the best load carrying capacity of adsorbed layer and balance between dispersibility to bio-base oil, as well as adsorption ability of the metal surface of carboxylic acid (Kamimura *et al.*, 2006). From literature, the friction coefficient is directly proportional to unsaturation (Lundgren *et al.*, 2008). We can see from the figure that at a concentration of 0.050 (w/w) %, SCMS-OA display much higher WSD reduction capability compared to SCMS-SA. Nevertheless, at concentration of 0.050 (w/w) %, of additives, WSD exhibit slightly increase here and then decreases as concentration increases. This is happened due to SCMS nanoparticles are at scarce and the primary wear mechanism is abrasive wear. With the increase in additives concentration, protection film

formed at the contact region which then prevent the asperities on the mating surface from direct contact between each other (Zhang, 2016).

The difference in WSD between SCMS-SA and SCMS-OA can be related to the structural properties of surface capping film and the rate of penetration of lubricant oil (Doig *et al.*, 2013). Increased wear size occurs when the rate of lubricant penetration increase, which induces the additives into more intimate contact with metal surface. Compared to stearic acid, oleic acid in SCMS-OA nanoparticles possess a cis-isomer structure with a bended alkyl chain, thus lowering the monolayer's thickness surrounding the core nanoparticles and increasing the additives' metal adsorption (Wood *et al.*, 2016). Furthermore, the presence of one double bond on the backbone of oleic acid provides an implicit rigidity and reported lower lubricant penetration into the surfactant film. Thus, SCMS-OA tend to adsorb more on the metal surface under similar tribological conditions.

Figures shown in Table 4.6 show the SEM metallographs at $250 \times$ magnification to accommodate the size of scar and measure the dimension. Scar using bio-based lubricant oil only and bio-based lubricant oil with SCMS nanoparticles additives show distinctly unique visible features. Bigger scar size of bio-based lubricant oil can be seen in the presence of increased wear. The topography of smooth surface ball bearing getting rougher due to the enhanced asperity-asperity contacts, followed by debris of wear (Kumar Dubey *et al.*, 2013). Moreover, the groove size appears to be larger, and the distance between each groove is much wider. Scar size due to the bio-based lubricant oil added with nanoparticles is much smaller in size. The presence of a dark third body deposited between the groove indicate the presence of tribo-layer of nanoparticles additives, which results in friction and wear reduction. This phenomenon can further confirm the fact that SCMS nanoparticles is an excellent antiwear and friction improver additives in a bio-based lubricant.

Table 4.6: Wear scar images of bio-based lubricant oil without additive and bio-based lubricant oil containing 0.025 to 0.125 (w/w) % additive

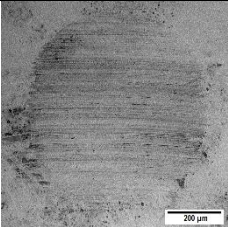
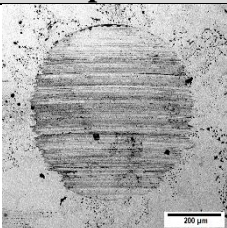
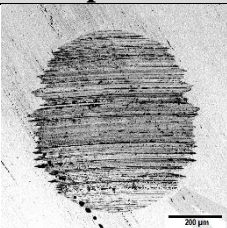
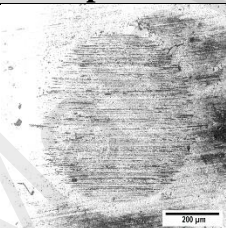
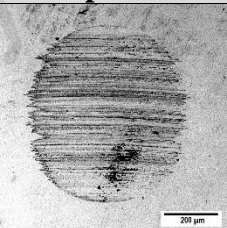
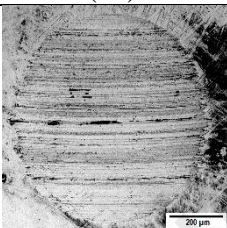
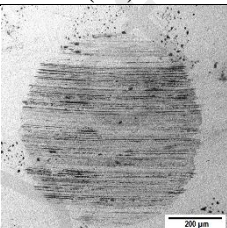
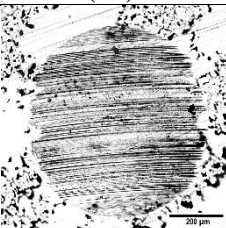
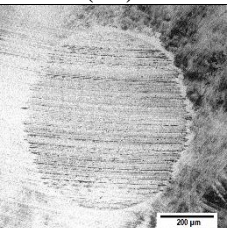
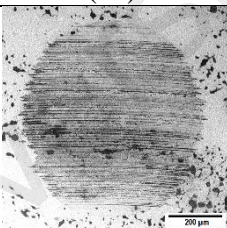
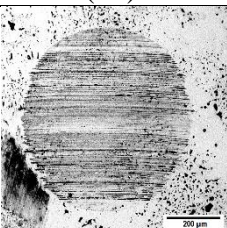
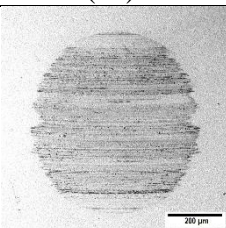
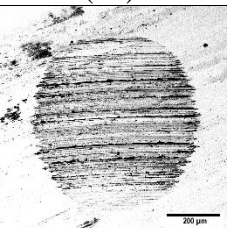
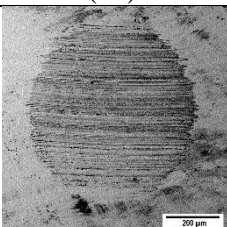
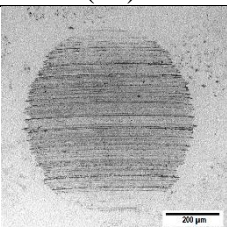
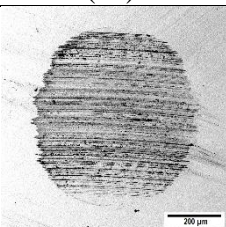
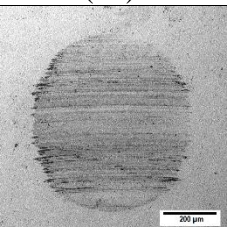
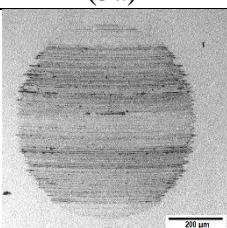
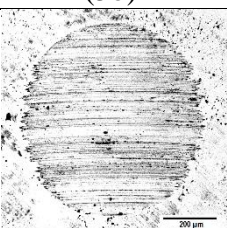
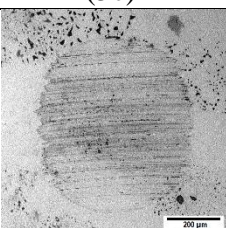
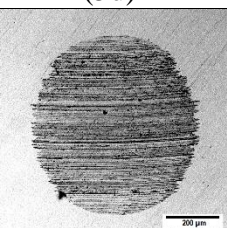
Additive Loading (w/w) %	Bio-based lubricant oil without additive			
0	 <p style="text-align: center;">(1)</p>			
	SCMS-CA nanoparticles	SCMS-LA nanoparticles	SCMS-SA nanoparticles	SCMS-OA nanoparticles
0.025	 <p style="text-align: center;">(2a)</p>	 <p style="text-align: center;">(2b)</p>	 <p style="text-align: center;">(2c)</p>	 <p style="text-align: center;">(2d)</p>
0.050	 <p style="text-align: center;">(3a)</p>	 <p style="text-align: center;">(3b)</p>	 <p style="text-align: center;">(3c)</p>	 <p style="text-align: center;">(3d)</p>
0.075	 <p style="text-align: center;">(4a)</p>	 <p style="text-align: center;">(4b)</p>	 <p style="text-align: center;">(4c)</p>	 <p style="text-align: center;">(4d)</p>
0.100	 <p style="text-align: center;">(5a)</p>	 <p style="text-align: center;">(5b)</p>	 <p style="text-align: center;">(5c)</p>	 <p style="text-align: center;">(5d)</p>
0.125	 <p style="text-align: center;">(6a)</p>	 <p style="text-align: center;">(6b)</p>	 <p style="text-align: center;">(6c)</p>	 <p style="text-align: center;">(6d)</p>

Figure 4.16 shows the graph of the wear scar diameter vs. applied load for both the bio-based lubricant oil without additive and bio-based lubricant oil with the addition of 0.075 (w/w) % SCMS-LA nanoparticles. From the trend of the plot, samples with additives reported smaller WSD compared to the samples without additives at all load parameters, and at 1600 N, samples with additives reported the largest WSD difference with a 39.75 % size reduction. Small differences in WSD at low loads compared to higher difference at high loads from the graph indicate that SCMS-LA nanoparticles as additives improves the capacity of carrying load and increase the operation of lubricant oil at extreme loads.

Furthermore, both samples showed that the starting point of the incipient seizure on the contact surface occurred at 400 N, and point of last non-seizure ends at 800 N. Incipient seizure reveals that the lubrication film is collapsing, leading to metal-metal contact, and cause test ball scar diameter to no longer be on the compensation line. The highest test load that yield largest WSD is 1600 N prior to both samples reaching the weld point at 1800 N. The weld point is the load at which the lubricant thoroughly fails and evaporates, leading to metal-metal fusion to take place due to the excessive heat and high pressure being generated between two rubbing surfaces. Figure 4.17 display schematic plot of WSD vs. applied load from (Totten *et al.*, 2003).

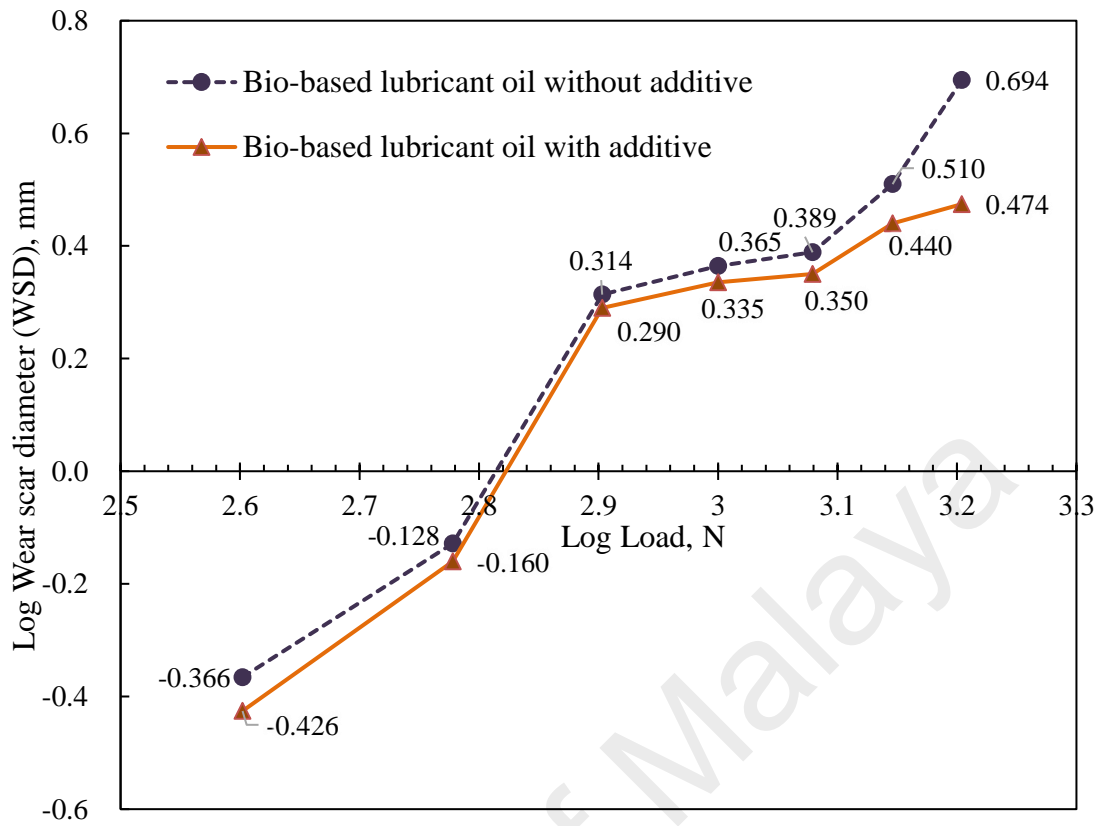


Figure 4.16: Relationship between load and wear scar diameter (WSD) of bio-based lubricant oil only and bio-based lubricant oil containing 0.075 (w/w) % SCMS-LA nanoparticles at different load 400 to 1,800 N.

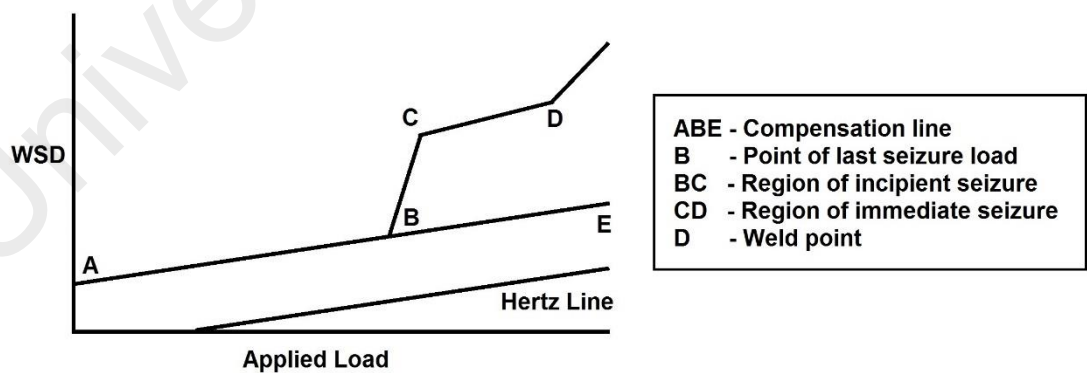


Figure 4.17: Schematic plot of WSD against applied load

Images in Table 4.7 show the morphologies of the worn surface lubricated with bio-based lubricant oil, with and without additives at different applied loads. It can be seen that the WSD of the latter image is much smaller and its worn surface smoother. The applied load and scar size is almost directly proportional. Fatty acid capping SCMS nanoparticles in bio-based lubricant oil can be effective in reducing friction when it is able to form metallic soap molecules to protect the surface of the metal. However, this protective film will collapse if the load becomes too much from high temperature and pressure between the contacting surface generated from a large amount of friction (Gellman & Spencer, 2002).

At higher loads, starting from 1200 N, as shown in Table 4.7 (5-7a) along the edge of the metal surface, the material transfer during adhesion can be ascertained, as per (5-7b). Images in Table 4.7 (7a) shows the highest material transfer, severe wear, cross hatching crack, and delamination compared to (7b). This anomaly occurs after the fracture of oil film, resulting in metallic contact. This metal-to-metal contact induced the adhesion of micro asperities and plastic deformation of the surface. Thus, it shows that the additive in the lubricant (SCMS-LA nanoparticles) is able to actively protect the surface and reduce material transfer from wear and friction.

Table 4.7: Surface morphology of wear scar formed on the ball after EP test using calibrated optical microscope

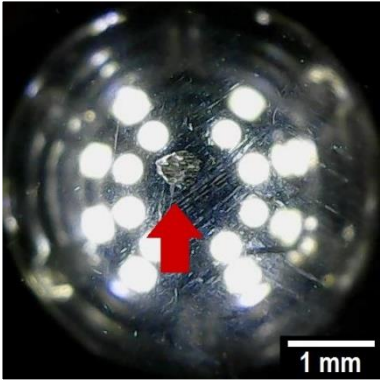
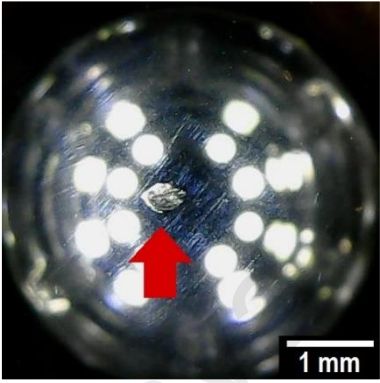
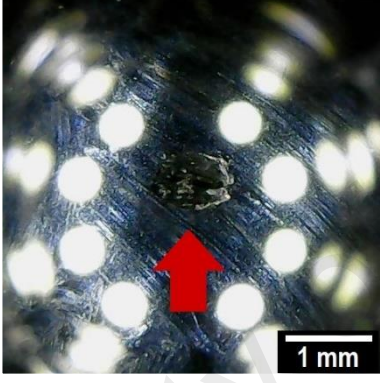
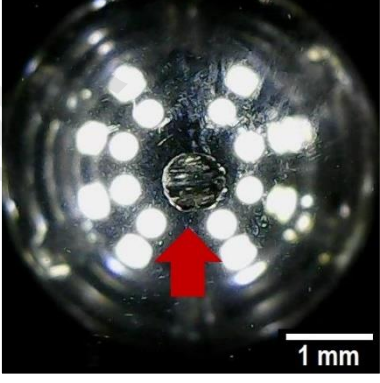
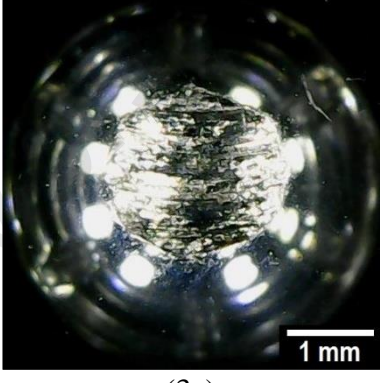
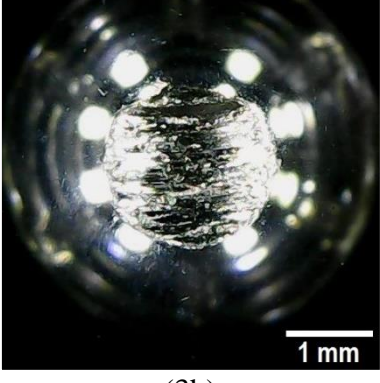
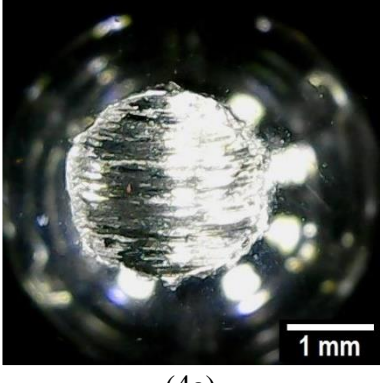
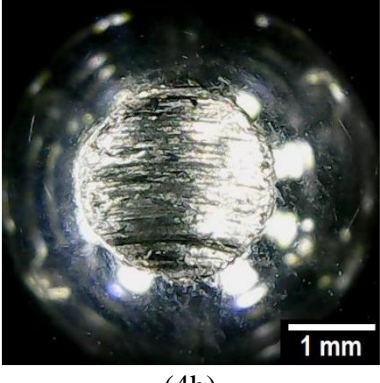
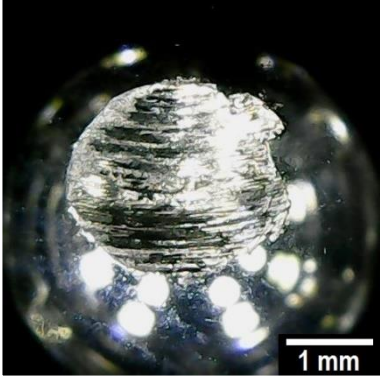
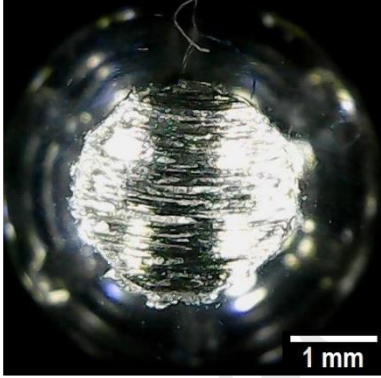
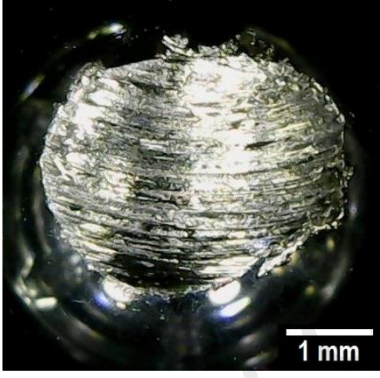
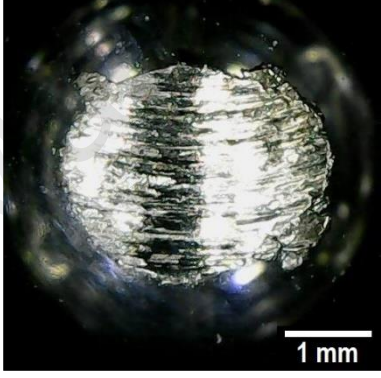
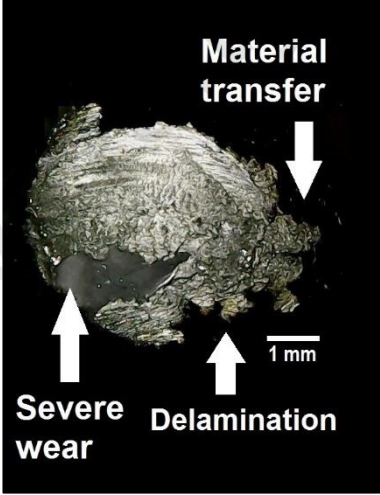
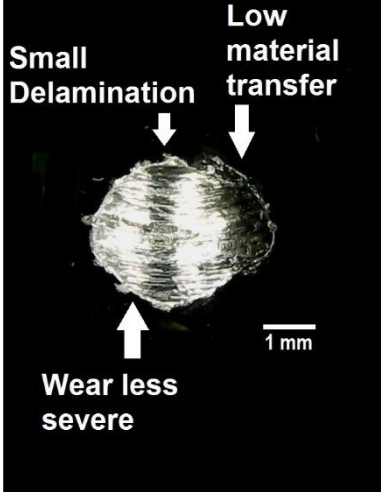
Applied Load (N)	Bio-based lubricant oil only	Bio-based lubricant oil with addition 0.075 (w/w) % SCMS-LA
400	 <p data-bbox="675 745 730 779">(1a)</p>	 <p data-bbox="1160 745 1216 779">(1b)</p>
600	 <p data-bbox="675 1171 730 1205">(2a)</p>	 <p data-bbox="1160 1171 1216 1205">(2b)</p>
800	 <p data-bbox="675 1597 730 1630">(3a)</p>	 <p data-bbox="1160 1597 1216 1630">(3b)</p>
1000	 <p data-bbox="675 2022 730 2056">(4a)</p>	 <p data-bbox="1160 2022 1216 2056">(4b)</p>

Table 4.7, continued

Table 4.7, continued

Applied Load (N)	Bio-based lubricant oil only	Bio-based lubricant oil with addition 0.075 (w/w) % SCMS-LA
1200	 <p>(5a)</p>	 <p>(5b)</p>
1400	 <p>(6a)</p>	 <p>(6b)</p>
1600	 <p>(7a)</p>	 <p>(7b)</p>
1800	Welded	Welded

4.5 Physiochemical study of formulated bio-based lubricant oil

Among various type of SCMS nanoparticles studied in this research, SCMS-LA nanoparticles in bio-based lubricant oil shows the optimised and best antiwear and antifriction behaviour. Thus, it was selected for further analyses of its physiochemical properties, such as sedimentation, dispersion, viscosity, and density. The difference between surface capped and uncapped molybdenum sulphide will be detailed and discussed.

4.5.1 Sedimentation Study

Sedimentation test and dispersion analysis was conducted to determine the colloidal stability of SCMS nanoparticles as an additive in bio-based lubricant oil. The dispersibility of the additives will begin stabilising as soon as the agitation in blending process stops and dispersion is more or less stable based on the ability of nanoadditives to remain suspended (Ilie & Covaliu, 2016). If the additive loaded into bio-based lubricant oil are well dispersed, the formation of sediments will be minimised.

Table 4.8 illustrate the stability of uncapped molybdenum sulphide (UCMS) nanoparticles and molybdenum sulphide nanoparticles capped with lauric acid (SCMS-LA) at different concentrations, ranging from 0.025 to 0.125 (w/w) % in PETC ester. The dispersing stabilities of additives in bio-based lubricant oil can be analysed from the aspect of light transmittance. Higher light transmittance can pass through bio-based lubricant oil sample, proving that more nanoadditives settled due to gravitational effect. Most common dispersed phase (additives) is denser than the continuous phase (bio-based oil), thus the additives will sediment to the bottom of bio-base oil with the passage of time. From the results, bio-based lubricant oil containing UCMS nanoparticles show greater sedimentation based on the clarity of the continuous phase and higher sediment at the bottom of the bottle, even at just 7 days compared to the SCMS-LA nanoparticles. It

is also confirmed that the dispersibility of capped molybdenum sulphide is far better than its uncapped counterpart at all range of loading concentration. It was suggested that long-aliphatic chain of fatty acid grafted on molybdenum sulphide nanoparticles on the surface formed lipophilic groups, which helps disperse the adducts in the bio-based oil.

Table 4.8: Digital images of the dispersion and sedimentation behaviour of SCMS-LA and UCMS nanoparticles after loading after 7 and 30 days for various additive concentration

Additive Loading (w/w) %	SCMS-LA nanoparticles			UCMS nanoparticles		
	After Loading	After 7 days	After 30 days	After Loading	After 7 days	After 30 days
0	 0	 0	 0	 0	 0	 0
0.025	 0.025	 0.025	 0.025	 0.025	 0.025	 0.025
0.050	 0.050	 0.050	 0.050	 0.050	 0.050	 0.050

Table 4.8, continued

Table 4.8, continued

Additive Loading (w/w) %	SCMS-LA nanoparticles			UCMS nanoparticles		
	After Loading	After 7 days	After 30 days	After Loading	After 7 days	After 30 days
0.075						
	0.075	0.075	0.075	0.075	0.075	0.075
0.100						
	0.100	0.100	0.100	0.100	0.100	0.100
0.125						
	0.125	0.125	0.125	0.125	0.125	0.125

The model of fatty acid monolayer surrounding SCMS nanoparticles were established and displayed in Figure 4.18 based on the results of the nanoparticles characterisation. Since molybdenum sulphide nano-core was embedded in the monolayer of fatty acid, the dispersion capability in organic solvent, especially in PETC ester, was improved accordingly, as the alkyl chain in fatty acid exhibit polar behaviour. The schematic diagram in Figure 4.19 represent the interaction between SCMS nanoparticles with bio-based lubricant oil.

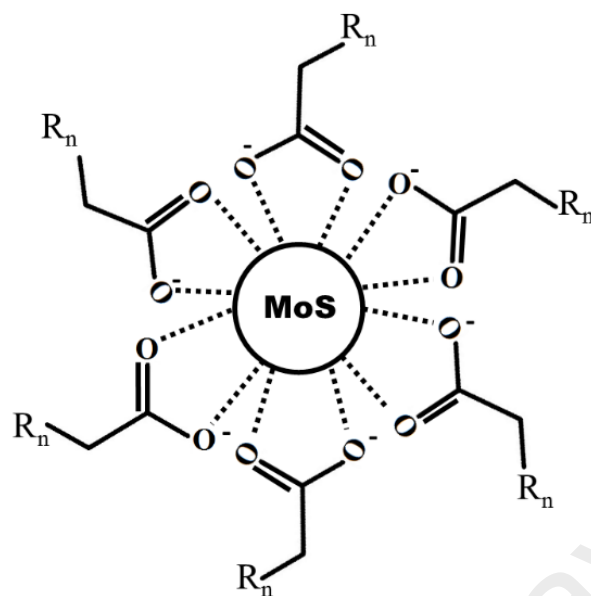


Figure 4.18: Model of SCMS nanoparticles where R is long alkyl chain with carbon number (n), n=4,10,16 (saturated) and 16 (unsaturated) for SCMS-CA, SCMS-LA, SCMS-SA and SCMS-OA respectively

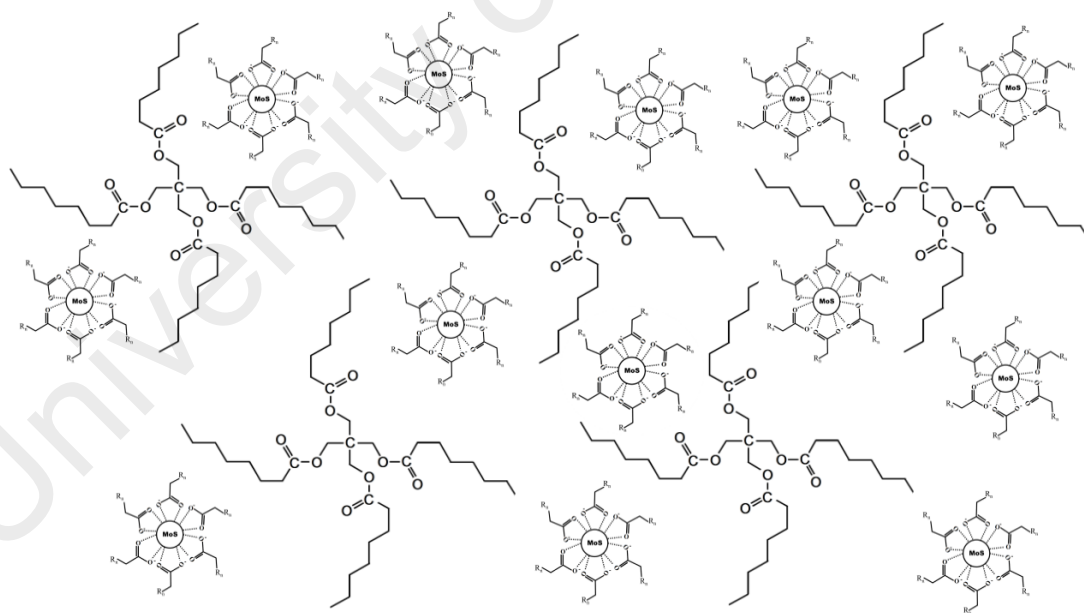


Figure 4.19: Schematic diagram of single layer of fatty acid capped molybdenum sulphide nanoparticles in bio-based lubricant oil (PETC ester)

4.5.2 Microscopic Dispersion Analysis

To further investigate the dispersion and agglomeration of SCMS nanoparticles in bio-based lubricant oil, dispersion analysis was carried out using optical microscopy. Images in Table 4.9 shows the dispersion and agglomeration of SCMS-LA and UCMS nanoparticles. The concentration of the SCMS-LA and UCMS nanoparticles ranged from 0.025 - 0.125 (w/w) %. Many large UCMS nanoparticles aggregates were seen in the images of UCMS nanoparticles suspension, even at all range of additive concentration (as shown in Table 4.9 (1-5a)). However, at low concentrations of SCMS-LA nanoparticles, the size of the aggregates decreased after the modification of molybdenum sulphide surface with fatty acid. As the concentration of SCMS-LA increases, the aggregates begin to appear (Table 4.9 (5b)), but at a much lesser rate compared to the UCMS nanoparticles (Table 4.9 (5a)).

The immense aspect ratio and remarkably small diameter of the UCMS nanoparticles resulted in very intense Van der Waals interactions between each particle (C. S. Chen *et al.*, 2005). Unmodified UCMS were coagulated and aggregated. Due to the presence of the capping layer surrounding the SCMS-LA nanoparticles, the hydrophilic segment (alkyl chain) of lauric acid were dispersed into the PETC ester, causing the appearance of lauric hindrance force that separates them from one another. However, at high concentrations, the aggregation of SCMS-LA nanoparticles could still occur due to overcrowding, and the additives lack the space for efficient dispersion.

Table 4.9: Metallographic micrographs of UCMS and SCMS-LA nanoparticles at different loading percentage

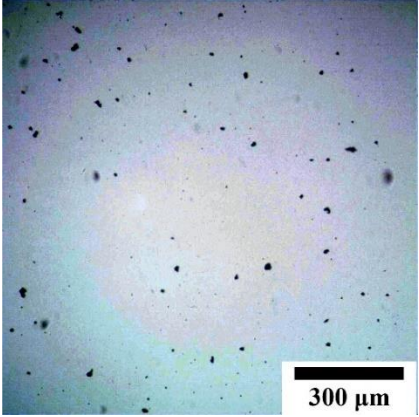
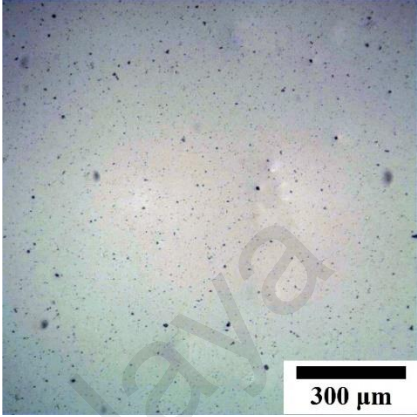
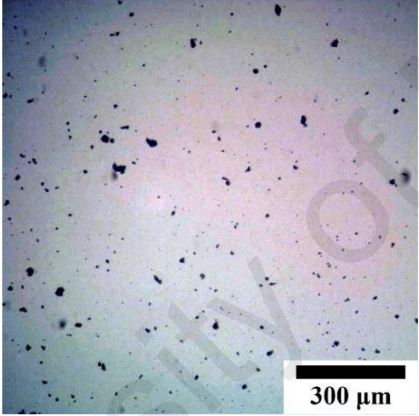
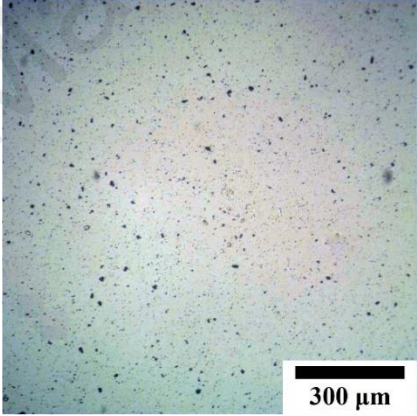
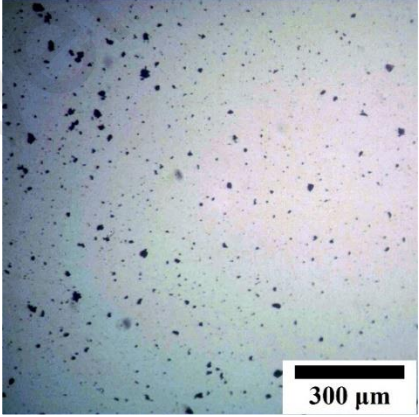
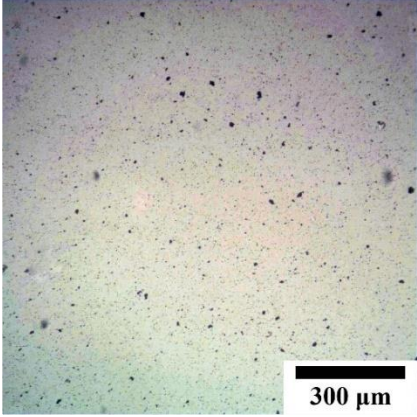
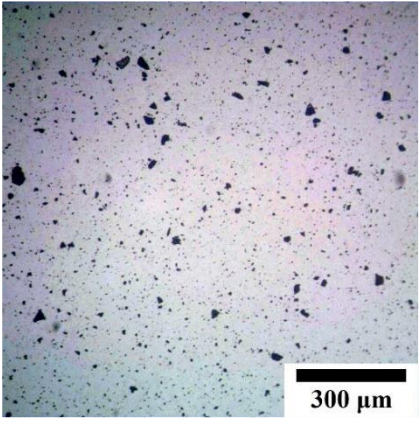
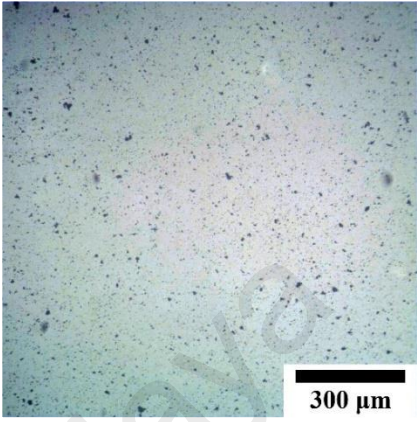
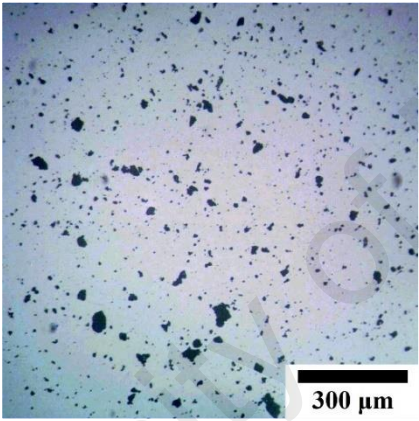
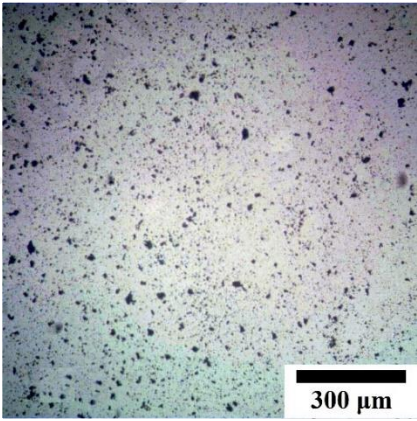
Additive Loading (w/w) %	UCMS nanoparticles	SCMS-LA nanoparticles
0.025	 <p>(1a)</p>	 <p>(1b)</p>
0.050	 <p>(2a)</p>	 <p>(2b)</p>
0.075	 <p>(3a)</p>	 <p>(3b)</p>

Table 4.9, continued

Table 4.9, continued

Additive Loading (w/w) %	UCMS nanoparticles	SCMS-LA nanoparticles
0.100	 <p style="text-align: center;">(4a)</p>	 <p style="text-align: center;">(4b)</p>
0.125	 <p style="text-align: center;">(5a)</p>	 <p style="text-align: center;">(5b)</p>

4.5.3 Viscosity Analysis

Table 4.10 shows the kinematic viscosity at test temperatures of 40 and 100°C. The viscosity index (VI) of formulated bio-based lubricant oil sample consist of additives ranging from 0 - 0.125 (w/w) %. From the results, there is no significant difference in the viscosity before and after the addition of additives at both temperatures. The viscosity of all samples were between 29.7 - 30.0 cSt, and 5.9 - 6.0 cSt for temperatures 40 and 100 °C, respectively. As the concentration of the additives increases, viscosity remains almost similar, which suggests that additive loading does not affect viscosity at both test temperatures. Moreover, there is no significant difference in viscosity between UCMS and SCMS-LA nanoparticles added lubricants at both test temperatures, which proves

that the modification of the surface of the nanoparticles with capping agent does not affect the viscosity of bio-based lubricant oil.

Table 4.10: Kinematic viscosity at 40 and 100 °C and viscosity index of formulated bio-based lubricant oil, loaded with SCM-LA and UCMS nanoparticles at concentration up to 0.125 (w/w) %.

Additives Loading (w/w) %	UCMS nanoparticles			SCMS-LA nanoparticles		
	Viscosity (cSt)		Viscosity Index, (VI)	Viscosity (cSt)		Viscosity Index, (VI)
	40 °C	100 °C		40 °C	100 °C	
0	29.8	5.9	147	29.8	5.9	147
0.025	30.0	5.9	147	29.7	5.9	148
0.050	30.0	5.9	148	29.8	5.9	150
0.075	30.0	5.9	148	30.0	6.0	151
0.100	30.0	6.0	149	29.8	6.0	151
0.125	30.0	6.0	149	29.7	6.0	154

However, there is significant difference in the VI between bio-based lubricant oil before and after the addition of additives. Literature points out that if the VI increases, the rate of viscosity will be lower with increasing temperature of the lubricant oil. (Zulkifli et al., 2014). Therefore, additives that can improve the VI of lubricant oil is preferred, as the performance of the lubrication is affected by temperature fluctuations. Figure 4.20 shows that as the concentration of additive load increases, VI also increases. Between the UCMS and SCMS-LA nanoparticles being added into the bio-based lubricant oil, the latter exhibit higher increment, while the maximum VI for SCMS-LA and UCMS added lubricant is recorded as high as 154 and 149, respectively. The VI results proves that the SCMS-LA nanoparticles improve not only wear and friction, but enhance the VI of bio-based lubricant oil. The enhancement of the VI is attributed to the presence of hydroxyl functional group surrounding SCMS-LA nanoparticles, which can affect the lubricating performance of bio-based lubricant oil (Quinchia et al., 2014).

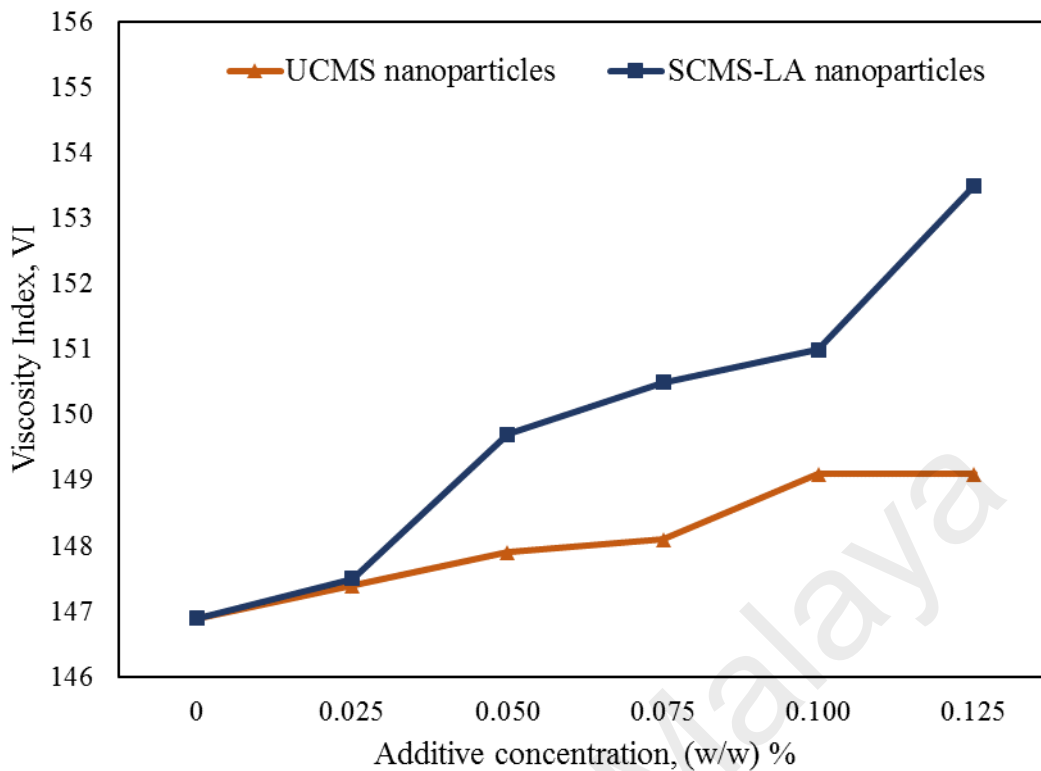


Figure 4.20: Relationship between additive concentration and viscosity index of UCMS and SCMS-LA nanoparticles added bio-based lubricant oil

4.5.4 Density Analysis

Table 4.11 compare the density at 15 °C of the bio-based lubricant oil in pristine form and bio-based lubricant oils infused with SCMS-LA and UCMS nanoparticles at concentrations between 0.025 - 0.125 (w/w) %. The density of both bio-based lubricants with and without additives are almost similar, within 0.958 - 0.960 g/cm³ throughout the different concentrations of additives. This shows that even at higher concentrations of additives, the density of the lubricant remains almost similar. There is also no significant difference between UCMS and SCMS-LA nanoparticles, which implies that the modification of nanoparticles using capping agent does not affect the density of lubricant oil.

Table 4.11: Density at 15 °C of formulated bio-based lubricant oil, loaded with SCM-LA and UCMS nanoparticles at concentration up to 0.125 (w/w) %.

Additives Loading (w/w) %	Density at 15 °C, (g/cm ³)	
	UCMS nanoparticles	SCMS-LA nanoparticles
0	0.958	0.958
0.025	0.959	0.958
0.050	0.959	0.960
0.075	0.959	0.959
0.100	0.959	0.960
0.125	0.959	0.959

University of Malaya

CHAPTER 5: CONCLUSIONS AND RECOMMENDATIONS

5.1 Conclusion

The objectives of this work have been successfully accomplished. The following conclusions can be drawn based on the results reported in the previous subsections.

i. Synthesis of SCMS nanoparticles

SCMS nanoparticles were successfully synthesised via the solvothermal route using a freshly prepared organometallic precursor and thioacetamide in a hexane solvent. This reaction was conducted at a high temperature and pressure inside an autoclave vessel, yielding favourable dark brown powder.

ii. Characterisation of SCMS nanoparticles

It was found that all types of SCMS (SCMS-CA, SCMS-LA, SCMS-SA and SCMS-OA nanoparticles) have average particles sizes between 62 - 84 nm. Moreover, based on elemental study, it was confirmed that the presence of fatty acid layer surrounding molybdenum sulphide nanoparticles and the composition by percentage of capping agent are within 47.19 % (SCMS-SA nanoparticles) to 78.41 % (SCMS-CA nanoparticles). It was proposed that this fatty acid compound was chemisorbed in the form of carboxylate onto the surface of the core nanoparticles. Furthermore, among various type of fatty acids, oleic acid was proven to possess the strongest monolayer bound surrounding molybdenum sulphide nanoparticles.

- iii. Study on the effect of capping agent and concentration on tribological performance of formulated bio-based lubricant oil

The experimental results showed that bio-based lubricant oil containing SCMS-LA nanoparticles at a concentration of 0.075 (w/w) % reduces the CoF by a factor of 15.40 % compared to the pure bio-based lubricant oil. The SCMS nanoparticles functions as an antifriction additive by being embedded into the worn surfaces and pan furrow on the metal surface. In terms of antiwear performance, the addition of 0.1 (w/w) % of SCMS-OA nanoparticles into bio-based lubricant oil resulted in the best antiwear performance, at 14.96 % reduction, proving that SCMS-OA, at this concentration has the best load carrying capacity of adsorbed layer and balance between dispersibility to bio-base oil, as well as carboxylate adsorption ability on metal surfaces. It is concluded that the wear reduction rate of SCMS nanoparticles increased with increasing alkyl chain length of capping layer.

- iv. Study on the extreme pressure on tribological properties of formulated bio-based lubricant oil

Formulated bio-based lubricant oil with the addition of 0.075 (w/w) % SCMS-LA nanoparticles additive was used in this study based on its efficiency in reducing friction. At lower loads, bio-based lubricant oil with additives reports small CoF reduction, while at higher loads, the CoF reduction increases up to the welding point. In terms of antiwear performance, bio-based lubricant oil with SCMS nanoparticles as an additive shows less severe wear, lower material transfer, smaller cross hatching crack, and delamination at extreme loads, suggesting that SCMS nanoparticles can effectively improve load-carrying capacity of the bio-based lubricant oil over a wide range of applied load.

v. Physiochemical and dispersibility study of formulated bio-based lubricant oil

SCMS-LA and UCMS nanoparticles at various concentration were added into the bio-based lubricant oil used in this study. It was confirmed that SCMS-LA nanoparticles showed slower aggregation and sedimentation, better dispersibility, and longer dispersion stability at all concentration tested compared with UCMS nanoparticles due to the presence of capping layer surrounding SCMS-LA nanoparticles and hydrophilic segment (alkyl chain) of lauric acid. It was efficiently dispersed in base oil, precipitating the presence of lauric hindrance force, forcing the nanoparticles to separate from each other.

In terms of viscosity, increasing concentrations of nanoparticles loaded into bio-based lubricant oil resulted in higher VI, while SCMS-LA nanoparticles showed better VI compared to UCMS nanoparticles. This proves that the SCMS-LA can highly improve VI of bio-based lubricant oil as high lubricant with high VI is preferred. However, in the density study of formulated bio-based lubricant oil, it was concluded that the addition of SCMS-LA and UCMS nanoparticles and increasing the concentration of additives do not affect density.

5.2 Recommendations for future work

In this work, four different types of SCMS nanoparticles were synthesised and blended into one type of bio-based lubricant oil at various concentrations. The four ball wear tester were used to study their tribological activities. Several suggestions and recommendations noted for further development are proposed:

- i. To investigate the influence of SCMS nanoparticles on the tribological behaviour of different sources of bio-based oil. Different sources of oil have different chemistry and compositions which can lead into different wear and friction behaviours.
- ii. To examine the effect of different test temperature and speed on tribological properties of SCMS nanoparticles added bio-based lubricant oil. Wear and friction resistance are strongly affected by speed and temperatures thus this test can increase understanding on additives behaviour in different test environment.
- iii. To characterise the tribological characteristics using alternative friction and wear tester, such as high frequency reciprocating rig (HFRR) tester and ball/pin on disc wear tester. These instruments can characterise friction under different lubrication situation such as under disc configuration and multidirectional wear condition.

REFERENCES

- Adhvaryu, A., Erhan, S. Z., & Perez, J. M. (2002). Wax appearance temperatures of vegetable oils determined by differential scanning calorimetry: effect of triacylglycerol structure and its modification. *Thermochimica Acta*, 395(1–2), 191-200. doi:[http://dx.doi.org/10.1016/S0040-6031\(02\)00180-6](http://dx.doi.org/10.1016/S0040-6031(02)00180-6)
- Afanasiev, P. (2008). Synthetic approaches to the molybdenum sulfide materials. *Chimie*, 159-182.
- Afanasiev, P., Xia, G.-F., Berhault, G., Jouguet, B., & Lacroix, M. (1999). Surfactant-Assisted Synthesis of Highly Dispersed Molybdenum Sulfide. *Chemistry of Materials*, 3216-3219.
- Analysts, G. I. (2015, February 4 2015). *Lubricating Oil and Greases - A Global Strategic Business Report*. Market Research Report Collections. Retrieved from <http://www.strategyr.com/pressMCP-2757.asp>
- Aziz, N. A. M., Yunus, R., Rashid, U., & Syam, A. M. (2014). Application of response surface methodology (RSM) for optimizing the palm-based pentaerythritol ester synthesis. *Industrial Crops and Products*, 62, 305-312. doi:<http://dx.doi.org/10.1016/j.indcrop.2014.08.040>
- Bakunin, V. N., Kuzmina, G. N., Kasrai, M., Parenago, O. P., & Bancroft, G. M. (2006). Tribological behavior and tribofilm composition in lubricated systems containing surface capped molybdenum sulphide nanoparticles. *Tribology Letters Volume 22*, 289-296.
- Barnes, A. M., Bartle, K. D., & Thibon, V. R. A. (2001). A review of zinc dialkyldithiophosphates (ZDDPS): characterisation and role in the lubricating oil. *Tribology International*, 34(6), 389-395. doi:[http://dx.doi.org/10.1016/S0301-679X\(01\)00028-7](http://dx.doi.org/10.1016/S0301-679X(01)00028-7)
- Bart, J. C., Cavallaro, S., & Gucciardi, E. (2012). *Biolubricants: Science and technology*: Elsevier.
- Barth, H. G. (1984). *Modern Methods of Particle Size Analysis*: Wiley.
- Beck, Á., Pölcsmann, G., Eller, Z., & Hancsók, J. (2014). Investigation of the effect of detergent–dispersant additives on the oxidation stability of biodiesel, diesel fuel and their blends. *Biomass and Bioenergy*, 66, 328-336. doi:<http://dx.doi.org/10.1016/j.biombioe.2014.03.050>
- Becker, L. C., Bergfeld, W. F., Belsito, D. V., Hill, R. A., Klaassen, C. D., Liebler, D. C., Snyder, P. W. (2015). Safety Assessment of Pentaerythrityl Tetraesters as Used in Cosmetics. *International journal of toxicology*, 34(2 suppl), 99S-112S.
- Bratton, W. K., Cotton, F. A., Debeau, M., & Walton, R. A. (1971). Vibrational Studies of Dinuclear Compounds Containing Quadruply Bonded Pairs Of Molybdenum and Rhenium Atoms. *Journal of Coordination Chemistry*, 1(2), 121-131. doi:10.1080/00958977108070753

- Cai, M., Liang, Y., Zhou, F., & Liu, W. (2011). Tribological Properties of Novel Imidazolium Ionic Liquids Bearing Benzotriazole Group as the Antiwear/Anticorrosion Additive in Poly(ethylene glycol) and Polyurea Grease for Steel/Steel Contacts. *ACS Applied Materials & Interfaces*, 3(12), 4580-4592. doi:10.1021/am200826b
- Campanella, A., Rustoy, E., Baldessari, A., & Baltanás, M. A. (2010). Lubricants from chemically modified vegetable oils. *Bioresource Technology*, 101(1), 245-254.
- Chen, C. S., Chen, X. H., Xu, L. S., Yang, Z., & Li, W. H. (2005). Modification of multi-walled carbon nanotubes with fatty acid and their tribological properties as lubricant additive. *Carbon*, 43(8), 1660-1666. doi:http://dx.doi.org/10.1016/j.carbon.2005.01.044
- Chen, S., & Liu, W. (2006). Oleic acid capped PbS nanoparticles: Synthesis, Characterization and tribological properties. *Materials Chemistry and Physics*, 183-189.
- Chen, S., Liu, W., & Yu, L. (1998). Preparation of DDP-coated PbS nanoparticles and investigation of the antiwear ability of the prepared nanoparticles as additive in liquid paraffin. *Wear*, 218(2), 153-158. doi:http://dx.doi.org/10.1016/S0043-1648(98)00220-8
- Chikan, V., & Kelley, D. F. (2002). Size-Dependent Spectroscopy of MoS₂ Nanoclusters. *Journal of Physical Chemistry B*, 3794-3804.
- Choi, C., & Jung, M. (2012). Extreme Pressure Properties of Multi-Component Oil-Based Nanofluids. *Journal of Nanoscience and Nanotechnology*, 12(4), 3237-3241. doi:10.1166/jnn.2012.5596
- Choo, J.-H., Forrest, A. K., & Spikes, H. A. (2007). Influence of Organic Friction Modifier on Liquid Slip: A New Mechanism of Organic Friction Modifier Action. *Tribology Letters*, 27(2), 239-244. doi:10.1007/s11249-007-9231-z
- Dai, W., Kheireddin, B., Gao, H., & Liang, H. (2016). Roles of nanoparticles in oil lubrication. *Tribology International*, 102, 88-98. doi:http://dx.doi.org/10.1016/j.triboint.2016.05.020
- Dalmaz, G., Childs, T. H. C., Dowson, D., & Taylor, C. M. (1995). *Lubricants and Lubrication*: Elsevier Science.
- Dobias, B. (1993). *Coagulation and Flocculation: Theory and Applications*: CRC Press.
- Doig, M., Warrens, C. P., & Camp, P. J. (2013). Structure and friction of stearic acid and oleic acid films adsorbed on iron oxide surfaces in squalane. *Langmuir*, 30(1), 186-195.
- Dorinson, A., & Ludema, K. C. (1985). *Mechanics and Chemistry in Lubrication*: Elsevier Science.

- Duphil, D., Bastide, S., & Lévy-Clément, C. (2002). Chemical synthesis of molybdenum disulfide nanoparticles in an organic solution. *Journal of Materials Chemistry*, 12(8), 2430-2432.
- Dutt, N., Ghosh, T., Prasad, D., Rani, K., & Viswanath, D. (2007). *Viscosity of Liquids Theory, Estimation, Experiment, and Data*". Springer, 33, 444-553.
- Erhan, S. Z., & Asadauskas, S. (2000). Lubricant basestocks from vegetable oils. *Industrial Crops and Products*, 11(2), 277-282.
- Erhan, S. Z., Sharma, B. K., Liu, Z., & Adhvaryu, A. (2008). Lubricant Base Stock Potential of Chemically Modified Vegetable Oils. *Journal of Agricultural and Food Chemistry*, 56(19), 8919-8925. doi:10.1021/jf801463d
- Farnig, L. (2009). *Ashless Antiwear and Extreme-Pressure Additives Lubricant Additives* (pp. 213-249): CRC Press.
- Feinstein-Jaffe, I., & Maisuls, S. E. (1987). Chromium, molybdenum, and tungsten organometallic polymeric networks with aryldiisocyanide ligands. *Journal of Organometallic Chemistry*, 326(3), C97-C100. doi:http://dx.doi.org/10.1016/0022-328X(87)87016-X
- Fox, N. J., & Stachowiak, G. W. (2007). Vegetable oil-based lubricants—A review of oxidation. *Tribology International*, 40(7), 1035-1046. doi:http://dx.doi.org/10.1016/j.triboint.2006.10.001
- Gellman, A. J., & Spencer, N. D. (2002). Surface chemistry in tribology. *Proceedings of the Institution of Mechanical Engineers, Part J: Journal of Engineering Tribology*, 216(6), 443-461.
- Genuit, D., Afanasiev, P., & Vrinat, M. (2005). Solution synthesis of unsupported Co(Ni)-Mo-S hydrotreating catalysts. *Journal of Catalysis* 235, 302-317.
- Ghosh, P., & Das, M. (2014). Study of the influence of some polymeric additives as viscosity index improvers and pour point depressants – Synthesis and characterization. *Journal of Petroleum Science and Engineering*, 119, 79-84. doi:http://dx.doi.org/10.1016/j.petrol.2014.04.014
- Ghosh, S. K., Pal, A., Kundu, S., Nath, S., & Pal, T. (2004). Fluorescence quenching of 1-methylaminopyrene near gold nanoparticles: size regime dependence of the small metallic particles. *Chemical Physics Letters*, 395(4–6), 366-372. doi:http://dx.doi.org/10.1016/j.cplett.2004.08.016
- Gorbachev, O., Bouchet, M. I. D. B., Martin, J. M., Léonard, D., Le-Mogne, T., Iovine, R., . . . Héau, C. (2016). Friction reduction efficiency of organic Mo-containing FM additives associated to ZDDP for steel and carbon-based contacts. *Tribology International*, 99, 278-288. doi:http://dx.doi.org/10.1016/j.triboint.2016.03.035
- Green, L. (2015). *When and How to Use Friction Modifiers*. Machinery Lubrication. Retrieved from <http://www.machinerylubrication.com/Read/30336/friction-modifiers-use>

- Grossiord, C., Varlot, K., Martin, J. M., Le Mogne, T., Esnouf, C., & Inoue, K. (1998). MoS₂ single sheet lubrication by molybdenum dithiocarbamate. *Tribology International*, 31(12), 737-743. doi:http://dx.doi.org/10.1016/S0301-679X(98)00094-2
- Gupta, R. N., & Harsha, A. P. (2016). Synthesis, Characterization, and Tribological Studies of Calcium–Copper–Titanate Nanoparticles as a Biolubricant Additive. *Journal of Tribology*, 139(2), 021801-021801-021811. doi:10.1115/1.4033714
- Hsu, S. M., & Klaus, E. E. (1978). Estimation of the Molecular Junction Temperatures in Four-Ball Contacts by Chemical Reaction Rate Studies. *A S L E Transactions*, 21(3), 201-210. doi:10.1080/05698197808982875
- Hu, K., Hu, X., & Jiang, P. (2010). Large Scale Morphology-controlled synthesis of Nano-sized Molybdenum Disulphide Particle by Different Sulphur Sources. *International Journal of Material and Product Technology*, 378-387.
- Husnawan, M., Saifullah, M. G., & Masjuki, H. H. (2007). Development of friction force model for mineral oil basestock containing palm olein and antiwear additive. *Tribology International*, 40(1), 74-81. doi:http://dx.doi.org/10.1016/j.triboint.2006.02.062
- Hwang, Y., Lee, C., Choi, Y., Cheong, S., Kim, D., Lee, K., . . . Kim, S. H. (2011). Effect of the size and morphology of particles dispersed in nano-oil on friction performance between rotating discs. *Journal of Mechanical Science and Technology*, 25(11), 2853-2857. doi:10.1007/s12206-011-0724-1
- Hwang, Y., Lee, J.-K., Lee, J.-K., Jeong, Y.-M., Cheong, S.-i., Ahn, Y.-C., & Kim, S. H. (2008). Production and dispersion stability of nanoparticles in nanofluids. *Powder Technology*, 186(2), 145-153. doi:http://dx.doi.org/10.1016/j.powtec.2007.11.020
- Ilie, F., & Covaliu, C. (2016). Tribological Properties of the Lubricant Containing Titanium Dioxide Nanoparticles as an Additive. *Lubricants*, 4(2), 12.
- Jiang, L., Gao, L., & Sun, J. (2003). Production of aqueous colloidal dispersions of carbon nanotubes. *Journal of colloid and interface science*, 260(1), 89-94. doi:http://dx.doi.org/10.1016/S0021-9797(02)00176-5
- Kamimura, H., Chiba, T., Watanabe, N., Kubo, T., Nanao, H., Minami, I., & Mori, S. (2006). Effects of Carboxylic Acids on Friction and Wear Reducing Properties for Alkylmethylimidazolium Derived Ionic liquids. *Tribology Online*, 1(2), 40-43. doi:10.2474/trol.1.40
- Kamiya, H., & Iijima, M. (2010). Surface modification and characterization for dispersion stability of inorganic nanometer-scaled particles in liquid media. *Science and Technology of Advanced Materials*, 11(4), 044304. doi:10.1088/1468-6996/11/4/044304
- Kebblinski, P., Phillpot, S. R., Choi, S. U. S., & Eastman, J. A. (2002). Mechanisms of heat flow in suspensions of nano-sized particles (nanofluids). *International*

Journal of Heat and Mass Transfer, 45(4), 855-863.
doi:http://dx.doi.org/10.1016/S0017-9310(01)00175-2

- Khonsari, M. M., & Booser, E. R. (2001). *Applied Tribology: Bearing Design and Lubrication*: Wiley.
- Kondo, Y., Koyama, T., & Sasaki, S. (2013). Tribological Properties of Ionic Liquids.
- Kreivaitis, R., Padgurskas, J., Gumbytė, M., & Makarevičienė, V. (2014). The thermal stability of rapeseed oil as a base stock for environmentally friendly lubricants. *Mechanics*, 20(3), 338-343.
- Ku, B.-C., Han, Y.-C., Lee, J.-E., Lee, J.-K., Park, S.-H., & Hwang, Y.-J. (2010). Tribological effects of fullerene (C₆₀) nanoparticles added in mineral lubricants according to its viscosity. *International Journal of Precision Engineering and Manufacturing*, 11(4), 607-611. doi:10.1007/s12541-010-0070-8
- Kumar Dubey, M., Bijwe, J., & Ramakumar, S. S. V. (2013). PTFE based nano-lubricants. *Wear*, 306(1-2), 80-88.
doi:http://dx.doi.org/10.1016/j.wear.2013.06.020
- Lansdown, A. R. (1999). *Molybdenum Disulphide Lubrication*: Elsevier Science.
- Lawton, D., & Mason, R. (1965). The Molecular Structure of Molybdenum(II) Acetate. *Journal of the American Chemical Society*, 87(4), 921-922.
doi:10.1021/ja01082a046
- Li, W.-J., Shi, E.-W., Ko, J.-M., Chen, Z.-Z., Ogino, H., & Fukuda, T. (2003). Hydrothermal synthesis of MoS₂ nanowires. *Journal of Crystal Growth*, 418-422.
- Liang, K., Chianelli, R., Chien, F., & Moss, S. (1986). Structure of poorly crystalline MoS₂—a modeling study. *Journal of non-crystalline solids*, 79(3), 251-273.
- Limaye, M. V., Singh, S. B., Date, S. K., Kothari, D., Reddy, V. R., Gupta, A., Kulkarni, S. K. (2009). High coercivity of oleic acid capped CoFe₂O₄ nanoparticles at room temperature. *The Journal of Physical Chemistry B*, 113(27), 9070-9076.
- Lin, J., Wang, L., & Chen, G. (2011). Modification of Graphene Platelets and their Tribological Properties as a Lubricant Additive. *Tribology Letters*, 41(1), 209-215. doi:10.1007/s11249-010-9702-5
- Lin, Y.-C., Cho, Y.-H., & Chiu, C.-T. (2012). Tribological performance of EP additives in different base oils. *Tribology Transactions*, 55(2), 175-184.
- López-Quintela, M. A. (2003). Synthesis of nanomaterials in microemulsions: formation mechanisms and growth control. *Current Opinion in Colloid & Interface Science*, 8(2), 137-144. doi:http://dx.doi.org/10.1016/S1359-0294(03)00019-0
- Lugo, L., Canet, X., Comuñas, M. J. P., Pensado, A. S., & Fernández, J. (2007). Dynamic Viscosity under Pressure for Mixtures of Pentaerythritol Ester Lubricants with 32 Viscosity Grade: Measurements and Modeling. *Industrial & Engineering Chemistry Research*, 46(6), 1826-1835. doi:10.1021/ie061187r

- Lugt, P., Severt, R., Fogelströ, J., & Tripp, J. (2001). Influence of surface topography on friction, film breakdown and running-in in the mixed lubrication regime. *Proceedings of the Institution of Mechanical Engineers, Part J: Journal of Engineering Tribology*, 215(6), 519-533.
- Lundgren, S. M., Ruths, M., Danerlöv, K., & Persson, K. (2008). Effects of unsaturation on film structure and friction of fatty acids in a model base oil. *Journal of colloid and interface science*, 326(2), 530-536.
- Markets, M. A. (2015). *Automotive Coolant & Lubricant Market by Vehicle Type (Passenger Car, LCV, & HCV), Application (Coolant-Engine & HVAC, Lubricant-Engine, Brake, & Transmission), Region & by Aftermarket - Global Trends & Forecast to 2019*. AT 2981. Retrieved from <http://www.marketsandmarkets.com/Market-Reports/automotive-coolants-lubricants-market-254296375.html>
- Markit, I. (2015). *Lubricating Oil Additives*. Retrieved from <https://www.ihs.com/products/chemical-lubricating-oil-scup.html>
- Menezes, P. L., Ingole, S. P., Nosonovsky, M., Kailas, S. V., & Lovell, M. R. (2013). *Tribology for scientists and engineers*: Springer.
- Mobil, E. (2016). *The Outlook for Energy: A View to 2040*. Retrieved from <http://corporate.exxonmobil.com/en/energy/energy-outlook>
- Mortier, R. M., Orszulik, S. T., & Fox, M. F. (2010). *Chemistry and technology of lubricants (Vol. 107115)*: Springer.
- Mutyala, K. C., Singh, H., Fouts, J. A., Evans, R. D., & Doll, G. L. (2016). Influence of MoS₂ on the Rolling Contact Performance of Bearing Steels in Boundary Lubrication: A Different Approach. *Tribology Letters*, 61(2), 20. doi:10.1007/s11249-015-0638-7
- Nagendramma, P., & Kaul, S. (2012). Development of ecofriendly/biodegradable lubricants: An overview. *Renewable and Sustainable Energy Reviews*, 16(1), 764-774. doi:<http://dx.doi.org/10.1016/j.rser.2011.09.002>
- Nakada, M. (1994). Trends in engine technology and tribology. *Tribology International*, 27(1), 3-8. doi:[http://dx.doi.org/10.1016/0301-679X\(94\)90056-6](http://dx.doi.org/10.1016/0301-679X(94)90056-6)
- Nepomnyashchaya, E. K., Prokofiev, A. V., Velichko, E. N., Pleshakov, I. V., & Kuzmin, Y. I. (2016). Investigation of magneto-optical properties of ferrofluids by laser light scattering techniques. *Journal of Magnetism and Magnetic Materials*. doi:<http://dx.doi.org/10.1016/j.jmmm.2016.10.002>
- Nogueira, I., Dias, A. M., Gras, R., & Proghi, R. (2002). An experimental model for mixed friction during running-in. *Wear*, 253(5-6), 541-549. doi:[http://dx.doi.org/10.1016/S0043-1648\(02\)00065-0](http://dx.doi.org/10.1016/S0043-1648(02)00065-0)
- Otero, V., Sanches, D., Montagner, C., Vilarigues, M., Carlyle, L., Lopes, J. A., & Melo, M. J. (2014). Characterisation of metal carboxylates by Raman and infrared

spectroscopy in works of art. *Journal of Raman Spectroscopy*, 45(11-12), 1197-1206. doi:10.1002/jrs.4520.

- Panchal, T. M., Patel, A., Chauhan, D. D., Thomas, M., & Patel, J. V. (2017). A methodological review on bio-lubricants from vegetable oil based resources. *Renewable and Sustainable Energy Reviews*, 70, 65-70. doi:http://dx.doi.org/10.1016/j.rser.2016.11.105
- Panigrahi, P. K., & Pathak, A. (2013). Aqueous Medium Synthesis Route for Randomly Stacked Molybdenum Disulfide. *Journal of Nanoparticles*, 2013.
- Parento, O., Bakunin, V., Kuz'mina, G., Suslov, A. Y., & Vedeneeva, L. (2002). Molybdenum sulfide nanoparticles as new-type additives to hydrocarbon lubricants. Paper presented at the Doklady Chemistry.
- Park, J. Y., Aliaga, C., Renzas, J. R., Lee, H., & Somorjai, G. A. (2009). The Role of Organic Capping Layers of Platinum Nanoparticles in Catalytic Activity of CO Oxidation. *Catalysis Letters*, 129(1), 1-6. doi:10.1007/s10562-009-9871-8
- Patel, J. D., Mighri, F., & Ajji, A. (2012). Generalized chemical route to develop fatty acid capped highly dispersed semiconducting metal sulphide nanocrystal. *Material Research Bulletin* 47, 2016-2021.
- Patel, J. D., Mighri, F., & Ajji, A. (2012). Generalized chemical route to develop fatty acid capped highly dispersed semiconducting metal sulphide nanocrystals. *Materials Research Bulletin*, 47(8), 2016-2021.
- Peña-Parás, L., Maldonado-Cortés, D., Taha-Tijerina, J., García-Pineda, P., Garza, G. T., Irigoyen, M., . . . Sánchez, D. (2016). Extreme pressure properties of nanolubricants for metal-forming applications. *Industrial Lubrication and Tribology*, 68(1), 30-34. doi:doi:10.1108/ILT-05-2015-0069
- Peng, Y., Meng, Z., Zhong, C., Lu, J., Yang, Z., & Qian, Y. (2002). Tube- and ball-like amorphous MoS₂ prepared by a solvothermal method. *Materials Chemistry and Physics* 73, 327-329.
- Phenrat, T., Saleh, N., Sirk, K., Tilton, R. D., & Lowry, G. V. (2007). Aggregation and Sedimentation of Aqueous Nanoscale Zerovalent Iron Dispersions. *Environmental Science & Technology*, 41(1), 284-290. doi:10.1021/es061349a
- Prince, R. J. (2010). Base Oils from Petroleum. In R. M. Mortier, M. F. Fox, & S. T. Orszulik (Eds.), *Chemistry and Technology of Lubricants* (pp. 3-33). Dordrecht: Springer Netherlands.
- Qu, J., Luo, H., Chi, M., Ma, C., Blau, P. J., Dai, S., & Viola, M. B. (2014). Comparison of an oil-miscible ionic liquid and ZDDP as a lubricant anti-wear additive. *Tribology International*, 71, 88-97. doi:http://dx.doi.org/10.1016/j.triboint.2013.11.010
- Qu, M., Yao, Y., He, J., Ma, X., Liu, S., Feng, J., & Hou, L. (2016). Tribological performance of functionalized ionic liquid and Cu microparticles as lubricating

additives in sunflower seed oil. *Tribology International*, 104, 166-174. doi:<http://dx.doi.org/10.1016/j.triboint.2016.08.035>

Quinchia, L. A., Delgado, M. A., Reddyhoff, T., Gallegos, C., & Spikes, H. A. (2014). Tribological studies of potential vegetable oil-based lubricants containing environmentally friendly viscosity modifiers. *Tribology International*, 69, 110-117. doi:<http://dx.doi.org/10.1016/j.triboint.2013.08.016>

Raj, F. R. M. S., & Sahayaraj, J. W. (2010, 13-15 Nov. 2010). A comparative study over alternative fuel (biodiesel) for environmental friendly emission. Paper presented at the Recent Advances in Space Technology Services and Climate Change 2010 (RSTS & CC-2010).

Ramezani, M., & Schmid, S. R. (2015). Bio-based lubricants for forming of magnesium. *Journal of Manufacturing Processes*, 19, 112-117. doi:<http://dx.doi.org/10.1016/j.jmapro.2015.06.008>

Rapoport, L., Feldman, Y., Homyonfer, M., Cohen, H., Sloan, J., Hutchison, J. L., & Tenne, R. (1999). Inorganic fullerene-like material as additives to lubricants: structure–function relationship. *Wear*, 225–229, Part 2, 975-982. doi:[http://dx.doi.org/10.1016/S0043-1648\(99\)00040-X](http://dx.doi.org/10.1016/S0043-1648(99)00040-X)

Research, G. V. (2016). *Lubricant Additives Market Analysis By Product (Dispersants, Viscosity Index Modifiers, Detergents, Anti-Wear Additives, Antioxidants, Friction Modifiers), By Application (Automotive (HDV and LDV), Industrial (Metalworking Fluids, General Industrial Oil, Industrial Engine Oil)) And Segment Forecasts To 2024*. Retrieved from <http://www.grandviewresearch.com/industry-analysis/lubricant-additives-market>

Rudnick, L. R. (2009). *Lubricant additives: chemistry and applications*: CRC Press.

Schmidt, G., & Malwitz, M. M. (2003). Properties of polymer–nanoparticle composites. *Current Opinion in Colloid & Interface Science*, 8(1), 103-108. doi:[http://dx.doi.org/10.1016/S1359-0294\(03\)00008-6](http://dx.doi.org/10.1016/S1359-0294(03)00008-6)

Schneider, M. P. (2006). Plant-oil-based lubricants and hydraulic fluids. *Journal of the Science of Food and Agriculture*, 86(12), 1769-1780. doi:10.1002/jsfa.2559

Shahnazar, S., Bagheri, S., & Hamid, S. B. A. (2016). Enhancing lubricant properties by nanoparticle additives. *International Journal of Hydrogen Energy*.

Sharma, B. K., & Biresaw, G. (2016). *Environmentally Friendly and Biobased Lubricants*: CRC Press.

Sharma, R. V., & Dalai, A. K. (2013). Synthesis of bio-lubricant from epoxy canola oil using sulfated Ti-SBA-15 catalyst. *Applied Catalysis B: Environmental*, 142, 604-614.

Shia, Q., Tang, H., ZHUa, H., Tang, G., Zhang, K., Zhang, H., & LIa, C. (2014). Synthesis And Tribological Properties Of Ti-Doped NbSe₂ Nanoparticles. *Chalcogenide Letters*, 11(5), 199-207.

- Singh, A. K. (2011). Castor oil-based lubricant reduces smoke emission in two-stroke engines. *Industrial Crops and Products*, 33(2), 287-295. doi:http://dx.doi.org/10.1016/j.indcrop.2010.12.014
- Soni, S., & Agarwal, M. (2014). Lubricants from renewable energy sources—a review. *Green Chemistry Letters and Reviews*, 7(4), 359-382.
- Stachowiak, G. W., & Batchelor, A. W. (1993). *Engineering Tribology*: Elsevier Science.
- Stachowiak, G. W., & Batchelor, A. W. (2006). 3 - Lubricants and Their Composition *Engineering Tribology (Third Edition)* (pp. 51-101). Burlington: Butterworth-Heinemann.
- Stephenson, T. A., Bannister, E., & Wilkinson, G. (1964). 487. Molybdenum(II) carboxylates. *Journal of the Chemical Society (Resumed)*(0), 2538-2541. doi:10.1039/JR9640002538
- Stepina, V., & Vesely, V. (1992). *Lubricants and Special Fluids*: Elsevier Science.
- Sulek, M. W., Kulczycki, A., & Malysa, A. (2010). Assessment of lubricity of compositions of fuel oil with biocomponents derived from rape-seed. *Wear*, 268(1–2), 104-108. doi:http://dx.doi.org/10.1016/j.wear.2009.07.004
- Suslov, A. Y., Bakunin, V., Kuz'mina, G., Vedeneva, L., & Parenago, O. (2003). Surface-Capped Molybdenum Sulfide Nanoparticles—A Novel Type of Lubricant Additives. *ANNALS*, 24, 26.
- Swihart, M. T. (2003). Vapor-phase synthesis of nanoparticles. *Current Opinion in Colloid & Interface Science*, 8(1), 127-133. doi:http://dx.doi.org/10.1016/S1359-0294(03)00007-4
- Syahrullail, S., Zubil, B., Azwadi, C., & Ridzuan, M. (2011). Experimental evaluation of palm oil as lubricant in cold forward extrusion process. *International journal of mechanical sciences*, 53(7), 549-555.
- Talpin, D. V., Rogach, A. L., Mekis, I., Haubold, S., Kornowski, A., Haase, M., & Weller, H. (2002). Synthesis and surface modification of amino-stabilized CdSe, CdTe and InP nanocrystals. *Colloids and Surfaces A: Physicochemical and Engineering Aspects*, 202(2–3), 145-154. doi:http://dx.doi.org/10.1016/S0927-7757(01)01078-0
- Talib, N., & Rahim, E. A. (2016). The Effect of Tribology Behavior on Machining Performances When Using Bio-based Lubricant as a Sustainable Metalworking Fluid. *Procedia CIRP*, 40, 504-508. doi:http://dx.doi.org/10.1016/j.procir.2016.01.116
- Tang, Z., & Li, S. (2014). A review of recent developments of friction modifiers for liquid lubricants (2007–present). *Current Opinion in Solid State and Materials Science*, 18(3), 119-139.
- Totten, G. E., Westbrook, S. R., & Shah, R. J. (2003). *Fuels and Lubricants Handbook*. ASTM International (01-June-2003).

- Tzanakis, I., Hadfield, M., Thomas, B., Noya, S. M., Henshaw, I., & Austen, S. (2012). Future perspectives on sustainable tribology. *Renewable and Sustainable Energy Reviews*, 16(6), 4126-4140. doi:<http://dx.doi.org/10.1016/j.rser.2012.02.064>
- Wang, H., Xu, B., & Liu, J. (2013). *Micro and nano sulfide solid lubrication*: Springer Science & Business Media.
- Wang, M., Niu, Y., Zhou, J., Wen, H., Zhang, Z., Luo, D., Li, Y. (2016). The dispersion and aggregation of graphene oxide in aqueous media. *Nanoscale*, 8(30), 14587-14592.
- Wang, S., & He, D. (2011). Nanocrystalline MoS₂ through Directional Growth along the (002) Crystal Plane under High Pressure. *Material Chemistry and Physics* 130, 170-174.
- Watanabe, K., Kyomoto, M., Yamane, S., Ishihara, K., Takatori, Y., Tanaka, S., & Moro, T. (2016). Tribological Evaluation Of Pmpc-Grafted Hydrated Bearing Surface Using Multidirectional Pin-on-Disk Tester. *Bone & Joint Journal Orthopaedic Proceedings Supplement*, 98-B(SUPP 4), 121-121.
- Wie, J. M., & Fuerstenau, D. W. (1974). The effect of dextrin on surface properties and the flotation of molybdenite. *International Journal of Mineral Processing*, 1(1), 17-32. doi:[http://dx.doi.org/10.1016/0301-7516\(74\)90024-6](http://dx.doi.org/10.1016/0301-7516(74)90024-6)
- Wilcoxon, J. P., & Samara, G. A. (1995). Strong quantum-size effects in a layered semiconductor: MOS₂ nanocluster. *Physical Review B*, 7299-7302.
- Wood, M. H., Casford, M. T., Steitz, R., Zorbakhsh, A., Welbourn, R. J. L., & Clarke, S. M. (2016). Comparative Adsorption of Saturated and Unsaturated Fatty Acids at the Iron Oxide/Oil Interface. *Langmuir*, 32(2), 534-540. doi:10.1021/acs.langmuir.5b04435
- Xu, N., Zhang, M., Li, W., Zhao, G., Wang, X., & Liu, W. (2013). Study on the selectivity of calcium carbonate nanoparticles under the boundary lubrication condition. *Wear*, 307(1-2), 35-43. doi:<http://dx.doi.org/10.1016/j.wear.2013.07.010>
- Xu, Y., Wang, Q., Hu, X., Li, C., & Zhu, X. (2010). Characterization of the lubricity of bio-oil/diesel fuel blends by high frequency reciprocating test rig. *Energy*, 35(1), 283-287. doi:<http://dx.doi.org/10.1016/j.energy.2009.09.020>
- Yadav, G., Tiwari, S., & Jain, M. (2016). Tribological analysis of extreme pressure and anti-wear properties of engine lubricating oil using four ball tester.
- Yamamoto, Y., & Gondo, S. (1989). Friction and Wear Characteristics of Molybdenum Dithiocarbamate and Molybdenum Dithiophosphate. *Tribology Transactions*, 32(2), 251-257. doi:10.1080/10402008908981886
- Yang, C. W., Hwang, M. J., & Huang, B. N. (2002). An analysis of factors affecting price volatility of the US oil market. *Energy Economics*, 24(2), 107-119. doi:[http://dx.doi.org/10.1016/S0140-9883\(01\)00092-5](http://dx.doi.org/10.1016/S0140-9883(01)00092-5)

- Zabinski, J. S., & McDevitt, N. T. (1996). Raman Spectra of Inorganic Compounds Related to Solid State Tribochemical Studies. Retrieved from
- Zahid, R. (2016). Study of tribological properties of lubricating oil blend added with graphene nanoplatelets. *J. Mater. Res*, 2.
- Zeng, X., Li, J., Wu, X., Ren, T., & Liu, W. (2007). The tribological behaviors of hydroxyl-containing dithiocarbamate-triazine derivatives as additives in rapeseed oil. *Tribology International*, 40(3), 560-566. doi:<http://dx.doi.org/10.1016/j.triboint.2006.05.005>
- Zhang, C., Zhang, S., Song, S., Yang, G., Yu, L., Wu, Z., Zhang, P. (2014a). Preparation and tribological properties of surface-capped copper nanoparticle as a water-based lubricant additive. *Tribology Letters*, 54(1), 25-33.
- Zhang, C., Zhang, S., Song, S., Yang, G., Yu, L., Wu, Z., . . . Zhang, P. (2014b). Preparation and Tribological Properties of Surface Capped Copper nanoparticle as a Water Based Lubricant Additives. *Tribology Letter*, 25-33.
- Zhao, Y., Kuai, L., Liu, Y., Wang, P., Arandiyani, H., Cao, S., . . . Geng, B. (2015). Well-Constructed Single-Layer Molybdenum Disulfide Nanorose Cross-Linked by Three Dimensional-Reduced Graphene Oxide Network For Superior Water Splitting And Lithium Storage Property. *Scientific Reports*, 5.
- Zheng, T., Bott, S., & Huo, Q. (2016). Techniques for Accurate Sizing of Gold Nanoparticles Using Dynamic Light Scattering with Particular Application to Chemical and Biological Sensing Based on Aggregate Formation. *ACS Applied Materials & Interfaces*, 8(33), 21585-21594. doi:[10.1021/acsami.6b06903](https://doi.org/10.1021/acsami.6b06903)
- Zhmud, B., & Pasalskiy, B. (2013). Nanomaterials in lubricants: an industrial perspective on current research. *Lubricants*, 1(4), 95-101.
- Zhou, G., Zhu, Y., Wang, X., Xia, M., Zhang, Y., & Ding, H. (2013). Sliding tribological properties of 0.45% carbon steel lubricated with Fe₃O₄ magnetic nano-particle additives in baseoil. *Wear*, 301(1-2), 753-757. doi:<http://dx.doi.org/10.1016/j.wear.2013.01.027>
- Zhou, J., Yang, J., Zhang, Z., Liu, W., & Xue, Q. (1999). Study on the structure and tribological properties of surface-modified Cu nanoparticles. *Materials Research Bulletin*, 34(9), 1361-1367. doi:[http://dx.doi.org/10.1016/S0025-5408\(99\)00150-6](http://dx.doi.org/10.1016/S0025-5408(99)00150-6)
- Zulkifli, N., Masjuki, H., Kalam, M., Yunus, R., & Azman, S. (2014). Lubricity of Bio-Based Lubricant Derived From Chemically Modified Jatropha Methyl Ester. *Jurnal Tribologi*, 1, 18-39.

LIST OF PUBLICATIONS AND PAPERS PRESENTED

Technical paper: -

Sharul Hafiq Roslan, Sharifah Bee Abd Hamid, Nurin Wahidah Mohd Zulkifli, (2017)
"Synthesis, characterisation and tribological evaluation of surface capped molybdenum sulphide nanoparticles as efficient antiwear bio-based lubricant additives", Industrial Lubrication and Tribology, Vol. 69 Issue: 3, pp.378386, <https://doi.org/10.1108/ILT0920160212>

Proceedings paper: -

Roslan, S. H.; Zulkifli, N. W. M.; Hamid S. B. A. (2016). "Production and tribological study of surface capped molybdenum sulphide nanoparticles for bio-based lubricant additives." Proceedings of International Conference on Advanced Processes and Systems in Manufacturing (APSIM 2016): 97-98.